



Adolescent Identity Search Algorithm (AISA): A novel metaheuristic approach for solving optimization problems

Esref Bogar ^{a,*}, Selami Beyhan ^b

^a Department of Electronic and Automation, Denizli Vocational School of Technical Sciences, Pamukkale University, 20070, Denizli, Turkey

^b Faculty of Engineering, Electrical and Electronics Engineering, Izmir Democracy University, Uckuyular District, Gursel Aksel Blvd, No:14, 35140 Karabaglar, Izmir, Turkey



ARTICLE INFO

Article history:

Received 20 October 2019

Received in revised form 16 May 2020

Accepted 23 June 2020

Available online 27 June 2020

Keywords:

Optimization

Metaheuristics

IIR system identification

Inverse kinematics problem

AISA

ABSTRACT

This paper proposes a novel population-based metaheuristic optimization algorithm, called Adolescent Identity Search Algorithm (AISA), which is inspired by the process of identity development/search of adolescents. AISA simulates the identity formation behavior of adolescents in the peer group. This behavior is modeled mathematically to solve optimization problems. The proposed algorithm is evaluated on thirty-nine well-known unimodal, multimodal, fixed-dimensional multimodal, composite and CEC 2019 benchmark functions to test exploration, exploitation, local optima avoidance, and convergence properties. The results are verified by an extensive comparative study with thirteen state-of-art metaheuristic algorithms. Furthermore, AISA has been used to solve IIR system identification and inverse kinematics problem of a seven Degrees Of Freedom (7-DOF) robot manipulator considered as the real-life engineering applications. The overall optimization results demonstrate that AISA possesses a strong and robust capability to produce superior performance over other competitor metaheuristic algorithms in solving various complex numerical optimization problems.

© 2020 Elsevier B.V. All rights reserved.

1. Introduction

Optimization is the process of finding the best value of a set of variables to minimize or maximize an objective function. Optimization has become an important area of work in practice and theory to reach certain goals by using the resources available in a system in the most efficient way. In terms of real world problems, optimization problems are frequently encountered in a wide variety of fields including engineering, business, economics, transportation and more. Generally, optimization problems are divided into various categories whether they are constrained or unconstrained, discrete or continuous, static or dynamic, single or multi-objective [1].

Many real-life optimization problems have high complexity, nonlinear constraints, interdependencies amongst variables and a wide range of solutions [2]. Therefore, finding a solution to such an optimization problem is considered as a challenging task. In order to solve them, many researchers have proposed optimization methods that are typically classified as mathematical programming approaches and metaheuristic methods. The former ones are not always efficient in dealing with many large-scale real-world multimodal, non-continuous and non-differentiable

problems [3]. Therefore, metaheuristic approaches have been designed as alternative seekers and have become very popular over the last four decades due to four major reasons: simplicity, flexibility, derivation-free mechanism, and local optima avoidance [4]. However, they do not guarantee an exact solution but provide acceptable results in a reasonable time.

In metaheuristic approaches, there are two indispensable components directly related to the search capability of an algorithm: exploration (diversification) and exploitation (intensification). The exploration strives to find promising solutions by spanning deeply unexplored regions. In other words, it focuses on improving the diversity of the solutions. On the contrary, the exploitation aims to enhance the quality of solutions by seeking locally around promising solutions obtained by the exploration. These components conflict and hinder each other [5]. Therefore, an optimizer should be designed by considering a right and reasonable balance between them. Otherwise, undesirable scenarios may occur such as being trapped in local optima and immature convergence.

Based on the source of inspiration, metaheuristics can be broadly decomposed into four main categories: Evolutionary Algorithms (EAs), Swarm Intelligence (SI), Physics/Chemistry-based and Human-based algorithms [6].

EAs are inspired by the Darwinian evolution in nature and imitate biological evolutionary behaviors such as recombination,

* Corresponding author.

E-mail addresses: ebogar@pau.edu.tr (E. Bogar), [\(S. Beyhan\)](mailto:selami.beyhan@idu.edu.tr).

mutation, and selection. Some of the most renowned are Genetic Algorithm (GA) [7], Differential Evolution (DE) [8], Evolution Strategy (ES) [9], Estimation of Distribution Algorithms (EDA) [10] and Biogeography-Based Optimization (BBO) [11].

SI algorithms are abstracted from the behaviors of groups of animals (foraging, mating, migration, and etc.). The most popular SI algorithm is Particle Swarm Optimization (PSO) [12] that imitates intelligent social behavior of bird flock. Other popular examples of SI algorithms are Ant Colony Optimization (ACO) [13], Artificial Bee Colony (ABC) [14], Cat Swarm Optimization (CSO) [15], Cuckoo Search (CS) [16], Firefly Algorithm (FA) [17], Bat Algorithm (BA) [18], Krill Herd (KH) [19], Fruit Fly Optimization Algorithm (FOA) [20], Gray Wolf Optimizer (GWO) [4], Weighted Superposition Attraction (WSA) [21], Artificial Algae Algorithm (AAA) [22], Crow Search Algorithm (CSA) [23], Whale Optimization Algorithm (WOA) [24], Grasshopper Optimization Algorithm (GOA) [25], Salp Swarm Algorithm (SSA) [26], Emperor Penguin Optimizer (EPO) [1], Mouth Brooding Fish (MBF) [27], Squirrel Search Algorithm (SSA) [28] and Pathfinder Algorithm (PFA) [29]. Apart from these, others can be obtained from [30].

Physics/Chemistry-based algorithms mimic certain physical/chemical laws, including electrical charges, gravity, river systems, motion, and etc. Simulated Annealing (SA) [31], Big-Bang Big-Crunch (BB-BC) [32], Gravitational Search Algorithm (GSA) [33], Chemical Reaction Optimization (CRO) [34], Charged System Search (CSS) [35], Ray Optimization (RA) [36], Black Hole (BH) [37], Gases Brownian Motion Optimization (GBMO) [38], Ions Motion Algorithm [39], Vortex Search (VS) [40] and Multi-Verso Optimizer (MVO) [6] are some optimizers in this category. In addition, more can be obtained from [41].

As the last category of metaheuristics, Human-based algorithms are inspired by human behaviors and characteristics. Some of well-regarded algorithms related to this category are Tabu Search (TS) [42], Teaching-Learning-Based Optimization (TLBO) [43], Mine Blast Algorithm (MBA) [44], Interior Search Algorithm (ISA) [45], Exchange Market Algorithm (EMA) [46], Human Behavior-Based Optimization (HBBO) [47], Volleyball Premier League (VPL) [48] and Social Engineering Optimizer (SEO) [49].

Although many optimization algorithms, which are successful in solving optimization problems of the literature, the scientific community still continue to develop new optimization algorithms so as to enhance solutions of the current problems and solve unprecedented complex problems. The reason of continuous development lies on the “No-Free-Lunch” (NFL) theorem [50]. NFL theorem states that there is no universal algorithm for solving all optimization problems. This implies that an optimization algorithm may yield satisfactory solutions on some problems but unsatisfactory solutions on other problems [51]. Therefore, the scientific optimization community is trying to develop new better optimization techniques.

In light of the developments in optimization literature, this paper proposes a novel, intriguing and powerful human behavior based optimization algorithm called “Adolescent Identity Search Algorithm (AISA)” for solving numerical optimization problems. As is evident from its name, it simulates the process of identity search of adolescents. The inspirations behind the proposed method are the adolescent theory of the Erikson and our personal observations on adolescents that are detailed in corresponding section. The main contributions can be outlined as follows.

- A novel population-based metaheuristic approach is introduced and explained.
- The proposed algorithm is validation on 39 classical benchmark functions with different characteristics.

- A rigorous comparative study is performed with well-known metaheuristic optimization algorithms using statistical analysis, scalability analysis, Wilcoxon signed-rank test, computational time analysis and convergence analysis.
- Two adaptive IIR system identification problems in both actual and reduced order are solved by the proposed algorithm.
- Optimization capability of AISA as well as other optimizers are investigated on the inverse kinematics problem of a seven Degrees Of Freedom (7-DOF) robot manipulator.

The rest of this paper is structured as follows. The proposed Adolescent Identity Search Algorithm (AISA) is introduced in Section 2 with a feature selection methodology. Section 3 presents structural comparison of AISA with other optimizers. Section 4 presents experimental comparisons of the literature optimization methods and proposed method in solving well-known benchmark problems. The application results for the engineering problems are provided in Section 5. The obtained results are presented and discussed in Section 6. Finally, some concluding remarks and scope for future work are listed in Section 7.

2. Adolescent Identity Search Algorithm (AISA)

Adolescence (from Latin adolescere, meaning to grow up) is typically described as a phase of maturation that is a period of physical and psychological transition between childhood and adulthood [52]. According to the World Health Organization (WHO), an adolescent is defined as any person between ages 10 and 19.

The adolescent experiences profound and exciting physical, social, emotional and intellectual changes during adolescence. Moreover, the adolescent strives to find himself, prove himself, make a lifestyle, determine aims, establish sexual relations, regulate human relations, and etc. Therefore, the adolescent makes a mysterious journey throughout this period when often seeking answers to the question “Who am I?” [53]. Thus, identity essentially refers to how a person answers this question [54]. In other words, it is a combination of different identity options/features such as behaviors, preferences, thoughts, abilities and beliefs that an individual has acquired in this process.

According to Erikson, who is a prominent developmental theorist, identity is formed in adolescence as an adolescent becomes more independent and explores/commitments different alternatives or roles in their communities [55]. In addition, Marcia elaborated on Erikson’s concept of identity and proposed four identity statuses such as achievement, foreclosure, moratorium and diffusion statuses by focusing on two basic elements such as exploration and commitment [56]. Each identity status expresses a combination of exploration and commitment at different levels.

The adolescent interacts with other members of the society and attempts to form his/her identity by using feedback from these social interactions. Generally, the adolescent tends to move away from the family to become an independent individual. In contrast, the adolescent’s identity can be shaped by peers since adolescents spend most of their time in school, playfield and so on. Regardless of structure and norms, any peer group plays an important role in adolescent development. This group may have a positive or negative effect on the adolescent and serves as a station for the identity formation of the adolescent. Moreover, experiences in the peer group have an important contribution to the self-efficacy, self-control, self-regularity ability, self-awareness and self-esteem [57]. Especially, adolescents in peer group develop their ability to make decisions and take responsibility in an environment where adults do not exist.

The modeling of the identity formation processes of adolescents in the peer group is actually a challenging task since

the group structure can be affected by many factors such as age, gender, location, ethnicity and culture, educational level and socio-economic status. For that reason, based on the developmental theories and the experiences during our own adolescence, a progress for adolescent identity search/exploration (inspiration and main steps of the proposed algorithm) have been modeled in three main principles/cases:

- An adolescent may form his/her own identity by observing and reasoning the behaviors, values, beliefs and attitudes of the society [58].
- Identity may form by imitating a role model, who are perceived as having high status, power, and prestige [59,60].
- The adolescent may adopt negative/undesirable identity option such as smoking, substance use, early sexual behavior and bullying within the group [61].

In this study, optimization based on adolescent behaviors stated above is summarized as follows. Adolescent behavior reaches maturity in most of the healthy individuals due to human intelligence. This behavior shows that the individuals selected in optimization will reach their optimal values after a certain period of time. In addition, it is known that some individuals have better behavior within the framework of community norms. This is considered to be the individual who optimizes the cost function better in optimization. If no adolescent reaches optimal values, this is seen as the failure to solve the optimization problem. This is also a possible situation in optimization and is regarded as possible social problems in the future for the society. Identity search of an adolescent characterized by Marcia's achievement identity status that refers to individuals who have made a commitment after a period of active exploration is mathematically modeled to solve numeric optimization problems as follows.

2.1. Implementation of AISA

Notations: Throughout this subsection, matrices and vectors are denoted by boldface upper case letters and boldface lower case letters, respectively. The superscripts $(\cdot)^{-1}$ and $(\cdot)^T$ denote the inverse and transpose operators, respectively.

Consider that AISA is implemented on an unconstrained single-objective optimization problem defined as

$$\begin{aligned} \min f(x_1, x_2, \dots, x_n) \\ b_j \leq x_j \leq \bar{b}_j, \quad j = 1, 2, \dots, n \end{aligned} \quad (1)$$

where $f(\cdot)$ is an objective function to be minimized, x_j represents the j th decision variable, n denotes the number of decision variables or the dimension of problem, b_j and \bar{b}_j are the lower and upper bounds of j th variable, respectively.

2.1.1. Random initialization

Similar to other population-based optimization algorithms, AISA starts by generating a random initial population within the boundaries of solution space. In other words, an artificial peer group is created. It is assumed that there is N number of adolescents in this group and identity of each adolescent consists of n identity features (number of variables). Furthermore, identity of i th adolescent $\{\mathbf{x}^i\}_{i=1,2,\dots,N}$ can be specified by a vector and it can be obtained as

$$x_j^i = b_j + U(0, 1)_j \times (\bar{b}_j - b_j), \quad i = 1, 2, \dots, N; j = 1, 2, \dots, n \quad (2)$$

where x_j^i represents the j th identity feature of i th adolescent and $U(0, 1)$ is a uniformly distributed random number in the

range $[0, 1]$. A population containing all adolescents with their identities can be represented in the following matrix,

$$\mathbf{X} = \begin{bmatrix} x_1^1 & x_2^1 & \cdots & x_n^1 \\ x_1^2 & x_2^2 & \cdots & x_n^2 \\ \vdots & \vdots & \ddots & \vdots \\ x_1^N & x_2^N & \cdots & x_n^N \end{bmatrix}_{N \times n} \quad (3)$$

where \mathbf{X} is called as population matrix.

2.1.2. Fitness evaluation

The fitness value of each adolescent is calculated by substituting the adolescent identity (values of decision variable) into predefined-fitness function. The calculated fitness values are stored in

$$\mathbf{f}(\mathbf{X}) = \begin{bmatrix} f_1[x_1^1, x_2^1, \dots, x_n^1] \\ f_2[x_1^2, x_2^2, \dots, x_n^2] \\ \vdots \\ f_N[x_1^N, x_2^N, \dots, x_n^N] \end{bmatrix}_{N \times 1} \quad (4)$$

where $\mathbf{f}(\mathbf{X})$ represents fitness vector of current solution population.

2.1.3. Generate new identity

As with many metaheuristic algorithms, the generation of new search agents is performed iteratively until a user-predefined stop criterion is satisfied. In fact, the aim is to evolve solution vectors throughout an iterative process.

As mentioned previously, three behaviors may occur during the identity exploration of adolescents in peer group. It is assumed that each adolescent/individual randomly selects only one of the situations in each iteration, which means that the individual has a dynamic selection strategy founded upon his or her impulses. The identity formation can be mathematically modeled as follows.

Case 1. An adolescent may form his/her own identity by observing and then reasoning the behaviors, values, beliefs and attitudes of peer group. It is assumed that the adolescent may mimic them by identifying the best features (the best hairstyle, the most hardworking, the best football skills and etc.) in the group. Specifically, the best features are here found by a feature selection process using an orthogonal function approximation.

For each iteration, there is constructed an approximate model between the current population vectors and their fitness values. Partially, it can be considered as an online modeling of black box optimization problem. In the approximate model, the identities of the individuals are separately used as model inputs and their fitness values are used as model outputs. After the approximate orthogonal function model estimated, contributions of all identity features expressed as partial fitness values to the objective function are calculated separately. Between the partial fitness values corresponding to any identity feature of all individuals, the best identity feature is selected as a minimal or maximal value according to the minimization or maximization problem. Then, this procedure is applied for all identity features. In the modeling process, the function approximation performance has no direct importance for the feature selection. Instead the main task is here to establish the best identity structure that directs individuals to the local solution of the problem.

In order to construct an approximate model between the individuals and their fitness values, a Chebyshev functional-link network (CFLN) has been used and optimized by Least Squares Estimation (LSE). The CFLN is one of the well-known orthogonal function approximation models which has fast and accurate approximation capability especially for online approximation

problems [62]. Additionally, the CFLN allows to find partial fitness values since final output of model is expressed as linear combination of partial outputs of input variables.

Chebyshev polynomials are very suitable for function approximation since they are orthogonal, have recurrence relations and span a dense set in definition interval $[-1, 1]$ [63]. For $x \in [-1, 1]$, the Chebyshev polynomials $\{T_k(x)\}_{k=0,1,2,\dots}$ are generated via the following recurrence equation,

$$T_k(x) := \begin{cases} 1, & : \text{if } k = 0 \\ x, & : \text{if } k = 1 \\ 2xT_{k-1}(x) - T_{k-2}(x), & : \text{if } k \geq 2 \end{cases} \quad (5)$$

where k is the degree of Chebyshev polynomials.

One of the CFLNs was constructed in [62] and proven effective. In order to find partial fitness value, a CFLN is designed and used with no-intercept term. It is preferred since it does not require an iterative procedure to learn the model with good accuracy and provides the opportunity to find partial fitness value for each input variable. The topology of a proposed orthogonal Chebyshev network is given in Fig. 1 as a multiple-input single-output feedforward network.

The inputs/identities are directly mapped through orthogonal Chebyshev polynomials. Then using the regressor matrix and outputs, the weighting parameters are estimated by LSE. First, input samples (population) for the CFLN model are normalized in $[-1, 1]$ as

$$\hat{x}_j^i = 2 \frac{(x_j^i - b_j)}{(b_j - b_j)} - 1, \quad i = 1, 2, \dots, N; j = 1, 2, \dots, n. \quad (6)$$

where \hat{x}_j^i is normalized value the j th identity feature of i th adolescent. The normalized inputs/identities can be represented by the following matrix,

$$\hat{\mathbf{X}} = \begin{bmatrix} \hat{x}_1^1 & \hat{x}_2^1 & \dots & \hat{x}_n^1 \\ \hat{x}_1^2 & \hat{x}_2^2 & \dots & \hat{x}_n^2 \\ \vdots & \vdots & \ddots & \vdots \\ \hat{x}_1^N & \hat{x}_2^N & \dots & \hat{x}_n^N \end{bmatrix}_{N \times n} \quad (7)$$

where $\hat{\mathbf{X}}$ is the normalized input matrix that is applied to the orthogonal function model. Then, regressor matrix Ψ and sub-regressor vector ψ of each input element are defined as follows.

$$\begin{aligned} \Psi &= \begin{bmatrix} T_1(\hat{x}_1^1) & \dots & T_k(\hat{x}_1^1) & \dots & \dots & T_1(\hat{x}_n^1) & \dots & T_k(\hat{x}_n^1) \\ T_1(\hat{x}_1^2) & \dots & T_k(\hat{x}_1^2) & \dots & \dots & T_1(\hat{x}_n^2) & \dots & T_k(\hat{x}_n^2) \\ \vdots & \ddots & \vdots & \ddots & \ddots & \vdots & \ddots & \vdots \\ T_1(\hat{x}_1^N) & \dots & T_k(\hat{x}_1^N) & \dots & \dots & T_1(\hat{x}_n^N) & \dots & T_k(\hat{x}_n^N) \end{bmatrix}_{N \times (n \times k)} \\ &= \begin{bmatrix} \psi_1^1 & \dots & \dots & \psi_n^1 \\ \psi_1^2 & \dots & \dots & \psi_n^2 \\ \vdots & \ddots & \ddots & \vdots \\ \psi_1^N & \dots & \dots & \psi_n^N \end{bmatrix}. \end{aligned} \quad (8)$$

The weighting factors of the approximate model are estimated using LSE as

$$\begin{aligned} \hat{\mathbf{w}} &= (\Psi^T \Psi)^{-1} \Psi^T \mathbf{f} \\ \hat{\mathbf{w}} &= [w_1^1 \dots w_k^1 \dots \dots w_1^n \dots w_n^n]_{1 \times (n \times k)}^T \\ &= [\mathbf{w}^1 \dots \dots \mathbf{w}^n]^T \end{aligned} \quad (9)$$

where $\mathbf{w}^j \in \mathbb{R}^{1 \times k}$ is the weight vector of j th input.

For each matrix element given in Eq. (7), the partial fitness value is obtained using Eq. (10) and stored as in Eq. (11).

$$\hat{f}_j^i = \psi_j^i \mathbf{w}^i. \quad (10)$$

$$\hat{\mathbf{F}} = \begin{bmatrix} \hat{f}_1^1 & \hat{f}_2^1 & \dots & \hat{f}_n^1 \\ \hat{f}_1^2 & \hat{f}_2^2 & \dots & \hat{f}_n^2 \\ \vdots & \vdots & \ddots & \vdots \\ \hat{f}_1^N & \hat{f}_2^N & \dots & \hat{f}_n^N \end{bmatrix}_{N \times n} \quad (11)$$

Finally, the best identity vector of current population consists of values in the population matrix (\mathbf{X}) given Eq in (3) corresponding to row indices with minimum values in each and every column of matrix in Eq. (11) and it can be found as

$$x_j^* = x_j^{m^i}, \quad m^i = \arg \min_l \left\{ \hat{f}_j^l \mid l = 1, 2, \dots, N \right\}, \quad \forall j \quad (12)$$

For this case, new identity (\mathbf{x}_{new}^i) of the i th adolescent is obtained as

$$\mathbf{x}_{new}^i = \mathbf{x}^i - r_1 (\mathbf{x}^i - \mathbf{x}^*) \quad (13)$$

where r_1 is a random number in the range of $[0, 1]$. \mathbf{x}^* is a set of the best identity features that each adolescent has created so far by observing and then evaluating the peers' identity features. The Eq. (13) represents that adolescent strive to acquire some new identities from its peer group which are approved as good behaviors.

Case 2. Identity may form by imitating a role model, who has high status, power, and prestige. Based on this, a role model can be selected as an individual with the best fitness value in the peer group. In this case, new identity of adolescent can be obtained as

$$\mathbf{x}_{new}^i = \mathbf{x}^i - r_2 (\mathbf{x}^p - \mathbf{x}^{rm}) \quad (14)$$

where r_2 is a random number in the range of $[0, 1]$ and \mathbf{x}^{rm} indicates the role model (best individual). For $p \neq rm$, \mathbf{x}^p is the p th adolescent. Part of the equation, $(\mathbf{x}^p - \mathbf{x}^{rm})$, is used to avoid immature convergence and shares similarity with Symbiotic Organisms Search (SOS) [64].

Case 3. The adolescent may adopt negative/undesirable identity feature such as smoking, substance use, early sexual activity or bullying and so on. It is assumed that the negative/undesirable identity feature (x^u) is a randomly selected element from the population matrix in order for the algorithm to have exploration capability. In this case, new identity of i th adolescent can be obtained as

$$\mathbf{x}_{new}^i = \mathbf{x}^i - r_3 (\mathbf{x}^i - \mathbf{x}^q), \quad (15)$$

where \mathbf{r}_3 is a $1 \times n$ row vector of uniformly distributed numbers in the interval $[0, 1]$. \mathbf{x}^q denotes negative identity vector written as follows.

$$\mathbf{x}^q = [x^u \quad x^u \quad \dots \quad x^u]_{1 \times n}^T. \quad (16)$$

As a result, in the new identity generation phase of the proposed approach, three cases are combined to be used as

$$\mathbf{x}_{new}^i = \begin{cases} \text{Case 1: } \mathbf{x}^i - r_1 (\mathbf{x}^i - \mathbf{x}^*), & r_4 \leq 1/3 \\ \text{Case 2: } \mathbf{x}^i - r_2 (\mathbf{x}^p - \mathbf{x}^{rm}), & 1/3 < r_4 \leq 2/3 \\ \text{Case 3: } \mathbf{x}^i - r_3 (\mathbf{x}^i - \mathbf{x}^q), & 2/3 < r_4 \end{cases} \quad (17)$$

where r_4 is a random number in $[0, 1]$ used as the selection strategy.

The algorithm has been conscientiously designed to possess different search capabilities. The first case serves the exploitation characteristic of the algorithm when \mathbf{x}^* is correctly estimated. Whatever the model's estimated, new solutions are obtained between minimum and maximum values of variables in the current population. In the second case, there is a tendency towards the best solution (the role model) and the focus is on exploitation. In

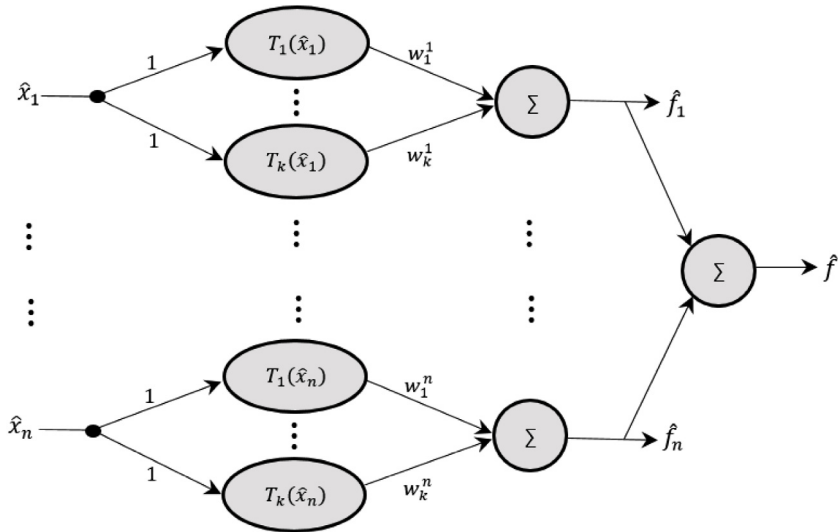


Fig. 1. Topology of a CFLN.

addition, the immature convergence is avoided by \mathbf{x}^p . Therefore, the first two cases have been developed for the exploitation ability of the algorithm. However, the third case brings an exploration capability to get rid of the local minima.

2.1.4. Boundary control mechanism

If a new individual goes beyond given the search space, a boundary control mechanism is activated. In other words, if any of the variables violate its limit range, such variables are randomly located within their limit range, that is, the violators are subjected to Eq. (2). This mechanism is the same as proposed in Backtracking Search Optimization Algorithm (BSA), which is highly effective in achieving population diversity that enables efficient searches in current and future generations [65].

2.1.5. Updating mechanism

The updating mechanism is used to decide whether the new identity is included in the population. Before the updating mechanism is applied, the fitness value of the adolescent's new identity is calculated. Then, if the new identity is better than the current identity, the current one is discarded from the population and also the new one is injected in the population instead. The same procedure is valid for each new identity. Thus, the searchers evolve to use in progressive evaluation. Many metaheuristics use a similar updating mechanism at the end of each iteration. However, AISA uses the updating mechanism at each evaluation. The intention behind this is to improve other solutions by injecting a more qualified solution into the population immediately.

In terms of identity formation process, it is also worth mentioning here that this updating mechanism simulates the reconsideration of commitment that involves comparing present commitment with possible alternative commitment since the current commitment is no longer satisfactory [66].

2.1.6. Stopping/termination criterion

Broadly, optimization algorithms complete the search task using one or a combination of four different stop criteria such as function tolerance, maximum number of function evaluations, maximum run time, and maximum number of iterations. In the present study, by associating adolescence period with the iterative process, the maximum number of iterations is considered as the termination criterion that means the end of puberty. The pseudocode of AISA is depicted in Algorithm 1.

Algorithm 1 Pseudocode for AISA

```

1: Begin:
2: Define input parameters ( $N, k, Max_{iter}$ )
3: Create the initial population  $[\mathbf{X}]_{N \times n}$  using Eq. (2)
4: Evaluate fitness of each adolescent
5: while the stopping criterion is not satisfied do
6:   Form the matrix  $\hat{\mathbf{X}}$  using Eq. (6)
7:   Form the regressor matrix  $\Psi$  and its sub-regressor vectors
    $(\psi^1, \dots, \psi^N)$  using Eq. (8)
8:   Compute the weighting vectors  $(\mathbf{w}^1, \dots, \mathbf{w}^n)$  using Eq. (9)
9:   Form the matrix  $\hat{\mathbf{F}}$  using Eq. (10)
10:  Find the best feature vector  $(\mathbf{x}^*)$  using Eq. (12)
11:  for  $i = 1$  to  $N$  do
12:    Update  $r_4 \sim U(0, 1)$ 
13:    if  $r_4 \leq 1/3$  then
14:      Update  $r_1 \sim U(0, 1)$ 
15:       $\mathbf{x}_{new}^i = \mathbf{x}^i - r_1 (\mathbf{x}^i - \mathbf{x}^*)$ 
16:    else if  $r_4 > 1/3 \wedge r_4 \leq 2/3$  then
17:      Update  $r_2 \sim U(0, 1)$ 
18:      Find the role model/the best solution  $(\mathbf{x}^{rm})$ 
19:      Randomly choose one of the adolescents  $p | p \neq rm$ 
20:       $\mathbf{x}_{new}^i = \mathbf{x}^i - r_2 (\mathbf{x}^p - \mathbf{x}^{rm})$ 
21:    else
22:      Update  $\mathbf{r}_3 \sim U(0, 1)^n$ 
23:      Generate the negative identity vector  $(\mathbf{x}^q)$ 
24:       $\mathbf{x}_{new}^i = \mathbf{x}^i - \mathbf{r}_3 (\mathbf{x}^i - \mathbf{x}^q)$ 
25:    end if
26:    Apply the boundary control mechanism
27:    Apply the updating mechanism
28:  end for
29: end while
30: Return the best optimal solution
31: End
```

3. Comparative analysis of AISA with other metaheuristics

The nature-inspired optimization algorithms are dramatically increasing in the optimization literature. Some studies have discussed that there is a critical doubt about the supposedly novel algorithms apparently similar to core ones [67–70]. One of the comprehensive comparisons stated that many modern metaheuristics could be considered to be versions of the same classical/core

algorithms such as GA, ACO, PSO, DE and ABC [69]. In addition, another one compared by subdividing the algorithms into two categories: procedure-based and equation-based [71]. Unlike many abstract comparisons, equation-based algorithms were mathematically compared and made a more perceptible comparison. Since AISA is an equation-based algorithm, it is compared with DE, PSO and ABC in terms of their search mechanisms and mathematical foundations.

Generally, equation-based metaheuristic optimizers use vector linear combination like gradient-based algorithms and their iterative update equations can be given as follows:

$$\mathbf{x}_i^{t+1} = \mathbf{x}_i^t + \Delta\mathbf{x}_i^t \quad (18)$$

where \mathbf{x}_i^t , \mathbf{x}_i^{t+1} and $\Delta\mathbf{x}_i^t$ indicate current solution, new solution and search (modification increment/mutation) vectors, respectively.

Now let us describe the updating equations of solutions in four algorithms such as DE, PSO, ABC and AISA.

- Differential Evolution (DE) [8]: The main mutation equation of DE can be expressed as

$$\mathbf{x}_i^{t+1} = \mathbf{x}_i^t + F(\mathbf{x}_j^t - \mathbf{x}_k^t) \quad (19)$$

which can be written as

$$\mathbf{x}_i^{t+1} = \mathbf{x}_i^t + \Delta\mathbf{x}_i^t, \quad \Delta\mathbf{x}_i^t = F(\mathbf{x}_j^t - \mathbf{x}_k^t) \quad (20)$$

where \mathbf{x}_i^t , \mathbf{x}_j^t and \mathbf{x}_k^t are three distinct solution vectors selected from the population. The scaling factor $F \in (0, 2)$ is a control parameter. After mutation operation, crossover operation is performed between the target vector and the mutant vector.

- Particle Swarm Optimization (PSO) [12]: The velocity v_i^t and position \mathbf{x}_i^t of i th particle at iteration t can be updated iteratively using

$$\mathbf{v}_i^{t+1} = \mathbf{v}_i^t + \Delta\mathbf{v}_i^t \quad (21)$$

$$\mathbf{x}_i^{t+1} = \mathbf{x}_i^t + \Delta\mathbf{x}_i^t \quad (22)$$

with

$$\Delta\mathbf{x}_i^t = \mathbf{v}_i^{t+1} = \mathbf{v}_i^t + \Delta\mathbf{v}_i^t \quad (23)$$

and

$$\Delta\mathbf{v}_i^t = c_1 r_1 (\mathbf{x}_{\text{Best}}^t - \mathbf{x}_i^t) + c_2 r_2 (\mathbf{g}_{\text{Best}}^t - \mathbf{x}_i^t) \quad (24)$$

where $\mathbf{x}_{\text{Best}}^t$ and $\mathbf{g}_{\text{Best}}^t$ denote the best particle position and best group position so far in all generations, r_1 and r_2 are independent uniform random numbers between 0 and 1. The parameters c_1 and c_2 are acceleration constants.

- Artificial Bee Colony (ABC) [14]: ABC consists of cascaded three phases such as employed bee, onlooker bee and scout bee. The movement of employed bees towards new food sources is realized by

$$\mathbf{x}_{ij}^{t+1} = \mathbf{x}_{ij}^t + \phi_{ij}(\mathbf{x}_{ij}^t - \mathbf{x}_{kj}^t) \quad (25)$$

which can be written as

$$\mathbf{x}_{ij}^{t+1} = \mathbf{x}_{ij}^t + \Delta\mathbf{x}_{ij}^t, \quad \Delta\mathbf{x}_{ij}^t = \phi_{ij}(\mathbf{x}_{ij}^t - \mathbf{x}_{kj}^t) \quad (26)$$

where k and j are randomly selected indices provided $k \neq i$. The ϕ_{ij} is a random value ranging in $[-1, 1]$. The movement equation of onlooker bees is the same as Eq. (25) but uses probabilistic information calculated from roulette wheel method. Moreover, a scout bee phase controlled by the predefined *Limit* is employed to diversify the population [14].

- Adolescent Identity Search Algorithm (AISA): The solution vectors of AISA can be updated iteratively using

$$\mathbf{x}_i^{t+1} = \mathbf{x}_i^t + \Delta\mathbf{x}_i^t \quad (27)$$

and

$$\Delta\mathbf{x}_i^t = \begin{cases} r_1 (\mathbf{x}_*^t - \mathbf{x}_i^t), & r_4 \leq 1/3 \\ r_2 (\mathbf{x}_{rm}^t - \mathbf{x}_p^t), & 1/3 < r_4 \leq 2/3 \\ r_3 (\mathbf{x}_q^t - \mathbf{x}_i^t), & 2/3 < r_4 \end{cases} \quad (28)$$

where r_1 , r_2 and r_4 are uniformly distributed random number in $[0, 1]$, r_3 is a vector of uniformly distributed numbers in the interval $[0, 1]$. \mathbf{x}_{rm}^t denotes the global best solution/role model, \mathbf{x}_p^t is randomly selected solution from population provided $rm \neq p$. \mathbf{x}_*^t and \mathbf{x}_q^t are two vectors that differ from solution vectors in the population.

3.1. AISA versus comparative algorithms

Metaheuristics are generally differentiated in relation to their solution updating strategies. AISA differs from the aforementioned algorithms from the following aspects:

- Although there are seemingly similar expression of \mathbf{x}_i^{t+1} in Eqs. (20), (22), (26) and (27), the expression of $\Delta\mathbf{x}_i^t$ is mathematically different in AISA.
- Many metaheuristic optimizers use the global best solution to generate new search agents in their exploitation processes; however, AISA uses a guide vector (\mathbf{x}_*^t) found by a feature selection process using an orthogonal function approximation that is a very distinguishing and unique property of AISA.
- AISA and PSO uses the global best solution. In PSO, new position of i th particle is governed by $\mathbf{x}_{\text{Best}}^t$ and $\mathbf{g}_{\text{Best}}^t$ that cumulative effect of both is considered. However, AISA is updated using \mathbf{x}_{rm}^t and another solution vector (\mathbf{x}_p^t).
- In exploration strategy of AISA, there is a tendency towards vector \mathbf{x}_q^t by using random vector r_3 while most of the algorithms randomly reinitialize the solutions.
- DE are mutated using only solution vectors in population; however, AISA are updated using two vectors that differ from solution vectors in the population. Moreover, DE uses a crossover strategy though it is not used in AISA.
- In ABC, solution matrix is divided into two regions for employed bees and onlooker bees in contrast to AISA. Moreover, ABC consists of cascaded three phases such as employed bee, onlooker bee and scout bee. However, AISA has three mechanisms (phases) manipulated by a random selection strategy.
- The boundary control mechanism of AISA is different from those of DE, PSO and ABC.

4. Experimental studies

This section first introduces benchmark test problems and a brief description of state-of-the-art metaheuristic algorithms used to compare with the proposed algorithm. Thereafter, the numerical experimental results are presented and analyzed in detail.

4.1. Benchmark test functions

In order to demonstrate its applicability and efficiency, the proposed methodology is tested on a set of thirty-nine benchmark functions listed in Tables 1–5 where n indicates the dimension of the function, *Range* denotes the function's search

Table 1
Unimodal benchmark functions.

Function	n	Range	F_{min}
$F_1(x) = \sum_{i=1}^n x_i^2$	10, 30, 50	$[-100, 100]^n$	0
$F_2(x) = \sum_{i=1}^n x_i + \prod_{i=1}^n x_i $	10, 30, 50	$[-10, 10]^n$	0
$F_3(x) = \sum_{i=1}^n \left(\sum_{j=1}^i x_j \right)^2$	10, 30, 50	$[-100, 100]^n$	0
$F_4(x) = \max_i \{ x_i , 1 \leq i \leq n \}$	10, 30, 50	$[-100, 100]^n$	0
$F_5(x) = \sum_{i=1}^{n-1} \left[100(x_{i+1} - x_i^2)^2 + (x_i - 1)^2 \right]$	10, 30, 50	$[-30, 30]^n$	0
$F_6(x) = \sum_{i=1}^n (x_i + 0.5)^2$	10, 30, 50	$[-100, 100]^n$	0
$F_7(x) = \sum_{i=1}^n i x_i^4 + \text{random}[0, 1)$	10, 30, 50	$[-1.28, 1.28]^n$	0

space, and F_{min} states the optimum value of minimization function. These benchmark functions can be organized into five categories according to their characteristic: unimodal, multimodal, fixed-dimension multimodal, composite and CEC 2019 benchmark functions.

The first category is unimodal test beds which consists of seven functions (F_1 – F_7) described in Table 1 and illustrated in 2-D contour plots in Fig. 2. These functions are perfectly suited for benchmarking the exploitation and convergence speed of algorithms since they have only one global optimum and wide search space.

The second category is multimodal test beds which consists of six functions (F_8 – F_{13}) described in Table 2 and illustrated in 2-D contour plots in Fig. 3. These functions have multiple local optima that are extremely eligible to examine the performance of an algorithm in terms of local optima avoidance and exploration.

The third category is fixed-dimension multimodal test beds which consists of ten functions (F_{14} – F_{23}) described in Table 3 (more detailed descriptions of constant parameters used can be seen in [33]) and illustrated in 2-D contour plots in Fig. 4. These functions include many local optima and a single global optima like multimodal functions. Therefore, they are suitable for benchmarking the exploration capacity of an algorithm.

Table 2
Multimodal benchmark functions.

Function	n	Range	F_{min}
$F_8(x) = \sum_{i=1}^n -x_i \sin(\sqrt{ x_i })$	10, 30, 50	$[-500, 500]^n$	$-418.9829 \times n$
$F_9(x) = \sum_{i=1}^n [x_i^2 - 10 \cos(2\pi x_i) + 10]$	10, 30, 50	$[-5.12, 5.12]^n$	0
$F_{10}(x) = -20 \exp \left(-0.2 \sqrt{\frac{1}{n} \sum_{i=1}^n x_i^2} \right) - \exp \left(\frac{1}{n} \sum_{i=1}^n \cos(2\pi x_i) \right) + 20 + e$	10, 30, 50	$[-32, 32]^n$	0
$F_{11}(x) = \frac{1}{4000} \sum_{i=1}^n x_i^2 - \prod_{i=1}^n \cos \left(\frac{x_i}{\sqrt{i}} \right) + 1$	10, 30, 50	$[-600, 600]^n$	0
$F_{12}(x) = \frac{\pi}{n} \left\{ \sin(\pi y_1) + \sum_{i=1}^{n-1} (y_i - 1)^2 [1 + \sin^2(\pi y_{i+1})] + (y_n - 1)^2 \right\} + \sum_{i=1}^n u(x_i, 10, 100, 4)$	10, 30, 50	$[-50, 50]^n$	0
$F_{13}(x) = 0.1 \left\{ \sin^2(3\pi y_1) + \sum_{i=1}^n (x_i - 1)^2 [1 + \sin^2(3\pi y_i + 1)] + (x_n - 1)^2 [1 + \sin^2(2\pi x_n + 1)] \right\} + \sum_{i=1}^n u(x_i, 5, 100, 4)$	10, 30, 50	$[-50, 50]^n$	0

The fourth category comprises six test functions (F_{24} – F_{29}) chosen from a CEC 2005 special session [72]. These benchmark functions, which are the shifted, rotated, expanded, and combined versions of some classical functions, are constructed to provide more challenging problems. Essentially, the classical/individual functions that compose each composite function are shifted randomly, stretched/compressed, rotated by their orthogonal rotation matrices calculated using Salmon's method [73], and combined using the Gaussian functions controlled by their coverage range. The functions are depicted in Table 4. It is also worth mentioning here that f_1, f_2, \dots, f_{10} indicate the individual functions used for composition. σ and λ indicate the coverage range and the stretch ($\lambda > 1$) or compression ($\lambda < 1$) factor of each individual function, respectively. Moreover, Fig. 5 shows the 2-D contour plots for each composite test function considered in this study. The reader can refer to [72] for detailed information about these functions and downloaded their Matlab codes from the following link: <http://www.ntu.edu.sg/home/epnsugan/>.

The fifth category consists of ten modern CEC 2019 benchmark beds known as “The 100-Digit Challenge”. These single objective benchmark beds are well-suited for benchmarking since they have a substantially complex structure including different properties such as multimodal and non-separable. In order to save space here these functions (F_{30} – F_{39}) are simply described in Table 5. Their mathematical formulation and characteristics are described in detail in [74]. The last seven functions illustrated in 2-D contour plots in Fig. 6 are shifted and rotated versions of basic functions, while others are not rotated due to their fully parameter dependent and not defined for 2 dimensions.

4.2. State-of-the-art metaheuristic algorithms for comparison

To verify the performance of the proposed algorithm, the thirteen well-regarded optimization algorithms are used for comparison. As detailed information can be obtained from the literature, a brief description of the competitor algorithms is presented in the discussion below. Furthermore, the links for the codes of algorithms implemented in this study are provided in Appendix.

- *Particle Swarm Optimization (PSO)* [12]: Particle Swarm Optimization (PSO) is a very popular population-based stochastic optimization algorithm proposed by Kennedy and Eberhart. It is inspired by social behavior of fish schooling or bird flocking. Each particle can update its current position within the boundaries of the search space in relation to three factors: (i) the best solution obtained so far by the particle (self

Table 3
Fixed-dimension multimodal benchmark functions.

Function	n	Range	F_{min}
$F_{14}(x) = \left(\frac{1}{500} + \sum_{j=1}^{25} \frac{1}{j + \sum_{i=1}^2 (x_i - a_{ij})^6} \right)^{-1}$	2	$[-65.536, 65.536]^n$	0.998
$F_{15}(x) = \sum_{i=1}^{11} \left[a_i - \frac{x_1 (b_i^2 + b_i x_2)}{b_i^2 + b_i x_3 + x_4} \right]^2$	4	$[-5, 5]^n$	0.00030
$F_{16}(x) = 4x_1^2 - 2.1x_1^4 + \frac{1}{3}x_1^6 + x_1 x_2 - 4x_2^2 + 4x_2^4$	2	$[-5, 5]^n$	-1.0316
$F_{17}(x) = \left(x_2 - \frac{5.1}{4\pi^2} x_1^2 + \frac{5}{\pi} x_1 - 6 \right)^2 + 10 \left(1 - \frac{1}{8\pi} \right) \cos(x_1) + 10$	2	$[-5, 5]^n$	0.398
$F_{18}(x) = [1 + (x_1 + x_2 + 1)^2 (19 - 14x_1 + 3x_1^2 - 14x_2 + 6x_1 x_2 + 3x_2^2)] \times [30 + (2x_1 - 3x_2)^2 \times (18 - 32x_1 + 12x_1^2 + 48x_2 - 36x_1 x_2 + 27x_2^2)]$	2	$[-2, 2]^n$	3
$F_{19}(x) = - \sum_{i=1}^4 c_i \exp \left(- \sum_{j=1}^3 a_{ij} (x_j - p_{ij})^2 \right)$	3	$[1, 3]^n$	-3.86
$F_{20}(x) = - \sum_{i=1}^4 c_i \exp \left(- \sum_{j=1}^6 a_{ij} (x_j - p_{ij})^2 \right)$	6	$[0, 1]^n$	-3.32
$F_{21}(x) = - \sum_{i=1}^5 [(X - a_i)(X - a_i)^T + c_i]^{-1}$	4	$[0, 10]^n$	-10.1532
$F_{22}(x) = - \sum_{i=1}^7 [(X - a_i)(X - a_i)^T + c_i]^{-1}$	4	$[0, 10]^n$	-10.4028
$F_{23}(x) = - \sum_{i=1}^{10} [(X - a_i)(X - a_i)^T + c_i]^{-1}$	4	$[0, 10]^n$	-10.5363

Table 4
Composite benchmark functions.

Function	n	Range	F_{min}
$F_{24}(CF_1)$:			
$f_1, f_2, f_3, \dots, f_{10}$ = Sphere function			
$[\sigma_1, \sigma_2, \sigma_3, \dots, \sigma_{10}] = [1, 1, 1, \dots, 1]$	10	$[-5, 5]^n$	0
$[\lambda_1, \lambda_2, \lambda_3, \dots, \lambda_{10}] = [5/100, 5/100, 5/100, \dots, 5/100]$			
$F_{25}(CF_2)$:			
$f_1, f_2, f_3, \dots, f_{10}$ = Griewank's function			
$[\sigma_1, \sigma_2, \sigma_3, \dots, \sigma_{10}] = [1, 1, 1, \dots, 1]$	10	$[-5, 5]^n$	0
$[\lambda_1, \lambda_2, \lambda_3, \dots, \lambda_{10}] = [5/100, 5/100, 5/100, \dots, 5/100]$			
$F_{26}(CF_3)$:			
$f_1, f_2, f_3, \dots, f_{10}$ = Griewank's function			
$[\sigma_1, \sigma_2, \sigma_3, \dots, \sigma_{10}] = [1, 1, 1, \dots, 1]$	10	$[-5, 5]^n$	0
$[\lambda_1, \lambda_2, \lambda_3, \dots, \lambda_{10}] = [1, 1, 1, \dots, 1]$			
$F_{27}(CF_4)$:			
f_1, f_2 = Ackley's function			
f_3, f_4 = Rastrigin's function			
f_5, f_6 = Weierstrass's function	10	$[-5, 5]^n$	0
f_7, f_8 = Griewank's function			
f_9, f_{10} = Sphere function			
$[\sigma_1, \sigma_2, \sigma_3, \dots, \sigma_{10}] = [1, 1, 1, \dots, 1]$			
$[\lambda_1, \lambda_2, \lambda_3, \dots, \lambda_{10}] = [5/32, 5/32, 1, 1, 5/0.5, 5/0.5, 5/100, 5/100, 5/100, 5/100]$			
$F_{28}(CF_5)$:			
f_1, f_2 = Rastrigin's function			
f_3, f_4 = Weierstrass's function			
f_5, f_6 = Griewank's function	10	$[-5, 5]^n$	0
f_7, f_8 = Ackley's function			
f_9, f_{10} = Sphere function			
$[\sigma_1, \sigma_2, \sigma_3, \dots, \sigma_{10}] = [1, 1, 1, \dots, 1]$			
$[\lambda_1, \lambda_2, \lambda_3, \dots, \lambda_{10}] = [1/5, 1/5, 5/0.5, 5/0.5, 5/100, 5/100, 5/32, 5/32, 5/100, 5/100]$			
$F_{29}(CF_6)$:			
f_1, f_2 = Rastrigin's function			
f_3, f_4 = Weierstrass's function			
f_5, f_6 = Griewank's function			
f_7, f_8 = Ackley's function	10	$[-5, 5]^n$	0
f_9, f_{10} = Sphere function			
$[\sigma_1, \sigma_2, \sigma_3, \dots, \sigma_{10}] = [0.1, 0.2, 0.3, 0.4, 0.5, 0.6, 0.7, 0.8, 0.9, 1]$			
$[\lambda_1, \lambda_2, \lambda_3, \dots, \lambda_{10}] = [0.1*1/5, 0.2*1/5, 0.3*5/0.5, 0.4*5/0.5, 0.5*5/100, 0.6*5/100, 0.7*5/32, 0.8*5/32, 0.9*5/100, 1*5/100]$			

Note: Sphere function, Rastrigin's function, Ackley's function and Griewank's function are sequentially $F_1(x)$, $F_9(x)$, $F_{10}(x)$ and $F_{11}(x)$ as presented in the Tables 1 and 2 ($n = 10$). Interested reader can see this technical report [72] for mathematical formulation of Weierstrass's function.

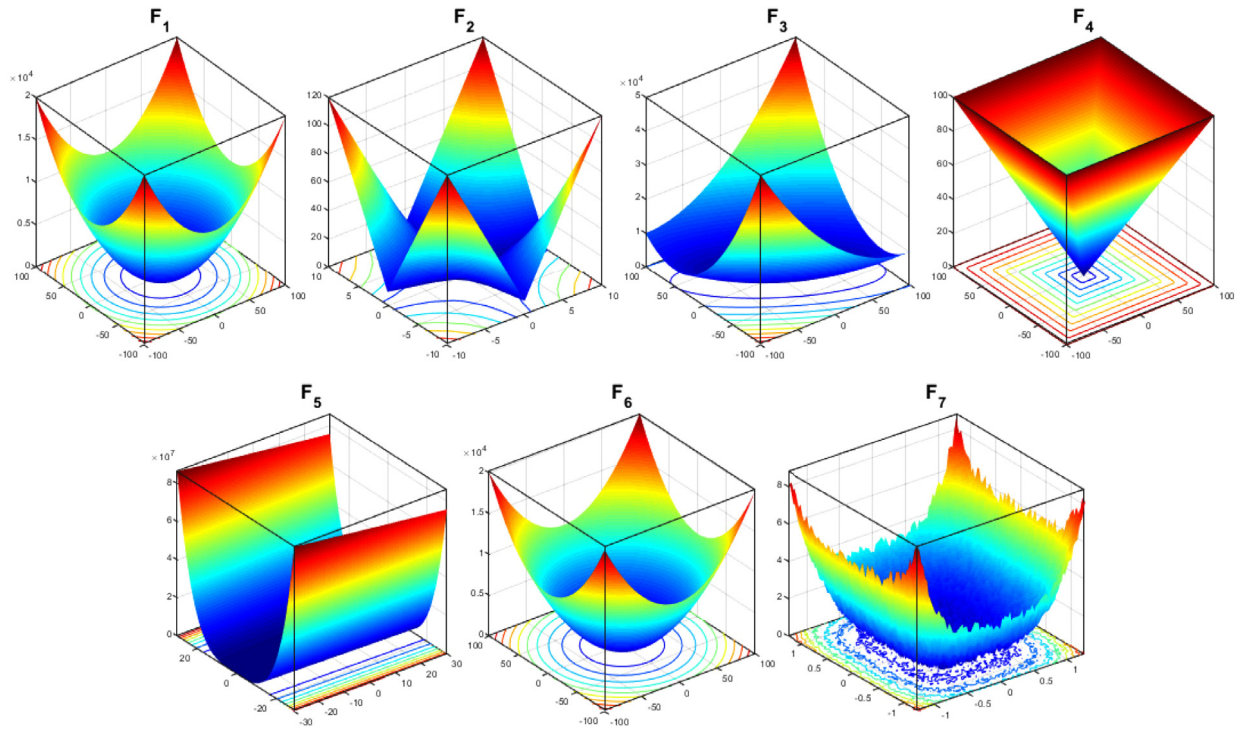


Fig. 2. 2-D contour plots of unimodal benchmark functions.

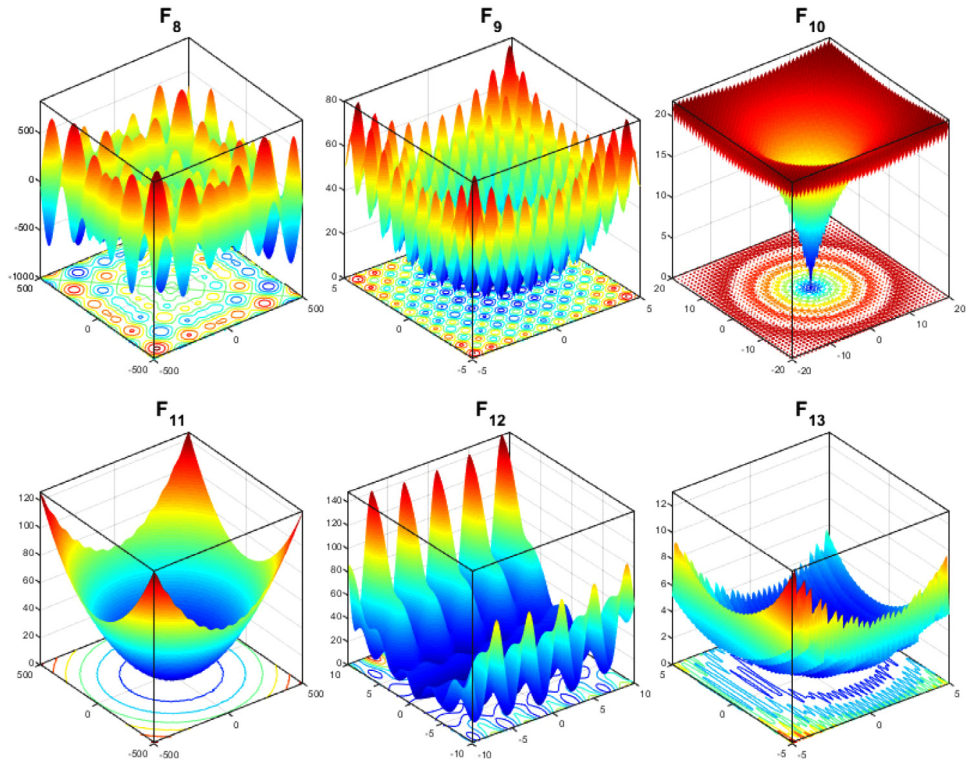


Fig. 3. 2-D contour plots of multimodal benchmark functions.

adjustment), (ii) the best solution obtained by the swarm (social adjustment), and (iii) the velocity of the particle in the previous iteration (inertia adjustment).

- **Artificial Bee Colony (ABC)** [14]: Artificial Bee Colony (ABC) is also another population-based stochastic optimization

algorithm proposed by Karaboga and Basturk. It mimics the foraging behavior of a swarm of bees. Artificial bee colony consists of three types of bees: (i) employed bees, who go to food sources previously visited by themselves, come back to the hive to share the nectar information of the sources

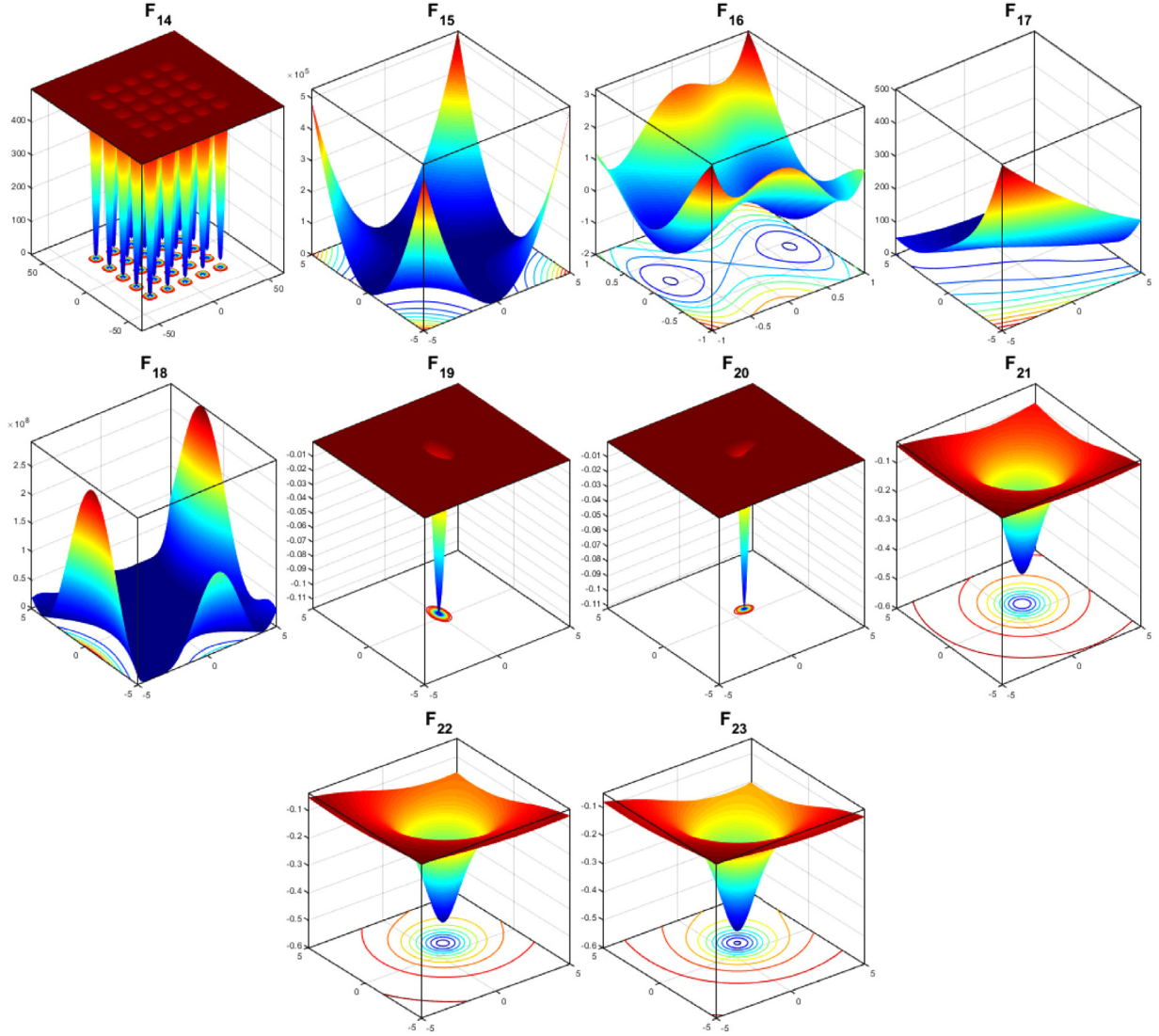


Fig. 4. 2-D contour plots of fixed-dimension multimodal benchmark functions.

with the bees waiting in the dance area, (ii) onlookers, who probabilistically chose food sources depending on information obtained by watching the dancing of employed bees, and (iii) the scouts, who consist of employed bees whose food source has been abandoned, and who are responsible for searching new food sources. This algorithm has been successfully applied to solve many optimization problems, as it is based on a concept that attempts to balance the exploration (carried out by employed bees and onlookers) and exploitation processes (carried out by the scouts).

- **Gravitational Search Algorithm (GSA)** [33]: Gravitational Search Algorithm (GSA) is a nature inspired algorithm developed by Rashedi et al. [33] which is based on the Newtonian gravity and law of motion. In GSA, each mass has four parameters, namely: position, inertial mass, active gravitational mass, and passive gravitational mass. Researchers have successfully applied the GSA algorithm/hybridized versions for solving various optimization problems due to its ability to find global optimum.
- **Bat Algorithm (BA)** [18]: The Bat Algorithm (BA) is a population-based metaheuristic optimization algorithm proposed by Yang. It is inspired by the echolocation behavior

of bats. Bats use natural sonar signals in order to navigate and prey. The BA algorithm has been designed and modeled mathematically based on the behavior of bats in chasing prey. Bats during chasing prey are in tendency to decrease the loudness and increase the rate of pulse emission. Further, to evaluate the performance of BA algorithm, it was tested on classical well-known test functions.

- **Gray Wolf Optimizer (GWO)** [4]: Gray Wolf Optimizer (GWO) is one of the most popular swarm intelligence techniques proposed by Mirjalili et al. [4]. Inspired by the behaviors of gray wolves in nature, GWO imitates the leadership hierarchy and hunting mechanism of gray wolves. This algorithm employs four type of gray wolves such as alpha, beta, delta, and omega to simulate the leadership hierarchy as well as the hunting, searching, encircling, and attacking mechanisms. This algorithm was applied on well-known test functions and real-life constrained optimization problems.
- **Moth-Flame Optimization (MFO)** [51]: Moth-Flame Optimization (MFO) is a recently developed nature-inspired based optimization algorithm proposed by Mirjalili. It is inspired by the navigation method of moths in nature called transverse orientation. In MFO, two main components are moths

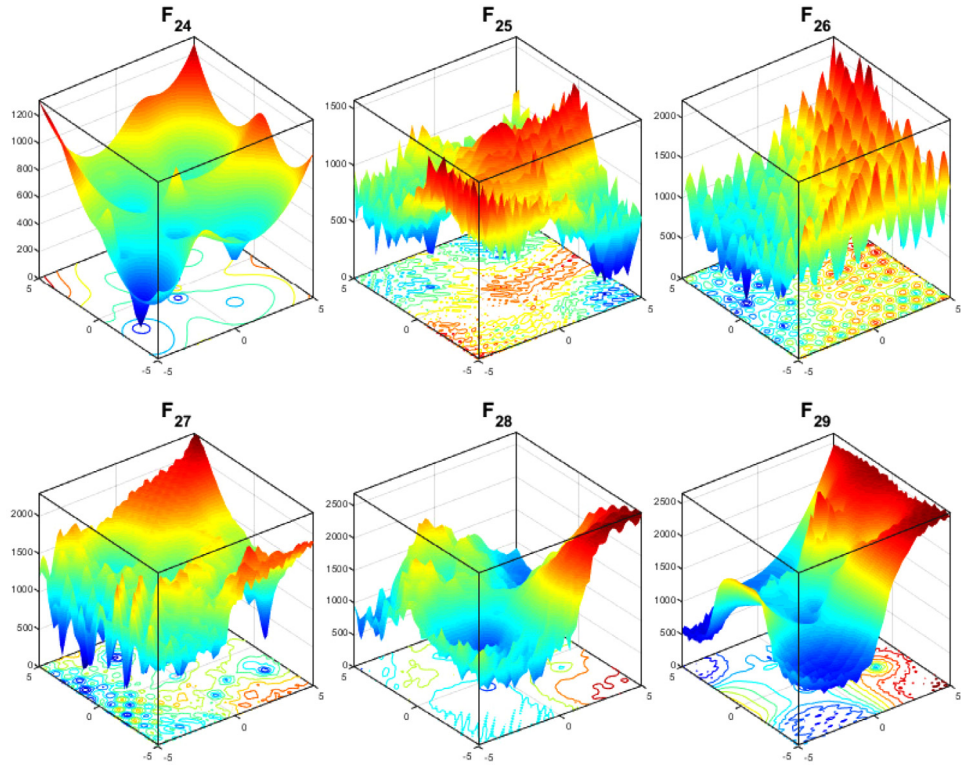


Fig. 5. 2-D contour plots of composite benchmark functions.

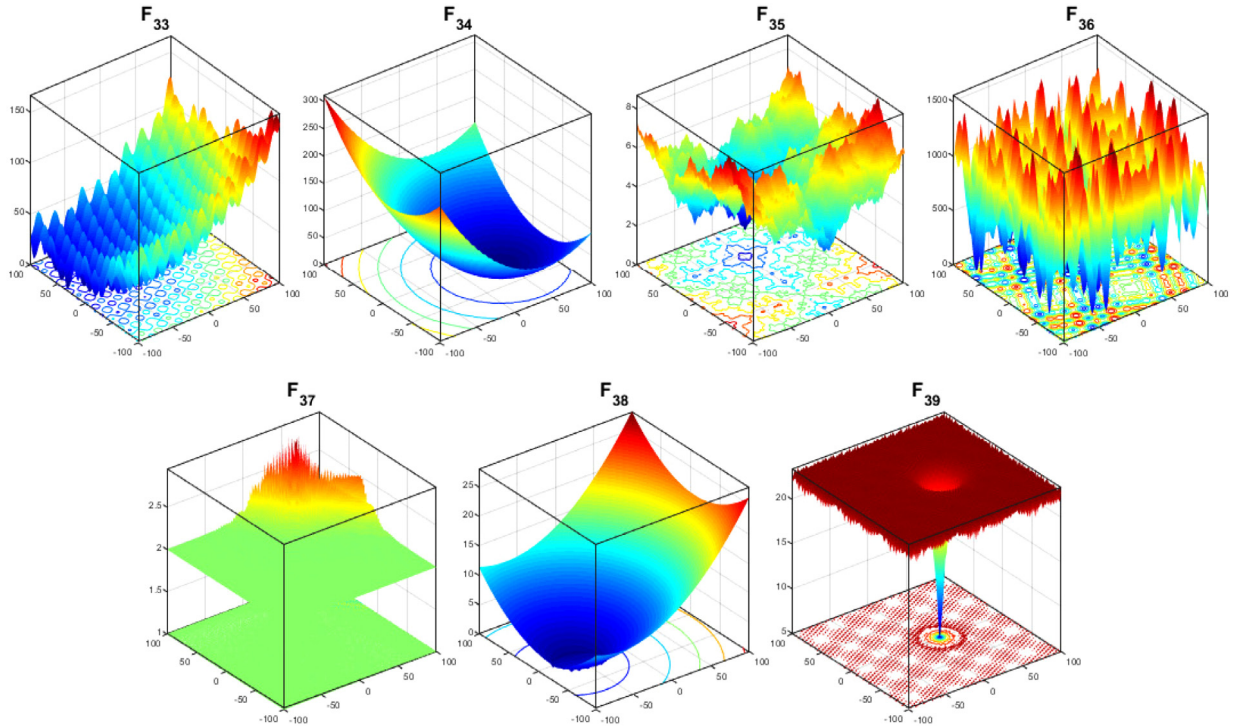


Fig. 6. 2-D contour plots of the last seven CEC 2019 benchmark functions.

and flames which are used to represent solutions. The moths are identified as actual search agents to find optimal solutions in the search space, while flames indicate the best positions of the moths obtained so far. The MFO possesses both local and global search capabilities, and also has

been proven its effectiveness in dealing with challenging optimization problems.

- **Vortex Search Algorithm (VS)** [40]: Vortex Search (VS) algorithm is a single-solution based metaheuristic algorithm proposed by Doğan and Ölmez for solving numerical

Table 5
CEC 2019 benchmark functions.

Function	<i>n</i>	Range	F_{min}
F_{30} (CEC01_2019) : Storn's Chebyshev polynomial fitting problem	9	$[-8192, 8192]^n$	1
F_{31} (CEC02_2019) : Inverse Hilbert matrix problem	16	$[-16384, 16384]^n$	1
F_{32} (CEC03_2019) : Lennard-Jones minimum energy cluster	18	$[-4, 4]^n$	1
F_{33} (CEC04_2019) : Rastrigin's function ($F_9(x)$)	10	$[-100, 100]^n$	1
F_{34} (CEC05_2019) : Griewank's function ($F_{11}(x)$)	10	$[-100, 100]^n$	1
F_{35} (CEC06_2019) : Weierstrass function	10	$[-100, 100]^n$	1
F_{36} (CEC07_2019) : Modified Schwefel's function	10	$[-100, 100]^n$	1
F_{37} (CEC08_2019) : Expanded Schaffer's F6 function	10	$[-100, 100]^n$	1
F_{38} (CEC09_2019) : Happy Cat function	10	$[-100, 100]^n$	1
F_{39} (CEC10_2019) : Ackley function ($F_{10}(x)$)	10	$[-100, 100]^n$	1

Interested reader can see this technical report [74] for more detailed information about these functions.

optimization problems which is inspired from the vortex pattern formed by the vortical flow of the stirred fluids. VS has a poor memory, and also a good balance between the exploration and exploitation by using an adaptive step size adjustment strategy.

- **Jaya Algorithm (JA)** [75]: Jaya Algorithm (JA) is a population-based metaheuristic algorithm developed by Rao. This algorithm is based on the hypothesis that each search candidate should move towards the best solution and away from the worst solution. In contrast to many metaheuristic algorithms, JA does not require any algorithm-specific parameters except for only common control parameters such as population size and number of maximum iteration. The reason behind the popularity of this algorithm overcomes the challenges of tuning and selecting the proper algorithm parameters.
- **Sine Cosine Algorithm (SCA)** [76]: Sine Cosine Algorithm (SCA), proposed by Mirjalili in 2016, is a promising population based stochastic optimization algorithm developed using a mathematical model based on sine and cosine functions. The SCA generates randomly the search agents, and then regenerates them within the boundary of the solution space by using the oscillations of the sine and cosine waves around the destination point (the best solution/agent obtained so far). The random and adaptive parameters used in the algorithm have an important role due to provide diversification and intensification.
- **Salp Swarm Algorithm (SSA)** [26]: Salp Swarm Algorithm/Optimizer (SSA) is a swarm-based metaheuristic technique recently proposed by Mirjalili et al. for solving single and multiple objectives optimization problems. It mimics the swarming behavior of salps during navigating and foraging in deep oceans. Salps form a swarm called salp chain that assists to achieve better locomotion during the foraging. The salp chain mechanism has been modeled mathematically by dividing the population into two groups: (i) leader, who is at the front of the chain and guides swarm, and (ii) followers, who are the rest of salps and follow each other. SSA exhibits high performance success in the solution of optimization problems with high dimensional and different characteristics.

• **Tree-seed Algorithm (TSA)** [77]: Tree-seed Algorithm (TSA) is a new and promising population-based metaheuristic algorithm proposed by Kiran for solving continuous optimization problems. It imitates the relationship between trees and their seeds. The TSA is smartly designed on two mechanisms manipulated by search tendency (ST) parameter. These mechanisms provide to balance exploitation and exploration capabilities of the TSA. Generally, this algorithm possesses efficient global search capability, simple implementation and computation time efficiency.

- **Differential Evolution (DE)** [8]: Differential Evolution (DE), proposed by Storn and Price in 1997, has an important place in evolutionary stochastic techniques due to its simple structure, easy implementation and effectiveness in dealing with challenging optimization problems. Initially, individuals represented by vectors in the population are randomly formed and then evolved iteratively using three main evolutionary operators of mutation, crossover and selection. It is also worth noting that there exist many DE variants with different mutation strategies to solve numerous real-life problems [78].
- **Evolution Strategy (ES)** [9,79]: Evolution Strategy (ES) is one of the most popular and versatile evolutionary algorithms. ES has a search paradigm inspired by natural evolution. It uses mutation, recombination, and selection operators for solving continuous or discrete optimization problems. The different variants of ES are defined by the abbreviations such as $(\mu + \lambda)$ -ES, (μ, λ) -ES where μ represents the number of parents, and λ represents the number of offspring.

4.3. Experimental setup

The experimentation has been performed on Matlab R2018(a) platform in the environment of Microsoft Windows 10 using 64 bit Core i-7 processor with 2.30 GHz and 8 GB main memory.

For the fair comparison of the proposed AISA algorithm with well-known and recent metaheuristic algorithms, the maximum number of function evaluations for all algorithms are set to $n \times 10,000$, which varies depending on the dimension of the problem (n). In addition, the control parameters of PSO are set as recommended in [80], the parameters of DE and ES are same with those set in [11], while others are same with specified/recommended setting in their original papers or codes available in Appendix. The used parameters of all algorithms are also tabulated in Table 6. The number of independent algorithmic runs are equal to 30 that have been utilized to generate the statistical results.

4.4. Performance comparison

In order to demonstrate the effectiveness of proposed algorithm, it is compared with thirteen well-known optimization algorithms on unimodal, multimodal, fixed-dimension multimodal, composite and CEC2019 benchmark functions. Moreover, a scalability study is performed on a set of 10-, 30- and 50-dimensional versions of the unimodal and multimodal functions to examine the impact of dimension on the results of AISA. For the quantitative comparison of algorithms, different performance indicators are utilized that are the best (Best), mean (Mean) and standard deviation (Std) of the solutions obtained over 30 independent runs.

4.4.1. Evaluation of 10-, 30- and 50-dimensional unimodal test functions F_1 – F_7

The unimodal test functions F_1 – F_7 are used to evaluate the exploitation capability of the metaheuristic algorithms. Tables 7–9 depict the performance of aforementioned algorithms on 10-,

Table 6

Initial values for the controlling parameters of algorithms.

Algorithm	Parameters	Values
AISA	Population size	30
	Number of Chebyshev polynomials (k)	3
PSO	Population size	30
	Cognitive and social constants	2, 2
	Inertial weight	[0.9 0.4]
ABC	Population size	40
	Number of food sources	Size of colony/2
	Limit	100
GSA	Population size	50
	Rnorm, Rpower, alpha, and G_0	2, 1, 20, 100
BA	Population size	20
	Loudness (A), pulse rate (r)	0.5, 0.5
	Frequency min and max	0, 2
GWO	Population size	30
	Control parameter (a)	[2 0]
MFO	Population size	30
	Convergence constant (r)	[-1 -2]
	Spiral factor (b)	1
VS	Number of neighborhood solutions	50
	Integration limit (x)	0.1
JA	Population size	25
SCA	Population size	30
	Parameter a	2
SSA	Population size	30
	Parameter c_1	[2 0]
TSA	Population size	20
	Search tendency (ST)	0.1
	Number of seeds	10%-25% of the number of trees
DE	Population size	50
	Scheme	DE/rand/1
	Scaling factor	0.5
ES	Crossover probability	0.5
	Population size	50
	Strategy	($\mu + \lambda$)
	λ	10
	σ	1

30- and 50-dimensional unimodal test functions, respectively. As per the results in these tables, AISA can obtain the best results on F_1, F_2, F_3, F_4, F_6 and F_7 functions with different dimensions. Moreover, AISA is considerably better than other competitors on F_2, F_3, F_4 and F_7 functions in all cases. The results reveal that proposed algorithm is very competitive as compared with other competitor algorithms and it has merit in terms of exploitation.

4.4.2. Evaluation of 10-, 30- and 50-dimensional multimodal test functions F_8 - F_{13}

In contrast to the unimodal functions, multimodal functions have many local optima whose number increases exponentially with dimension. Therefore, they are able to assess exploration ability of an algorithm. The results of the algorithms on 10-, 30- and 50-dimensional multimodal test functions are presented in Tables 10–12, respectively. These results show that the AISA has the first overall rank in solving 10-, 30- and 50-dimensional five multimodal functions F_9 - F_{13} and provides better results compared to other powerful metaheuristic algorithms. The results reveal that AISA can get rid of local optima and has exploration capability with high performance regardless of the dimension of problem.

4.4.3. Evaluation of fixed-dimension multimodal test functions F_{14} - F_{23}

As per the results in Table 13, AISA is able to find optimal solution for seven test functions (i.e., $F_{14}, F_{15}, F_{17}, F_{19}, F_{21}, F_{22}$ and

F_{23}) and also obtains competitive results in the other test cases. It is worth noting that, in contrast to large-dimensional multimodal functions, DE performs much better on these test problems and achieves the first overall rank. Overall, it can be concluded that AISA has high exploration capability.

4.4.4. Evaluation of composite test functions F_{24} - F_{29}

Composite test functions have been one of the attractive tools used to test the ability of optimization methods to escape from the local minima. However, their optimization is an extremely challenging task in practice since only a proper balance between exploration and exploitation enables to avoid from local optima. Table 14 depicts optimization results of all algorithms on composite test functions. As seen from Table 14, the proposed algorithm is the best optimizer in four test problems (F_{24}, F_{25}, F_{27} and F_{28}). In light of these findings, it can be stated that the AISA can well balance two cornerstones of optimization process: exploration and exploitation.

4.4.5. Evaluation of CEC 2019 test functions F_{30} - F_{39}

CEC 2019 test functions are compelling optimization problems. The quantitative comparison results of algorithms are presented in Table 15. As seen from this table, AISA performs the best on five challenging test functions ($F_{30}, F_{31}, F_{32}, F_{37}$ and F_{39}). The results demonstrate that AISA possesses a strong capability to produce superior performance over other competitor metaheuristic algorithms in solving complex CEC 2019 test functions.

4.4.6. Wilcoxon signed-rank test

Although fundamental statistical results are presented in aforementioned performance analysis, in order to make a more rigorous comparison as well as provide another insight into performance of the algorithms, the Wilcoxon Signed-Rank Test is utilized for pairwise comparisons. It is a non-parametric statistical hypothesis test which is used to determine whether two samples are statistically different populations or not [81]. The test is performed with a level of significance used to determine whether a hypothesis is rejected or accepted. The null hypothesis H_0 for this test is: "There is no difference between the medians of the solutions obtained after the same test problem is executed by algorithms A and B", that is, the medians of algorithms A and B are equal. To determine whether algorithm A achieved a statistically better solution than algorithm B, or if not, whether the alternative hypothesis H_1 is valid, the sizes of the ranks provided by the Wilcoxon Signed-Rank Test (i.e., $T+$ and $T-$, as defined in [65]) are examined [40].

The non-parametric statistical results of the AISA algorithm versus other algorithms based on the Wilcoxon Signed-Rank Test are found by using the solutions obtained as a result of 30 runs and p -value, $T+$ and $T-$ values are reported in Tables 16–24, with the statistical significance level $\alpha = 0.05$. In these tables, '+' and '-' indicate that both the null hypothesis is rejected and AISA has statistically superior and inferior performances, respectively. Apart from these, '=' indicates a failure to reject the null hypothesis, and also there is no statistical difference between two algorithms. In order to more easily observe the results, Table 25, which is formed by compiling the results in Tables 16–24, lists the Wilcoxon Signed-Rank Test results for each test category. Each cell in Table 25 shows the total count of the three statistical significance cases (+/-/-) in the pairwise comparison. Inspection of the results in Table 25, it may be observed that the proposed AISA algorithm performs better than the others. However, for fixed-dimension multimodal functions, AISA is in competition with TSA and DE algorithms and the numerical results provided for some algorithms such as PSO, ABC, TSA and DE is not sufficient to make a statistically convincing inference.

Table 7Results of unimodal benchmark functions ($F_1 - F_7$), with 10 dimensions.

<i>F</i>	AISA	PSO	ABC	GSA	BA	GWO	MFO	VS	JA	SCA	SSA	TSA	DE	ES
F_1	Best 0.00E+00	7.75E-89	2.79E-17	1.34E-18	1.22E+02	0.00E+00	1.34E-114	3.71E-33	1.02E-110	3.68E-114	1.58E-10	1.43E-110	1.21E-100	3.92E-02
	Mean 0.00E+00	1.32E-81	5.09E-17	3.04E-18	3.45E+03	0.00E+00	6.40E-108	8.13E-28	3.73E-106	5.81E-97	7.24E-10	5.30E-107	1.39E-97	1.84E-01
	Std 0.00E+00	7.04E-81	1.36E-17	9.38E-19	1.75E+03	0.00E+00	2.39E-107	3.24E-27	7.73E-106	2.17E-96	2.68E-10	2.37E-106	5.13E-97	1.16E-01
F_2	Best 8.86E-270	8.71E-50	1.56E-16	3.66E-09	1.73E-03	7.51E-232	3.29E-68	6.96E-16	1.86E-57	6.37E-73	3.24E-06	1.09E-69	4.62E-56	3.13E-02
	Mean 2.46E-256	5.77E-46	2.22E-16	5.19E-09	1.61E+01	7.45E-228	1.08E-63	6.50E-13	5.14E-56	4.46E-63	8.48E-06	7.68E-68	2.91E-55	8.17E-02
	Std 0.00E+00	1.64E-45	4.85E-17	7.96E-10	1.58E+01	0.00E+00	3.08E-63	1.87E-12	8.81E-56	2.00E-62	5.45E-06	1.27E-67	2.86E-55	2.53E-02
F_3	Best 0.00E+00	1.27E-31	7.46E-01	1.70E-18	5.65E+02	5.26E-206	3.97E-36	2.56E-19	8.37E-21	4.22E-59	3.85E-10	1.13E-18	2.24E-15	3.09E+01
	Mean 5.72E-285	6.81E-27	4.79E+00	5.60E-18	5.31E+03	2.18E-186	3.89E+02	1.76E-15	2.95E-18	1.61E-39	1.34E-09	4.45E-16	3.22E-14	3.93E+02
	Std 0.00E+00	1.41E-26	3.13E+00	2.02E-18	3.19E+03	0.00E+00	1.50E+03	4.47E-15	4.78E-18	8.79E-39	6.24E-10	1.03E-15	4.94E-14	3.42E+02
F_4	Best 2.19E-226	2.79E-24	4.39E-02	6.73E-10	1.55E+01	7.61E-134	9.20E-14	2.83E-14	4.06E-31	5.05E-37	1.10E-05	3.00E-21	2.40E-26	3.98E-01
	Mean 1.22E-215	8.13E-22	1.51E-01	1.11E-09	3.36E+01	1.20E-127	1.65E-01	1.48E-11	9.39E-30	5.42E-29	1.55E-05	1.11E-19	2.16E-25	9.27E-01
	Std 0.00E+00	1.60E-21	6.51E-02	2.00E-10	7.35E+00	4.23E-127	7.84E-01	4.92E-11	1.46E-29	2.35E-28	2.82E-06	9.65E-20	1.74E-25	3.44E-01
F_5	Best 0.00E+00	4.91E-03	1.10E-03	2.90E+00	4.12E+00	5.24E+00	1.69E-01	3.91E-01	1.01E-08	5.97E+00	7.03E-01	2.85E-02	3.62E-03	3.49E+00
	Mean 0.00E+00	2.15E+00	1.88E-01	3.08E+00	5.03E+04	6.33E+00	4.35E+01	1.71E+01	1.05E-01	6.61E+00	8.76E+01	2.17E+00	1.96E+00	5.58E+01
	Std 0.00E+00	1.12E+00	2.25E-01	1.28E-01	1.17E+05	7.01E-01	1.11E+02	4.49E+01	4.14E-01	4.18E-01	1.95E+02	1.42E+00	7.00E-01	4.05E+01
F_6	Best 0.00E+00	0.00E+00	3.50E-17	1.40E-18	7.98E+02	5.79E-06	0.00E+00	1.23E-32	8.16E-02	4.84E-02	1.47E-10	0.00E+00	0.00E+00	2.33E-02
	Mean 0.00E+00	0.00E+00	6.19E-17	2.98E-18	3.47E+03	1.24E-05	2.60E-32	2.04E-28	1.24E-01	2.14E-01	6.40E-10	0.00E+00	0.00E+00	2.05E-01
	Std 0.00E+00	0.00E+00	2.09E-17	7.68E-19	1.43E+03	2.69E-06	5.77E-32	4.27E-28	2.07E-02	1.08E-01	3.03E-10	0.00E+00	0.00E+00	1.51E-01
F_7	Best 1.14E-05	3.64E-04	3.17E-03	7.64E-04	2.49E-01	2.03E-06	1.80E-04	1.07E-04	2.07E-04	2.44E-05	2.08E-04	3.32E-04	2.60E-03	1.48E-03
	Mean 7.60E-05	1.49E-03	1.24E-02	3.31E-03	6.90E-01	8.07E-05	3.49E-03	1.36E-03	1.14E-03	3.28E-04	1.44E-03	1.13E-03	8.40E-03	4.02E-03
	Std 5.36E-05	9.63E-04	4.06E-03	1.71E-03	4.80E-01	8.50E-05	2.57E-03	7.69E-04	4.77E-04	3.39E-04	9.23E-04	5.00E-04	3.18E-03	2.09E-03

The bold values indicate the best solutions found by the algorithms.

Table 8Results of unimodal benchmark functions ($F_1 - F_7$), with 30 dimensions.

<i>F</i>	AISA	PSO	ABC	GSA	BA	GWO	MFO	VS	JA	SCA	SSA	TSA	DE	ES
F_1	Best 0.00E+00	9.00E-67	4.20E-16	4.98E-18	1.75E+03	0.00E+00	2.81E-88	6.01E-30	1.89E-109	1.03E-73	2.55E-09	1.56E-57	2.30E-89	2.57E-01
	Mean 0.00E+00	1.23E-61	5.65E-16	8.49E-18	9.63E+03	0.00E+00	2.00E+03	5.67E-27	5.40E-106	6.36E-57	3.95E-09	7.78E-56	1.66E-87	4.66E-01
	Std 0.00E+00	5.89E-61	8.41E-17	1.96E-18	5.17E+03	0.00E+00	4.84E+03	1.69E-26	1.35E-105	1.64E-56	7.24E-10	1.83E-55	2.37E-87	1.85E-01
F_2	Best 0.00E+00	9.44E-42	1.12E-15	1.21E-08	1.71E+00	0.00E+00	3.71E-55	1.20E-12	7.93E-61	1.67E-68	5.35E-05	1.08E-42	8.89E-51	1.74E-01
	Mean 0.00E+00	2.99E-38	1.48E-15	1.67E-08	3.19E+03	0.00E+00	4.20E+01	2.86E-07	1.48E-59	4.18E-58	4.31E-01	8.70E-42	4.48E-50	2.42E-01
	Std 0.00E+00	6.32E-38	1.94E-16	2.42E-09	1.29E+04	0.00E+00	2.44E+01	1.17E-06	2.12E-59	2.21E-57	7.09E-01	9.00E-42	3.51E-50	4.58E-02
F_3	Best 0.00E+00	5.28E-05	8.68E+02	3.82E-17	7.88E+03	9.49E-211	9.97E-10	4.53E-09	8.80E+02	7.66E-08	3.55E-08	8.90E+02	1.81E+03	5.10E+03
	Mean 0.00E+00	7.22E-04	2.77E+03	1.50E-02	2.84E+04	1.26E-181	1.83E+04	1.24E-07	7.78E+03	1.23E+01	6.74E-08	3.20E+03	4.39E+03	8.88E+03
	Std 0.00E+00	8.31E-04	8.39E+02	2.63E-02	2.13E+04	0.00E+00	1.18E+04	1.85E-07	6.05E+03	3.59E+01	2.17E-08	1.80E+03	1.78E+03	2.40E+03
F_4	Best 0.00E+00	7.52E-03	2.50E+01	1.65E-09	3.09E+01	7.51E-158	4.10E+01	5.45E-08	1.23E-07	4.48E-08	3.08E-04	5.45E-01	1.55E-10	2.81E+00
	Mean 0.00E+00	2.29E-02	3.51E+01	2.01E-09	4.50E+01	8.47E-153	6.26E+01	4.54E-06	9.13E-06	2.74E-02	1.81E-01	1.36E+00	1.37E-07	4.91E+00
	Std 0.00E+00	1.51E-02	5.27E+00	2.32E-10	8.72E+00	3.73E-152	1.11E+01	7.73E-06	1.01E-05	5.81E-02	3.05E-01	6.16E-01	7.50E-07	9.82E-01
F_5	Best 0.00E+00	5.73E-02	5.72E-03	1.86E+01	1.28E+01	2.51E+01	5.69E-02	1.95E+01	2.66E-14	2.63E+01	2.13E+01	1.92E+01	1.58E+01	3.24E+01
	Mean 2.55E+00	3.41E+01	1.18E-01	2.35E+01	3.84E+03	2.63E+01	2.68E+06	8.94E+01	2.54E-05	2.75E+01	8.43E+01	2.42E+01	1.77E+01	1.81E+02
	Std 2.10E+00	2.92E+01	1.32E-01	2.36E+01	1.21E+04	6.74E-01	1.46E+07	1.34E+02	9.74E-05	7.19E-01	1.34E+02	1.06E+01	6.25E-01	2.83E+02
F_6	Best 0.00E+00	0.00E+00	3.80E-16	7.62E-18	2.25E+03	1.07E-05	3.50E-30	1.57E-29	1.71E+00	2.98E+00	2.86E-09	0.00E+00	0.00E+00	2.25E-01
	Mean 0.00E+00	2.34E-32	5.65E-16	1.20E-17	9.42E+03	3.88E-01	2.67E+03	2.84E-27	2.54E+00	3.57E+00	4.76E-09	2.05E-34	0.00E+00	4.80E-01
	Std 0.00E+00	3.12E-32	8.47E-17	3.06E-18	4.88E+03	2.94E-01	5.23E+03	4.84E-27	5.24E-01	2.73E-01	1.14E-09	7.82E-34	0.00E+00	2.00E-01
F_7	Best 5.38E-06	6.68E-03	8.85E-02	7.34E-03	4.70E-01	1.26E-05	1.15E-02	2.07E-03	2.62E-03	2.42E-04	2.75E-03	3.36E-03	5.15E-02	7.47E-03
	Mean 4.34E-05	1.12E-02	1.58E-01	1.16E-02	1.01E+00	4.45E-05	5.28E+00	5.74E-03	6.81E-03	2.94E-03	7.55E-03	9.47E-03	7.94E-02	1.58E-02
	Std 2.72E-05	3.58E-03	3.82E-02	2.95E-03	3.64E-01	2.28E-05	1.06E+01	2.22E-03	3.38E-03	4.44E-03	2.46E-03	2.82E-03	1.47E-02	5.54E-03

The bold values indicate the best solutions found by the algorithms.

Table 9Results of unimodal benchmark functions ($F_1 - F_7$), with 50 dimensions.

<i>F</i>	AISA	PSO	ABC	GSA	BA	GWO	MFO	VS	JA	SCA	SSA	TSA	DE	ES	
F_1	Best	0.00E+00	4.22E-52	8.47E-16	1.39E-17	3.37E+03	0.00E+00	1.22E-69	3.37E-28	4.55E-97	2.65E-50	8.79E-09	2.07E-25	6.28E-74	1.29E-01
	Mean	0.00E+00	2.68E-48	1.33E-15	2.31E-17	1.30E+04	0.00E+00	9.67E+03	1.32E-26	9.55E-93	2.60E-33	1.10E-08	1.66E-24	1.50E-72	8.07E-01
	Std	0.00E+00	9.79E-48	2.51E-16	4.28E-18	6.74E+03	0.00E+00	1.10E+04	2.05E-26	1.79E-92	1.36E-32	1.30E-09	2.03E-24	2.00E-72	2.72E-01
F_2	Best	0.00E+00	1.25E-33	2.58E-15	2.27E-08	1.54E+00	0.00E+00	1.00E+01	1.52E-09	6.77E-55	6.75E-66	2.22E-02	9.65E-23	9.82E-44	3.18E-01
	Mean	0.00E+00	1.46E-28	3.20E-15	2.88E-08	2.87E+09	0.00E+00	6.73E+01	5.37E-06	2.10E-47	9.85E-55	1.12E+00	4.02E-22	5.40E-42	4.12E-01
	Std	0.00E+00	7.46E-28	3.55E-16	3.49E-09	1.56E+10	0.00E+00	3.42E+01	2.53E-05	1.15E-46	4.25E-54	1.14E+00	2.46E-22	3.11E-42	6.46E-02
F_3	Best	0.00E+00	3.31E-01	1.24E+04	8.92E-01	1.08E+04	2.59E-212	5.00E+03	9.78E-05	2.21E+04	8.42E+00	6.16E-07	2.06E+04	4.46E+04	1.73E+04
	Mean	0.00E+00	1.16E+00	1.64E+04	5.37E+00	5.57E+04	5.60E-179	3.71E+04	4.79E-04	5.68E+04	3.83E+03	1.06E-06	5.62E+04	6.70E+04	2.58E+04
	Std	0.00E+00	5.65E-01	2.30E+03	3.82E+00	4.19E+04	0.00E+00	2.44E+04	3.40E-04	1.45E+04	4.79E+03	2.23E-07	1.07E+04	7.54E+03	4.19E+03
F_4	Best	0.00E+00	5.82E-01	5.91E+01	2.22E-09	3.19E+01	9.36E-178	7.25E+01	3.09E-04	1.26E+01	1.21E-01	1.00E+00	3.49E+01	2.33E-04	6.10E+00
	Mean	0.00E+00	8.65E-01	6.64E+01	2.97E-09	4.52E+01	6.98E-171	8.35E+01	5.94E-03	1.97E+01	9.93E+00	8.40E+00	5.44E+01	4.90E-03	8.96E+00
	Std	0.00E+00	1.84E-01	3.52E+00	3.74E-10	7.05E+00	0.00E+00	4.32E+00	7.12E-03	2.95E+00	7.44E+00	3.85E+00	8.92E+00	2.07E-02	2.06E+00
F_5	Best	0.00E+00	6.32E+00	4.61E-03	3.54E+01	2.85E+01	4.50E+01	1.46E-01	4.28E+01	2.33E-13	4.70E+01	3.82E+01	4.29E+01	3.04E+01	7.37E+01
	Mean	3.89E+01	6.82E+01	2.02E-01	3.61E+01	5.15E+01	4.67E+01	5.37E+06	7.90E+01	6.37E-09	4.80E+01	7.24E+01	6.79E+01	3.56E+01	2.06E+02
	Std	1.33E+01	4.15E+01	3.46E-01	3.21E-01	4.23E+01	1.09E+00	2.03E+07	9.77E+01	1.62E-08	5.82E-01	4.25E+01	3.61E+01	9.41E+00	5.09E+01
F_6	Best	0.00E+00	7.40E-32	1.11E-15	1.53E-17	1.61E+03	1.25E+00	2.37E-26	3.40E-28	8.15E+00	7.42E+00	8.08E-09	2.03E-25	0.00E+00	2.77E-01
	Mean	0.00E+00	2.13E-30	1.38E-15	2.13E-17	1.33E+04	2.13E+00	8.32E+03	5.14E-27	1.45E+01	8.04E+00	1.11E-08	2.10E-24	0.00E+00	8.50E-01
	Std	0.00E+00	3.63E-30	1.80E-16	5.72E-18	8.14E+03	6.17E-01	9.85E+03	6.15E-27	6.09E+00	3.32E-01	1.68E-09	2.08E-24	0.00E+00	2.48E-01
F_7	Best	4.78E-06	1.04E-02	3.13E-01	1.41E-02	4.19E-01	1.20E-05	3.39E-01	5.22E-03	1.16E-02	1.46E-03	4.49E-03	2.44E-02	1.53E-01	1.47E-02
	Mean	2.27E-05	2.91E-02	4.72E-01	2.27E-02	6.22E-01	6.35E-05	1.55E+01	1.09E-02	2.51E-02	1.07E-02	1.61E-02	4.30E-02	1.91E-01	2.91E-02
	Std	1.32E-05	1.10E-02	6.13E-02	4.70E-03	1.27E-01	2.93E-05	2.09E+01	3.65E-03	7.97E-03	8.09E-03	4.38E-03	1.09E-02	2.17E-02	6.46E-03

The bold values indicate the best solutions found by the algorithms.

Table 10Results of multimodal benchmark functions ($F_8 - F_{13}$), with 10 dimensions.

<i>F</i>	AISA	PSO	ABC	GSA	BA	GWO	MFO	VS	JA	SCA	SSA	TSA	DE	ES
F_8	Best -4.19E+03	-3.16E+03	-4.19E+03	-2.07E+03	-3.12E+03	-3.50E+03	-3.72E+03	-4.19E+03	-4.19E+03	-2.83E+03	-3.32E+03	-4.19E+03	-4.19E+03	-4.19E+03
	Mean -4.19E+03	-2.54E+03	-4.19E+03	-1.53E+03	-1.89E+03	-2.82E+03	-3.10E+03	-3.92E+03	-3.75E+03	-2.42E+03	-2.92E+03	-4.12E+03	-4.18E+03	-4.19E+03
	Std 2.78E-12	3.01E+02	2.53E-12	2.32E+02	3.69E+02	3.37E+02	2.98E+02	1.96E+02	4.85E+02	1.74E+02	1.93E+02	1.01E+02	3.54E+01	4.33E-01
F_9	Best 0.00E+00	0.00E+00	0.00E+00	9.95E-01	1.19E+01	0.00E+00	6.96E+00	1.99E+00	9.05E+00	0.00E+00	6.96E+00	0.00E+00	0.00E+00	1.41E-02
	Mean 0.00E+00	2.02E+00	0.00E+00	3.08E+00	4.41E+01	0.00E+00	2.73E+01	1.59E+01	1.95E+01	0.00E+00	1.64E+01	1.64E+00	0.00E+00	9.77E-02
	Std 0.00E+00	1.27E+00	0.00E+00	1.58E+00	1.67E+01	0.00E+00	1.57E+01	7.88E+00	6.21E+00	0.00E+00	4.76E+00	1.55E+00	0.00E+00	6.30E-02
F_{10}	Best 8.88E-16	4.44E-15	4.44E-15	1.66E-09	1.29E+01	4.44E-15	8.88E-16	4.44E-15	4.44E-15	8.88E-16	7.88E-06	4.44E-15	8.88E-16	9.17E-02
	Mean 8.88E-16	4.56E-15	7.99E-15	2.54E-09	1.57E+01	4.44E-15	2.58E-01	1.66E-14	4.44E-15	3.38E-15	6.56E-01	4.44E-15	4.09E-15	2.61E-01
	Std 0.00E+00	6.49E-16	9.33E-16	4.19E-10	1.69E+00	0.00E+00	8.10E-01	1.69E-14	0.00E+00	1.66E-15	7.91E-01	0.00E+00	1.08E-15	9.87E-02
F_{11}	Best 0.00E+00	2.95E-02	0.00E+00	0.00E+00	1.47E+01	0.00E+00	4.67E-02	1.01E-01	1.51E-01	0.00E+00	9.10E-02	0.00E+00	0.00E+00	1.15E-01
	Mean 0.00E+00	1.19E-01	2.10E-03	4.11E-03	5.42E+01	3.06E-03	1.40E-01	2.78E-01	3.65E-01	7.01E-04	3.13E-01	6.07E-02	0.00E+00	3.28E-01
	Std 0.00E+00	1.05E-01	4.72E-03	5.65E-03	2.26E+01	6.07E-03	6.91E-02	1.23E-01	1.11E-01	3.72E-03	1.59E-01	5.33E-02	0.00E+00	1.21E-01
F_{12}	Best 4.71E-32	4.71E-32	3.48E-17	2.09E-20	5.63E+00	5.97E-07	4.71E-32	2.30E-25	4.73E-03	1.46E-02	3.33E-12	4.71E-32	4.71E-32	5.29E-04
	Mean 4.71E-32	4.72E-32	5.17E-17	5.58E-20	1.10E+05	3.30E-03	1.14E-01	1.58E-22	2.20E-02	4.78E-02	1.24E-01	4.71E-32	4.71E-32	5.92E-03
	Std 1.67E-47	2.49E-34	1.01E-17	2.04E-20	3.66E+05	1.05E-02	2.08E-01	3.16E-22	8.57E-03	2.76E-02	2.66E-01	1.67E-47	1.67E-47	7.04E-03
F_{13}	Best 1.35E-32	1.35E-32	2.62E-17	1.06E-19	1.26E+01	3.36E-06	1.35E-32	5.67E-25	1.35E-32	8.04E-02	1.59E-11	1.35E-32	1.35E-32	9.05E-04
	Mean 1.35E-32	1.35E-32	5.33E-17	5.71E-05	8.62E+05	1.32E-02	4.03E-03	6.35E-22	3.66E-04	2.06E-01	3.66E-04	1.35E-32	1.35E-32	1.58E-02
	Std 5.57E-48	5.57E-48	1.57E-17	3.13E-04	2.39E+06	3.42E-02	5.39E-03	2.70E-21	2.01E-03	7.87E-02	2.01E-03	5.57E-48	5.57E-48	1.06E-02

The bold values indicate the best solutions found by the algorithms.

Table 11Results of multimodal benchmark functions ($F_8 - F_{13}$), with 30 dimensions.

<i>F</i>	AISA	PSO	ABC	GSA	BA	GWO	MFO	VS	JA	SCA	SSA	TSA	DE	ES
F_8	Best -1.26E+04	-8.31E+03	-1.26E+04	-3.87E+03	-6.85E+03	-7.50E+03	-1.02E+04	-1.16E+04	-1.26E+04	-4.86E+03	-9.21E+03	-1.19E+04	-1.26E+04	-1.26E+04
	Mean -1.26E+04	-6.59E+03	-1.26E+04	-2.66E+03	-4.92E+03	-6.24E+03	-8.49E+03	-1.03E+04	-1.12E+04	-4.39E+03	-7.86E+03	-1.06E+04	-1.23E+04	-1.26E+04
	Std 1.85E-12	9.11E+02	3.06E-03	3.70E+02	1.13E+03	6.36E+02	8.15E+02	5.35E+02	2.27E+03	2.46E+02	7.31E+02	1.15E+03	5.20E+02	7.80E-01
F_9	Best 0.00E+00	1.19E+01	0.00E+00	9.95E+00	4.48E+01	0.00E+00	6.67E+01	4.97E+01	1.99E+01	0.00E+00	5.07E+01	6.96E+00	7.39E+01	1.00E-01
	Mean 0.00E+00	2.49E+01	1.44E-13	1.37E+01	1.01E+02	0.00E+00	1.51E+02	7.92E+01	8.31E+01	4.33E-05	7.23E+01	2.54E+01	9.15E+01	2.44E-01
	Std 0.00E+00	7.44E+00	1.37E-13	2.85E+00	3.68E+01	0.00E+00	4.13E+01	1.66E+01	5.95E+01	2.26E-04	1.62E+01	2.09E+01	7.68E+00	9.99E-02
F_{10}	Best 8.88E-16	7.99E-15	4.35E-14	2.01E-09	1.57E+01	4.44E-15	7.99E-15	2.93E-14	7.99E-15	4.44E-15	1.52E-05	4.44E-15	4.44E-15	9.79E-02
	Mean 1.01E-15	1.04E-14	5.13E-14	2.64E-09	1.71E+01	7.64E-15	1.60E+01	3.10E-02	4.04E+00	1.12E+01	1.81E+00	7.52E-15	6.10E-15	2.35E-01
	Std 6.49E-16	3.41E-15	6.75E-15	2.60E-10	8.79E-01	1.08E-15	6.79E+00	1.70E-01	7.28E+00	9.25E+00	8.10E-01	1.23E-15	1.80E-15	7.08E-02
F_{11}	Best 0.00E+00	0.00E+00	0.00E+00	0.00E+00	9.77E+01	0.00E+00	0.00E+00	1.11E-16	0.00E+00	0.00E+00	9.43E-09	0.00E+00	0.00E+00	3.06E-01
	Mean 0.00E+00	1.36E-02	3.34E-15	0.00E+00	1.99E+02	0.00E+00	1.81E+01	1.71E-02	1.14E-02	0.00E+00	1.23E-02	2.47E-04	0.00E+00	5.25E-01
	Std 0.00E+00	1.20E-02	6.88E-15	0.00E+00	6.89E+01	0.00E+00	4.37E+01	1.51E-02	1.26E-02	0.00E+00	1.21E-02	1.35E-03	0.00E+00	1.26E-01
F_{12}	Best 1.57E-32	1.57E-32	2.63E-16	3.25E-20	9.09E+00	6.55E-03	1.23E-31	4.09E-26	2.42E-01	2.01E-01	1.09E-11	1.57E-32	1.57E-32	4.85E-04
	Mean 1.57E-32	1.64E-32	5.54E-16	7.72E-20	6.62E+03	2.80E-02	2.49E-01	6.84E-02	5.39E+00	3.33E-01	1.24E+00	1.57E-32	1.57E-32	2.15E-03
	Std 5.57E-48	7.59E-34	1.15E-16	2.71E-20	3.49E+04	1.72E-02	7.29E-01	2.11E-01	3.42E+00	4.63E-02	2.13E+00	5.89E-35	5.57E-48	1.76E-03
F_{13}	Best 1.35E-32	1.35E-32	3.91E-16	6.08E-19	6.87E+01	6.63E-06	1.95E-30	4.24E-26	1.35E-32	1.83E+00	1.31E-10	1.35E-32	1.35E-32	8.97E-03
	Mean 1.35E-32	3.66E-04	5.60E-16	1.20E-18	4.16E+05	3.96E-01	1.09E-01	2.56E-03	4.00E-03	2.01E+00	3.63E-03	1.36E-32	1.35E-32	2.58E-02
	Std 5.57E-48	2.01E-03	7.82E-17	2.87E-19	1.33E+06	2.00E-01	3.87E-01	4.73E-03	6.01E-03	1.03E-01	5.91E-03	3.13E-34	5.57E-48	8.68E-03

The bold values indicate the best solutions found by the algorithms.

Table 12Results of multimodal benchmark functions ($F_8 - F_{13}$), with 50 dimensions.

<i>F</i>	AISA	PSO	ABC	GSA	BA	GWO	MFO	VS	JA	SCA	SSA	TSA	DE	ES
F_8	Best -2.09E+04	-1.31E+04	-2.09E+04	-4.54E+03	-1.27E+04	-1.08E+04	-1.65E+04	-1.82E+04	-2.09E+04	-6.59E+03	-1.47E+04	-1.91E+04	-1.42E+04	-2.09E+04
	Mean -2.08E+04	-1.08E+04	-2.09E+04	-3.43E+03	-8.43E+03	-9.02E+03	-1.39E+04	-1.66E+04	-1.96E+04	-5.91E+03	-1.25E+04	-1.73E+04	-1.20E+04	-2.09E+04
	Std 1.08E+03	1.36E+03	4.09E+01	5.06E+02	1.35E+03	9.54E+02	1.33E+03	9.04E+02	2.26E+03	3.77E+02	7.02E+02	1.70E+03	6.51E+02	7.12E-01
F_9	Best 0.00E+00	3.58E+01	1.71E-13	1.89E+01	9.95E+01	0.00E+00	1.82E+02	9.05E+01	5.17E+01	0.00E+00	6.17E+01	2.49E+01	2.30E+02	2.25E-01
	Mean 0.00E+00	6.06E+01	2.20E-11	2.56E+01	1.77E+02	0.00E+00	2.85E+02	1.42E+02	1.03E+02	5.31E-01	1.13E+02	4.73E+01	2.47E+02	3.71E-01
	Std 0.00E+00	1.23E+01	8.84E-11	4.06E+00	7.27E+01	0.00E+00	5.08E+01	2.97E+01	2.94E+01	2.81E+00	1.97E+01	1.04E+01	9.15E+00	1.17E-01
F_{10}	Best 8.88E-16	1.51E-14	9.33E-14	2.05E-09	1.53E+01	7.99E-15	1.25E+01	5.77E-14	5.77E-14	7.99E-15	1.37E+00	1.96E-13	7.99E-15	1.63E-01
	Mean 1.60E-15	2.28E-14	1.14E-13	2.82E-09	1.74E+01	8.47E-15	1.94E+01	1.45E-01	3.38E+00	1.22E+01	2.39E+00	4.64E-13	7.99E-15	2.42E-01
	Std 1.45E-15	9.00E-15	1.47E-14	2.91E-10	1.07E+00	1.54E-15	1.42E+00	4.49E-01	3.37E+00	9.82E+00	5.44E-01	2.17E-13	0.00E+00	4.67E-02
F_{11}	Best 0.00E+00	0.00E+00	8.88E-16	0.00E+00	1.80E+02	0.00E+00	0.00E+00	3.33E-16	0.00E+00	0.00E+00	1.19E-08	0.00E+00	0.00E+00	3.79E-01
	Mean 0.00E+00	5.26E-03	6.26E-15	5.45E-03	3.57E+02	0.00E+00	8.75E+01	5.01E-03	7.29E-03	1.45E-12	6.32E-03	0.00E+00	0.00E+00	6.06E-01
	Std 0.00E+00	6.43E-03	7.51E-15	1.87E-02	1.20E+02	0.00E+00	9.88E+01	6.45E-03	1.16E-02	6.76E-12	9.74E-03	0.00E+00	0.00E+00	1.38E-01
F_{12}	Best 9.42E-33	1.02E-32	1.04E-15	5.06E-20	1.02E+01	3.53E-02	5.07E-29	1.25E-26	9.08E+00	4.86E-01	7.98E-01	1.38E-13	9.42E-33	6.41E-04
	Mean 9.42E-33	7.39E-32	1.40E-15	2.07E-03	2.46E+01	6.65E-02	2.56E+07	2.46E-01	1.94E+01	5.93E-01	6.52E+00	3.17E-01	9.42E-33	2.18E-03
	Std 2.78E-48	1.72E-31	1.82E-16	1.14E-02	8.57E+00	2.28E-02	7.81E+07	4.26E-01	5.20E+00	8.34E-02	3.19E+00	1.12E+00	2.78E-48	2.82E-03
F_{13}	Best 1.35E-32	2.83E-32	7.87E-16	1.57E-18	1.33E+02	7.23E-01	2.70E-26	6.50E-26	1.35E-32	3.73E+00	3.23E-10	9.73E-13	1.35E-32	1.84E-02
	Mean 1.35E-32	2.56E-03	1.34E-15	2.26E-18	8.72E+03	1.45E+00	4.10E+07	3.30E-03	1.98E+00	4.19E+00	5.49E-03	4.01E-04	1.35E-32	4.15E-02
	Std 5.57E-48	4.73E-03	2.19E-16	4.29E-19	3.18E+04	3.11E-01	1.25E+08	5.12E-03	5.82E+00	1.98E-01	5.59E-03	2.00E-03	5.57E-48	1.29E-02

The bold values indicate the best solutions found by the algorithms.

Table 13Results of fixed-dimension multimodal benchmark functions ($F_{14} - F_{23}$).

<i>F</i>	AISA	PSO	ABC	GSA	BA	GWO	MFO	VS	JA	SCA	SSA	TSA	DE	ES
F_{14}	Best 9.98E-01	9.98E-01	9.98E-01	9.99E-01	9.98E-01	9.98E-01	9.98E-01	9.98E-01	9.98E-01	9.98E-01	9.98E-01	9.98E-01	9.98E-01	9.98E-01
	Mean 9.98E-01	2.71E+00	9.98E-01	5.53E+00	1.21E+01	5.73E+00	2.02E+00	9.98E-01	1.00E+00	1.92E+00	1.06E+00	9.98E-01	9.98E-01	4.29E+00
	Std 0.00E+00	2.53E+00	1.13E-16	4.08E+00	6.89E+00	4.53E+00	1.95E+00	1.91E-16	5.89E-03	1.91E+00	2.52E-01	0.00E+00	0.00E+00	5.30E+00
F_{15}	Best 3.07E-04	3.07E-04	4.09E-04	1.11E-03	7.32E-04	3.07E-04	5.85E-04	3.08E-04	3.07E-04	3.32E-04	4.01E-04	3.82E-04	3.07E-04	7.34E-04
	Mean 3.07E-04	7.54E-04	7.15E-04	2.55E-03	6.61E-03	4.35E-03	1.45E-03	7.85E-04	4.65E-04	9.65E-04	8.29E-04	6.29E-04	3.83E-04	3.17E-03
	Std 1.71E-19	2.16E-04	1.86E-04	1.27E-03	2.13E-02	8.14E-03	1.90E-03	3.14E-04	3.56E-04	4.19E-04	2.64E-04	9.82E-05	2.42E-04	3.84E-03
F_{16}	Best -1.03E+00	-1.03E+00	-1.03E+00	-1.03E+00	-1.03E+00	-1.03E+00	-1.03E+00	-1.03E+00	-1.03E+00	-1.03E+00	-1.03E+00	-1.03E+00	-1.03E+00	-1.03E+00
	Mean -1.03E+00	-1.03E+00	-1.03E+00	-1.03E+00	-1.00E+00	-1.03E+00	-1.03E+00	-1.03E+00	-1.03E+00	-1.03E+00	-1.03E+00	-1.03E+00	-1.03E+00	-1.03E+00
	Std 1.08E-15	6.32E-16	4.97E-16	5.05E-16	1.49E-01	3.18E-08	6.78E-16	5.00E-16	2.32E-05	3.06E-05	3.02E-14	6.71E-16	6.78E-16	1.30E-05
F_{17}	Best 3.98E-01	3.98E-01	3.98E-01	3.98E-01	3.98E-01	3.98E-01	3.98E-01	3.98E-01	3.98E-01	3.98E-01	3.98E-01	3.98E-01	3.98E-01	3.98E-01
	Mean 3.98E-01	3.98E-01	3.98E-01	3.98E-01	3.98E-01	3.98E-01	3.98E-01	3.98E-01	3.99E-01	3.98E-01	3.98E-01	3.98E-01	3.98E-01	3.98E-01
	Std 0.00E+00	0.00E+00	0.00E+00	0.00E+00	5.98E-10	7.02E-07	0.00E+00	0.00E+00	0.00E-03	2.32E-14	0.00E+00	0.00E+00	0.00E+00	1.64E-04
F_{18}	Best 3.00E+00	3.00E+00	3.00E+00	3.00E+00	3.00E+00	3.00E+00	3.00E+00	3.00E+00	3.00E+00	3.00E+00	3.00E+00	3.00E+00	3.00E+00	3.00E+00
	Mean 3.00E+00	3.00E+00	3.01E+00	3.00E+00	8.40E+00	3.00E+00	3.00E+00	3.00E+00	3.00E+00	3.00E+00	3.00E+00	3.00E+00	3.00E+00	3.00E+00
	Std 1.41E-15	1.47E-15	4.26E-02	4.04E-15	2.06E+01	2.41E-05	2.33E-15	3.70E-15	4.01E-04	4.89E-05	2.18E-13	1.23E-15	1.81E-15	7.63E-04
F_{19}	Best -3.86E+00	-3.86E+00	-3.86E+00	-3.86E+00	-3.86E+00	-3.86E+00	-3.86E+00	-3.86E+00	-3.86E+00	-3.86E+00	-3.86E+00	-3.86E+00	-3.86E+00	-3.86E+00
	Mean -3.86E+00	-3.86E+00	-3.86E+00	-3.86E+00	-3.84E+00	-3.86E+00	-3.86E+00	-3.86E+00	-3.86E+00	-3.86E+00	-3.86E+00	-3.86E+00	-3.86E+00	-3.86E+00
	Std 2.71E-15	2.68E-15	2.34E-15	2.40E-15	1.41E-01	2.61E-03	2.71E-15	2.07E-15	2.71E-15	2.56E-03	6.64E-14	2.71E-15	2.71E-15	5.32E-05
F_{20}	Best -3.32E+00	-3.32E+00	-3.32E+00	-3.32E+00	-3.32E+00	-3.32E+00	-3.32E+00	-3.32E+00	-3.23E+00	-3.32E+00	-3.32E+00	-3.32E+00	-3.32E+00	-3.32E+00
	Mean -3.31E+00	-3.28E+00	-3.32E+00	-3.32E+00	-3.27E+00	-3.25E+00	-3.26E+00	-3.27E+00	-3.28E+00	-3.22E+00	-3.32E+00	-3.29E+00	-3.24E+00	-3.24E+00
	Std 4.11E-02	5.83E-02	1.76E-15	1.36E-15	6.03E-02	1.07E-01	6.40E-02	6.03E-02	5.92E-02	4.22E-01	4.11E-02	1.37E-15	5.54E-02	5.54E-02
F_{21}	Best -1.02E+01	-1.02E+01	-1.02E+01	-1.02E+01	-1.02E+01	-1.02E+01	-1.02E+01	-1.02E+01	-6.64E+00	-1.02E+01	-1.02E+01	-1.02E+01	-1.02E+01	-1.02E+01
	Mean -1.02E+01	-8.55E+00	-1.02E+01	-7.39E+00	-5.47E+00	-9.48E+00	-6.80E+00	-1.02E+01	-7.45E+00	-2.83E+00	-8.06E+00	-1.01E+01	-1.02E+01	-6.23E+00
	Std 6.27E-15	2.52E+00	6.82E-07	3.50E+00	3.06E+00	1.75E+00	3.31E+00	5.86E-15	2.77E+00	2.18E+00	3.09E+00	5.18E-01	7.23E-15	3.74E+00
F_{22}	Best -1.04E+01	-1.04E+01	-1.04E+01	-1.04E+01	-1.04E+01	-1.04E+01	-1.04E+01	-1.04E+01	-7.09E+00	-1.04E+01	-1.04E+01	-1.04E+01	-1.04E+01	-1.04E+01
	Mean -1.04E+01	-1.00E+01	-1.04E+01	-1.04E+01	-5.62E+00	-9.87E+00	-8.05E+00	-1.04E+01	-8.18E+00	-3.89E+00	-9.01E+00	-1.03E+01	-1.04E+01	-5.86E+00
	Std 6.60E-16	1.34E+00	1.42E-03	8.08E-16	3.33E+00	1.62E+00	3.21E+00	1.19E-15	2.97E+00	1.93E+00	2.61E+00	3.00E-01	1.40E-15	3.54E+00
F_{23}	Best -1.05E+01	-1.05E+01	-1.05E+01	-1.05E+01	-1.05E+01	-1.05E+01	-1.05E+01	-1.05E+01	-1.05E+01	-1.05E+01	-8.34E+00	-1.05E+01	-1.05E+01	-1.05E+01
	Mean -1.05E+01	-9.92E+00	-1.05E+01	-1.05E+01	-4.62E+00	-1.03E+01	-7.09E+00	-1.05E+01	-8.14E+00	-4.87E+00	-9.74E+00	-1.05E+01	-1.05E+01	-6.11E+00
	Std 2.56E-15	1.91E+00	5.76E-03	1.98E-15	3.41E+00	1.48E+00	3.81E+00	1.62E-15	3.07E+00	1.95E+00	2.09E+00	2.70E-05	1.81E-15	3.70E+00

The bold values indicate the best solutions found by the algorithms.

Table 14Results of composite benchmark functions ($F_{24} - F_{29}$).

F	AISA	PSO	ABC	GSA	BA	GWO	MFO	VS	JA	SCA	SSA	TSA	DE	ES	
F_{24}	Best	0.00E+00	0.00E+00	1.59E-16	3.48E-18	4.92E-05	6.01E-01	0.00E+00	0.00E+00	6.74E+00	4.17E+01	2.83E-11	0.00E+00	0.00E+00	2.50E-02
	Mean	8.44E-30	8.00E+01	4.56E-03	9.48E-18	1.37E+02	8.64E+01	9.08E+01	2.33E+01	5.19E+01	1.03E+02	6.00E+01	5.81E+00	4.20E+01	2.67E+01
	Std	1.73E-29	8.05E+01	9.47E-03	3.53E-18	1.33E+02	1.03E+02	5.85E+01	5.04E+01	4.57E+01	3.81E+01	6.75E+01	1.90E+01	5.89E+01	4.50E+01
F_{25}	Best	1.77E+00	3.18E+00	4.99E+00	1.00E+02	3.57E+01	6.87E+00	0.00E+00	1.03E+01	4.74E+01	7.60E+01	6.18E+00	1.88E-01	0.00E+00	1.74E+00
	Mean	1.90E+01	1.16E+02	2.05E+01	1.89E+02	3.96E+02	1.30E+02	4.39E+01	2.54E+01	1.11E+02	1.03E+02	2.19E+01	4.31E+01	5.88E+01	1.00E+02
	Std	2.82E+01	9.48E+01	1.24E+01	3.06E+01	1.88E+02	1.11E+02	4.87E+01	1.08E+01	7.34E+01	8.53E+00	1.00E+01	4.52E+01	7.27E+01	8.99E+01
F_{26}	Best	1.11E+02	9.60E+01	9.79E+01	0.00E+00	2.53E+02	9.51E+01	1.26E+02	1.01E+02	1.88E+02	2.21E+02	1.01E+02	1.06E+02	9.43E+01	1.05E+02
	Mean	1.58E+02	1.62E+02	1.31E+02	5.70E+01	6.28E+02	1.93E+02	2.49E+02	1.85E+02	2.86E+02	3.21E+02	1.92E+02	1.49E+02	1.31E+02	1.73E+02
	Std	2.17E+01	3.78E+01	1.61E+01	7.09E+01	1.94E+02	5.49E+01	7.62E+01	4.44E+01	6.19E+01	6.65E+01	5.31E+01	2.81E+01	2.37E+01	3.74E+01
F_{27}	Best	2.00E+02	2.28E+02	2.94E+02	2.00E+02	5.02E+02	2.24E+02	3.16E+02	2.28E+02	3.40E+02	3.71E+02	2.62E+02	2.18E+02	2.00E+02	2.97E+02
	Mean	2.86E+02	3.10E+02	3.62E+02	4.84E+02	7.53E+02	4.03E+02	3.54E+02	3.07E+02	3.62E+02	4.09E+02	3.17E+02	3.14E+02	2.92E+02	4.09E+02
	Std	2.50E+01	2.32E+01	2.88E+01	1.50E+02	1.45E+02	1.49E+02	2.83E+01	3.38E+01	2.53E+01	2.02E+01	2.74E+01	2.59E+01	2.07E+01	9.87E+01
F_{28}	Best	0.00E+00	1.19E+00	5.78E+00	3.94E-15	1.96E+02	1.34E+00	4.37E+00	0.00E+00	1.12E+01	4.45E+01	1.19E+00	2.25E-03	0.00E+00	6.25E+00
	Mean	2.48E+00	9.71E+01	1.01E+01	2.17E+02	5.47E+02	1.43E+02	8.39E+01	3.52E+00	1.03E+02	9.90E+01	2.43E+01	3.19E+01	5.60E+01	8.99E+01
	Std	1.24E+00	8.97E+01	3.25E+00	4.74E+01	2.02E+02	1.63E+02	7.40E+01	2.25E+00	9.19E+01	5.32E+01	3.92E+01	3.58E+01	5.20E+01	1.14E+02
F_{29}	Best	4.01E+02	5.00E+02	4.10E+02	5.58E+02	5.67E+02	5.01E+02	4.41E+02	4.05E+02	5.25E+02	4.30E+02	4.02E+02	4.37E+02	5.00E+02	5.01E+02
	Mean	5.24E+02	7.74E+02	5.03E+02	7.16E+02	8.53E+02	8.60E+02	7.09E+02	4.98E+02	7.90E+02	5.17E+02	5.25E+02	5.19E+02	6.52E+02	6.45E+02
	Std	1.04E+02	1.84E+02	6.51E+01	8.09E+01	1.09E+02	1.22E+02	1.90E+02	1.77E+01	1.64E+02	7.10E+01	1.22E+02	7.47E+01	1.89E+02	1.90E+02

The bold values indicate the best solutions found by the algorithms.

Table 15Results of CEC 2019 benchmark functions ($F_{30} - F_{39}$).

<i>F</i>	AISA	PSO	ABC	GSA	BA	GWO	MFO	VS	JA	SCA	SSA	TSA	DE	ES	
F_{30}	Best	1.00E+00	9.03E+03	4.60E+05	1.70E+08	1.32E+08	8.22E+00	1.07E+03	3.04E+04	1.32E+06	2.98E+01	7.56E+03	2.09E+05	4.10E+00	5.24E+05
	Mean	1.00E+00	2.87E+07	2.03E+06	4.04E+08	9.68E+08	5.88E+03	1.64E+07	5.27E+05	4.49E+06	4.51E+05	5.24E+05	1.10E+06	1.39E+04	1.23E+07
	Std	0.00E+00	3.54E+07	8.30E+05	1.80E+08	6.87E+08	2.94E+04	3.33E+07	3.17E+05	2.02E+06	9.84E+05	4.28E+05	8.86E+05	5.13E+04	9.70E+06
F_{31}	Best	2.83E+00	1.54E+03	7.38E+02	1.23E+04	1.10E+04	4.84E+00	1.12E+02	1.20E+02	1.40E+02	1.00E+02	1.07E+03	5.15E+02	1.17E+03	
	Mean	3.21E+00	6.40E+03	2.07E+03	2.24E+04	2.15E+04	1.62E+02	2.05E+03	3.08E+02	2.77E+03	1.59E+03	3.71E+02	2.33E+03	1.06E+03	3.94E+03
	Std	2.14E-01	4.18E+03	5.92E+02	5.41E+03	8.11E+03	1.75E+02	2.79E+03	9.59E+01	6.60E+02	1.14E+03	2.46E+02	6.42E+02	2.60E+02	2.06E+03
F_{32}	Best	1.00E+00	1.00E+00	1.06E+00	1.41E+00	1.41E+00	1.00E+00	1.41E+00	1.00E+00	3.98E+00	3.72E+00	1.00E+00	3.37E+00	3.28E+00	1.07E+00
	Mean	1.33E+00	1.50E+00	1.52E+00	2.21E+00	7.86E+00	1.88E+00	6.55E+00	3.07E+00	7.46E+00	7.26E+00	2.41E+00	6.90E+00	4.97E+00	2.24E+00
	Std	1.66E-01	6.07E-01	1.94E-01	1.56E+00	3.17E+00	1.18E+00	2.58E+00	2.02E+00	1.65E+00	1.50E+00	1.45E+00	1.64E+00	7.89E-01	1.28E+00
F_{33}	Best	4.98E+00	1.69E+01	5.13E+00	2.39E+01	3.28E+01	5.00E+00	1.49E+01	6.97E+00	2.03E+01	3.25E+01	5.97E+00	5.13E+00	1.00E+00	8.13E+00
	Mean	1.29E+01	4.04E+01	9.93E+00	3.40E+01	8.81E+01	1.59E+01	3.03E+01	1.64E+01	3.23E+01	4.41E+01	2.25E+01	1.60E+01	9.56E+00	1.70E+01
	Std	4.41E+00	1.32E+01	1.87E+00	7.56E+00	3.39E+01	7.74E+00	1.35E+01	6.75E+00	7.86E+00	6.03E+00	9.52E+00	5.83E+00	4.37E+00	6.30E+00
F_{34}	Best	1.01E+00	1.03E+00	1.00E+00	1.00E+00	3.75E+01	1.17E+00	1.04E+00	1.04E+00	2.10E+00	2.75E+00	1.06E+00	1.01E+00	1.00E+00	1.22E+00
	Mean	1.07E+00	1.15E+00	1.02E+00	1.00E+00	1.13E+02	1.69E+00	4.17E+00	1.25E+00	2.27E+00	6.44E+00	1.28E+00	1.17E+00	1.05E+00	1.49E+00
	Std	3.87E-02	8.88E-02	1.03E-02	5.35E-03	5.04E+01	6.37E-01	8.03E+00	1.20E-01	1.10E-01	2.42E+00	1.10E-01	1.17E-01	6.30E-02	1.55E-01
F_{35}	Best	1.00E+00	1.00E+00	1.43E+00	1.00E+00	1.18E+01	1.12E+00	2.22E+00	1.00E+00	3.72E+00	4.96E+00	1.20E+00	1.00E+00	1.00E+00	1.41E+00
	Mean	1.76E+00	3.66E+00	2.34E+00	2.98E+00	1.42E+01	2.46E+00	5.38E+00	1.35E+00	5.85E+00	7.02E+00	3.41E+00	1.21E+00	1.85E+00	3.33E+00
	Std	5.49E-01	1.37E+00	5.13E-01	1.36E+00	1.10E+00	1.19E+00	1.76E+00	6.25E-01	1.36E+00	1.47E+00	1.63E+00	4.06E-01	7.67E-01	1.04E+00
F_{36}	Best	2.42E+02	1.35E+02	3.38E+01	7.07E+02	5.37E+02	1.80E+02	3.59E+02	1.33E+02	7.74E+02	6.22E+02	1.28E+02	2.93E+02	3.30E+01	3.72E+01
	Mean	3.95E+02	8.01E+02	1.88E+02	1.16E+03	1.36E+03	5.09E+02	1.03E+03	5.11E+02	1.18E+03	1.14E+03	7.63E+02	8.94E+02	3.09E+02	3.41E+02
	Std	7.05E+01	2.88E+02	7.50E+01	2.70E+02	4.22E+02	1.77E+02	3.73E+02	2.36E+02	2.00E+02	2.08E+02	3.63E+02	2.80E+02	1.73E+02	2.27E+02
F_{37}	Best	2.23E+00	3.14E+00	3.04E+00	4.60E+00	4.36E+00	2.67E+00	3.42E+00	1.96E+00	3.76E+00	3.37E+00	3.06E+00	3.54E+00	2.53E+00	2.67E+00
	Mean	3.12E+00	4.04E+00	3.41E+00	5.27E+00	5.25E+00	3.62E+00	4.53E+00	3.55E+00	4.20E+00	4.19E+00	3.75E+00	3.87E+00	3.24E+00	3.69E+00
	Std	3.88E-01	4.85E-01	2.32E-01	2.17E-01	2.73E-01	4.03E-01	3.42E-01	5.27E-01	2.30E-01	3.14E-01	3.70E-01	1.89E-01	2.86E-01	4.47E-01
F_{38}	Best	1.04E+00	1.09E+00	1.10E+00	1.01E+00	2.41E+00	1.09E+00	1.10E+00	1.03E+00	1.20E+00	1.22E+00	1.10E+00	1.11E+00	1.09E+00	1.16E+00
	Mean	1.09E+00	1.19E+00	1.15E+00	1.03E+00	4.22E+00	1.17E+00	1.35E+00	1.15E+00	1.41E+00	1.49E+00	1.21E+00	1.17E+00	1.14E+00	1.37E+00
	Std	2.27E-02	7.68E-02	2.55E-02	1.30E-02	9.55E-01	8.41E-02	1.66E-01	7.44E-02	8.38E-02	1.15E-01	9.41E-02	2.91E-02	2.61E-02	9.64E-02
F_{39}	Best	2.16E+00	2.10E+01	2.83E+00	1.00E+00	2.10E+01	7.07E+00	2.10E+01	1.00E+00	2.11E+01	2.12E+01	2.16E+00	2.12E+01	2.02E+01	2.10E+01
	Mean	1.22E+01	2.11E+01	1.85E+01	1.83E+01	2.10E+01	2.09E+01	2.12E+01	1.90E+01	2.13E+01	2.14E+01	2.04E+01	2.13E+01	2.11E+01	2.10E+01
	Std	9.09E+00	9.21E-02	5.91E+00	6.91E+00	5.61E-05	2.61E+00	1.73E-01	6.10E+00	9.05E-02	7.17E-02	3.44E+00	6.57E-02	2.30E-01	1.71E-02

The bold values indicate the best solutions found by the algorithms.

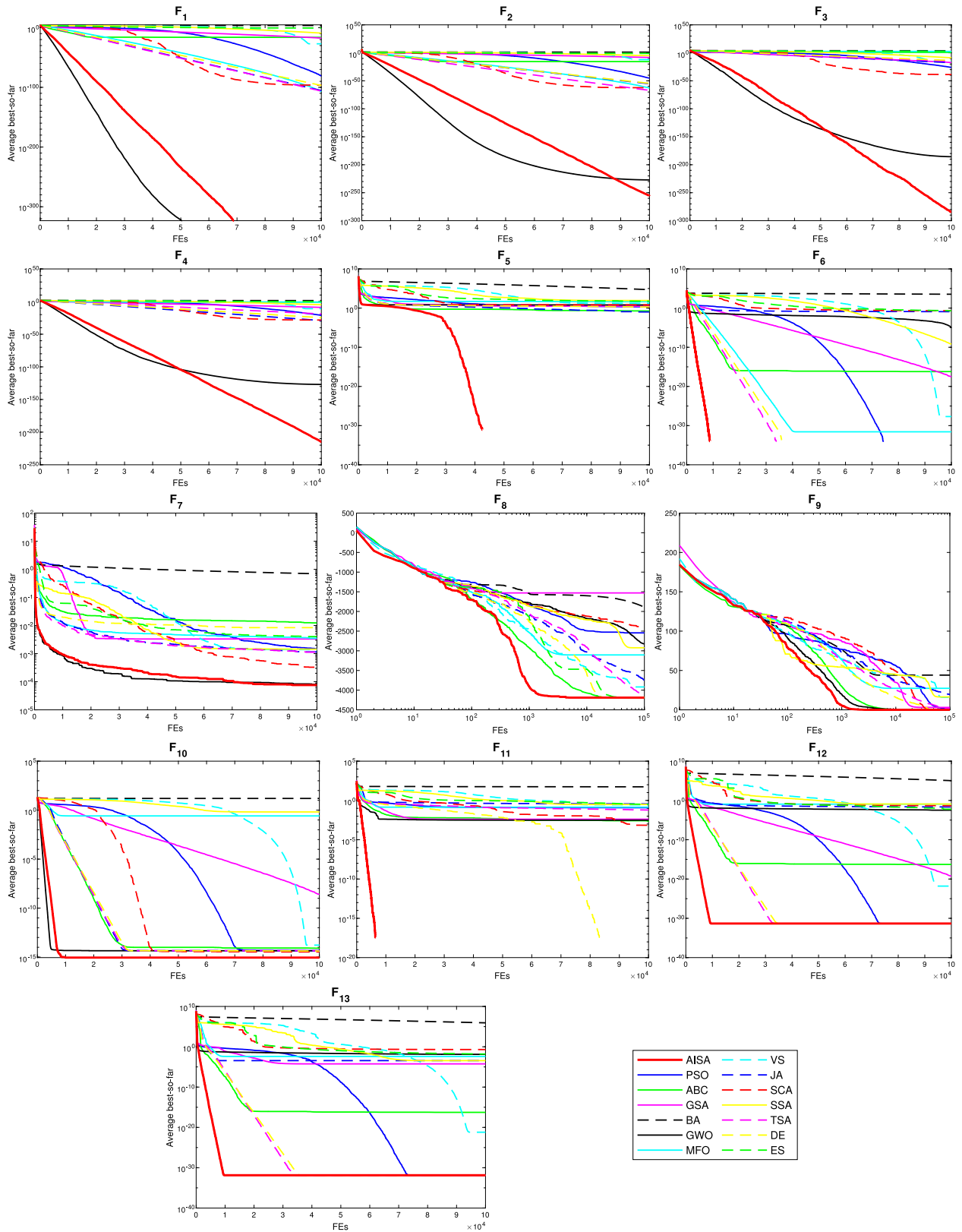


Fig. 7. Convergence curves of the algorithms on F_1 - F_{13} with 10 dimensions.

4.4.7. Convergence analysis

In this part, in order to further check the efficacy of the proposed algorithm, convergence behavior of the algorithms is

investigated on all benchmark functions. Figs. 7–11 show the convergence curves of AISA and other competitive algorithms while optimizing the test functions. It should be noted that average

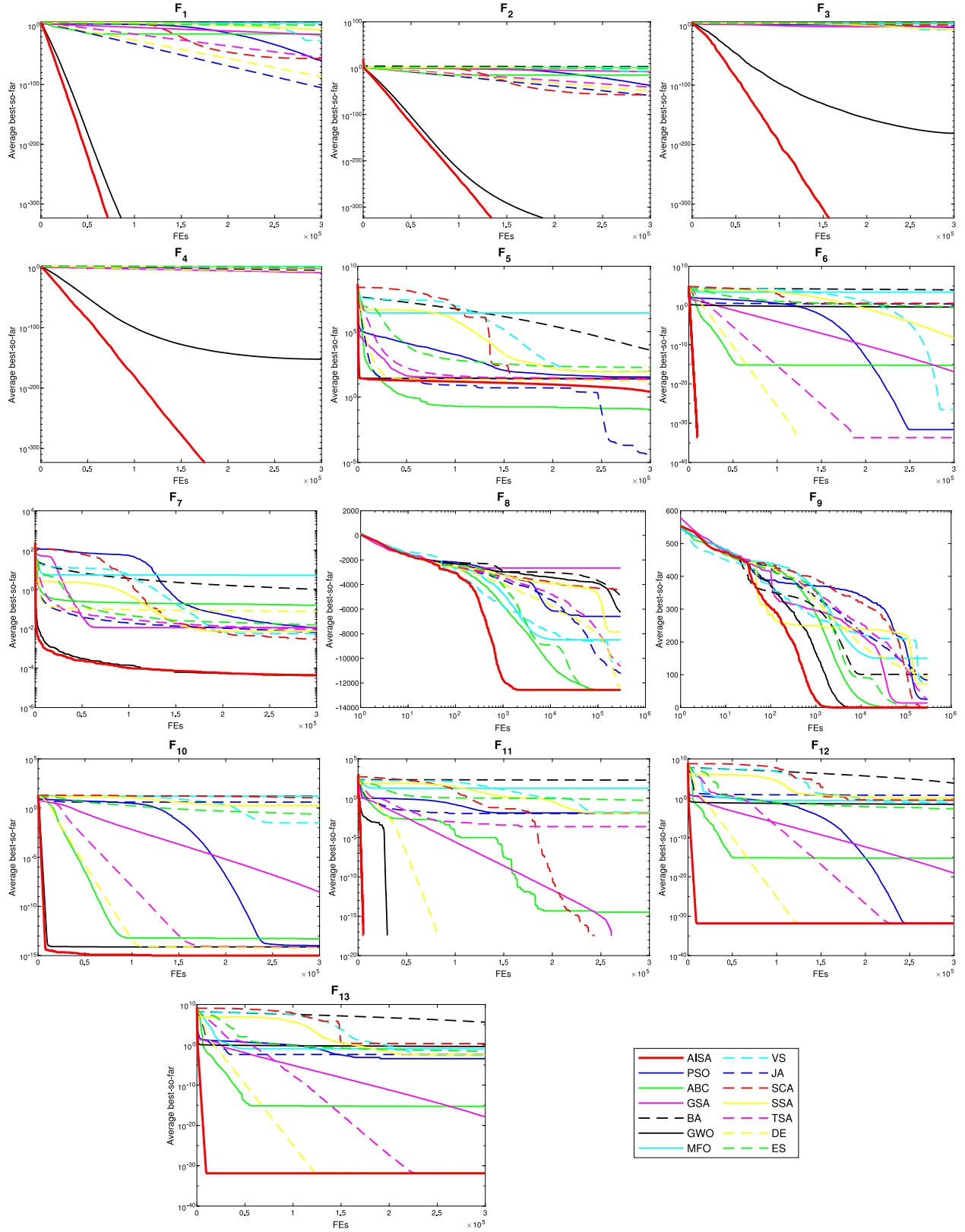


Fig. 8. Convergence curves of the algorithms on F_1 – F_{13} with 30 dimensions.

best-so-far is the average of the best solution obtained so far in each function evaluation (FE) over 30 runs.

Fig. 7 shows convergence performance of the algorithms on 10-dimensional unimodal and multimodal functions. It is observed that the AISA algorithm performs much better than other

competitors, except for F_1 . Figs. 8 and 9 indicate the curves on 30- and 50-dimensional unimodal and multimodal functions, respectively. It is seen that AISA can converge quickly to the optimal solution with less calculation, except for function F_5 . These results indicate that AISA achieves consistent

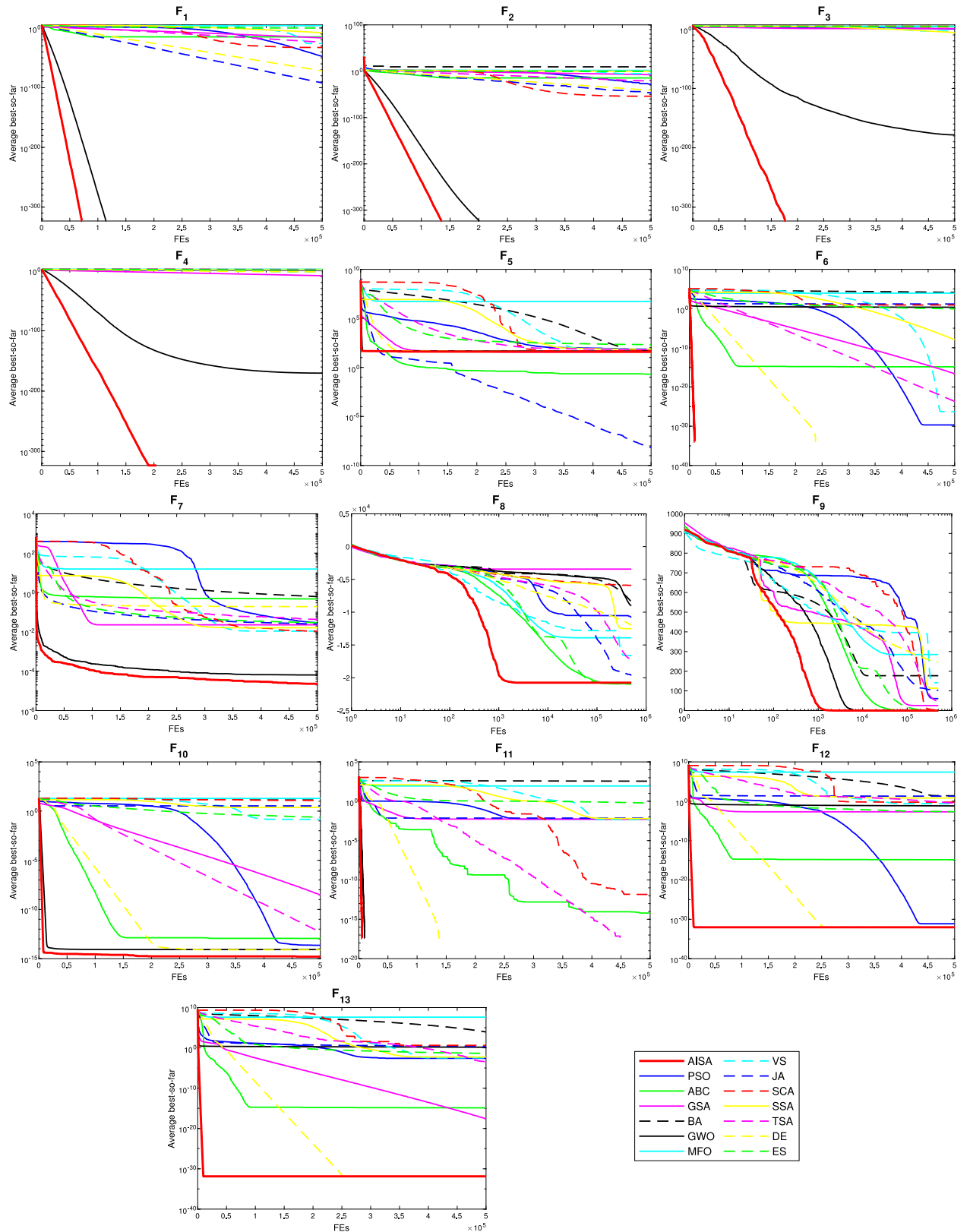


Fig. 9. Convergence curves of the algorithms on F_1 – F_{13} with 50 dimensions.

convergence success on both unimodal and multimodal functions with different dimensions. In addition, Figs. 10 and 11 present the convergence history of all algorithms on remainder functions, AISA exhibits a remarkable convergence rate in more than half

of the functions and achieves a steady state. Within general framework of convergence analysis, the results reveal that AISA is very competitive as compared to other competitor algorithms in terms of the convergence rate.

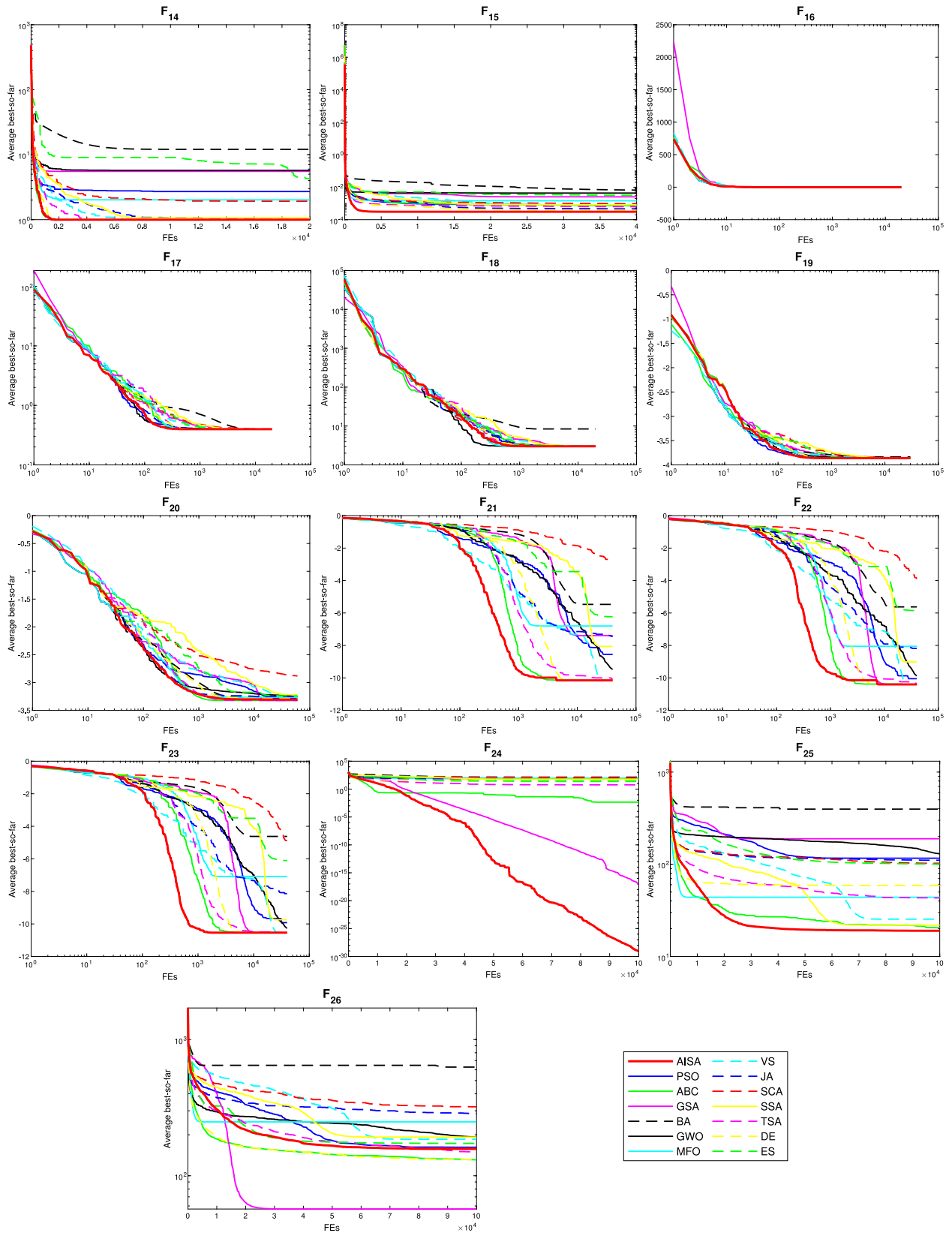
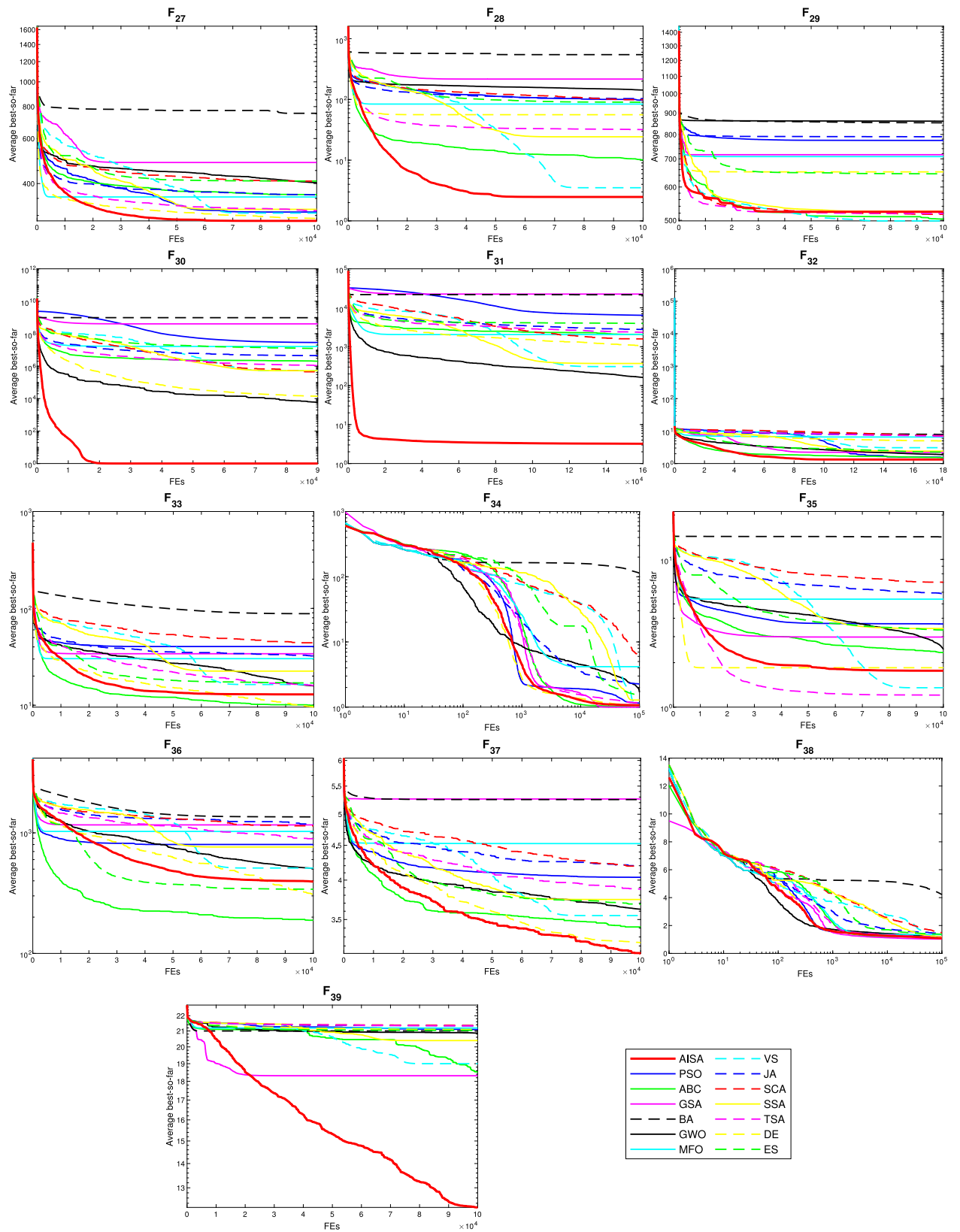


Fig. 10. Convergence curves of the algorithms on F_{14} – F_{26} .

4.5. Computational time analysis

Another assessment measure to judge the performance of the algorithms is investigated, which is the running time taken by the

optimizers. Fig. 12 visually compares the total running time for each algorithm, which is the sum of running times for 30 times over all benchmark functions such as unimodal functions with 10, 30 and 50 dimensions, multimodal functions with 10, 30 and

Fig. 11. Convergence curves of the algorithms on F_{27} – F_{39} .

50 dimensions, fixed-dimension multimodal functions, composite functions and CEC 2019 functions. The figure demonstrates that the total running time of AISA is 12 545 s on all problems. AISA

performs faster than well-established optimizers such as GSA, DE and ES. It should be noted that the execution time cost of AISA is due to the extra calculation required by the CFLN optimized by

Table 16The results of two-sided Wilcoxon signed-rank test with $\alpha = 0.05$ for $F_1 - F_7$ with 10 dimensions.

<i>F</i>	PSO	ABC	GSA	BA	GWO	MFO	VS	JA	SCA	SSA	TSA	DE	ES
F_1 (T+, T-)	p-value (0, 465)	1.73E-06 (0, 465)	1.73E-06 (0, 465)	1.73E-06 (0, 465)	1 (0, 0)	1.73E-06 (0, 465)	1.73E-06 (0, 465)	1.73E-06 (0, 465)	1.73E-06 (0, 465)	1.73E-06 (0, 465)	1.73E-06 (0, 465)	1.73E-06 (0, 465)	1.73E-06 (0, 465)
	Winner	+	+	+	=	+	+	+	+	+	+	+	+
F_2 (T+, T-)	p-value (0, 465)	1.73E-06 (0, 465)	1.73E-06 (0, 465)	1.73E-06 (0, 465)	1.73E-06 (0, 465)	1.73E-06 (0, 465)	1.73E-06 (0, 465)	1.73E-06 (0, 465)	1.73E-06 (0, 465)	1.73E-06 (0, 465)	1.73E-06 (0, 465)	1.73E-06 (0, 465)	1.73E-06 (0, 465)
	Winner	+	+	+	=	+	+	+	+	+	+	+	+
F_3 (T+, T-)	p-value (0, 465)	1.73E-06 (0, 465)	1.73E-06 (0, 465)	1.73E-06 (0, 465)	1.73E-06 (0, 465)	1.73E-06 (0, 465)	1.73E-06 (0, 465)	1.73E-06 (0, 465)	1.73E-06 (0, 465)	1.73E-06 (0, 465)	1.73E-06 (0, 465)	1.73E-06 (0, 465)	1.73E-06 (0, 465)
	Winner	+	+	+	=	+	+	+	+	+	+	+	+
F_4 (T+, T-)	p-value (0, 465)	1.73E-06 (0, 465)	1.73E-06 (0, 465)	1.73E-06 (0, 465)	1.73E-06 (0, 465)	1.73E-06 (0, 465)	1.73E-06 (0, 465)	1.73E-06 (0, 465)	1.73E-06 (0, 465)	1.73E-06 (0, 465)	1.73E-06 (0, 465)	1.73E-06 (0, 465)	1.73E-06 (0, 465)
	Winner	+	+	+	=	+	+	+	+	+	+	+	+
F_5 (T+, T-)	p-value (0, 465)	1.73E-06 (0, 465)	1.73E-06 (0, 465)	1.73E-06 (0, 465)	1.73E-06 (0, 465)	1.72E-06 (0, 465)	1.73E-06 (0, 465)	1.73E-06 (0, 465)	1.73E-06 (0, 465)	1.73E-06 (0, 465)	1.73E-06 (0, 465)	1.73E-06 (0, 465)	1.73E-06 (0, 465)
	Winner	+	+	+	=	+	+	+	+	+	+	+	+
F_6 (T+, T-)	p-value (0, 0)	1 (0, 0)	1.73E-06 (0, 465)	1.73E-06 (0, 465)	1.73E-06 (0, 465)	1.73E-06 (0, 465)	3.51E-06 (0, 406)	1.73E-06 (0, 465)	1.73E-06 (0, 465)	1.73E-06 (0, 465)	1.73E-06 (0, 465)	1 (0, 0)	1.73E-06 (0, 465)
	Winner	=	+	+	=	+	+	+	+	+	+	=	+
F_7 (T+, T-)	p-value (0, 465)	1.73E-06 (0, 465)	1.73E-06 (0, 465)	1.73E-06 (0, 465)	0.39333 (274, 191)	1.73E-06 (0, 465)	1.92E-06 (1, 464)	1.73E-06 (0, 465)	5.79E-05 (37, 428)	1.73E-06 (0, 465)	1.73E-06 (0, 465)	1.73E-06 (0, 465)	1.73E-06 (0, 465)
	Winner	+	+	+	=	+	+	+	+	+	+	+	+
Total (+/-/-)	6/1/0	7/0/0	7/0/0	7/0/0	5/2/0	7/0/0	7/0/0	7/0/0	7/0/0	7/0/0	6/1/0	6/1/0	7/0/0

Table 17The results of two-sided Wilcoxon signed-rank test with $\alpha = 0.05$ for $F_1 - F_7$ with 30 dimensions.

<i>F</i>	PSO	ABC	GSA	BA	GWO	MFO	VS	JA	SCA	SSA	TSA	DE	ES
F_1 (T+, T-)	p-value (0, 465)	1.73E-06 (0, 465)	1.73E-06 (0, 465)	1.73E-06 (0, 465)	1 (0, 0)	1.72E-06 (0, 465)	1.73E-06 (0, 465)	1.73E-06 (0, 465)	1.73E-06 (0, 465)	1.73E-06 (0, 465)	1.73E-06 (0, 465)	1.73E-06 (0, 465)	1.73E-06 (0, 465)
	Winner	+	+	+	=	+	+	+	+	+	+	+	+
F_2 (T+, T-)	p-value (0, 465)	1.73E-06 (0, 465)	1.73E-06 (0, 465)	1.73E-06 (0, 465)	1 (0, 0)	1.59E-06 (0, 465)	1.73E-06 (0, 465)	1.73E-06 (0, 465)	1.73E-06 (0, 465)	1.73E-06 (0, 465)	1.73E-06 (0, 465)	1.73E-06 (0, 465)	1.73E-06 (0, 465)
	Winner	+	+	+	=	+	+	+	+	+	+	+	+
F_3 (T+, T-)	p-value (0, 465)	1.73E-06 (0, 465)	1.73E-06 (0, 465)	1.73E-06 (0, 465)	1.73E-06 (0, 465)	1.73E-06 (0, 465)	1.73E-06 (0, 465)	1.73E-06 (0, 465)	1.73E-06 (0, 465)	1.73E-06 (0, 465)	1.73E-06 (0, 465)	1.73E-06 (0, 465)	1.73E-06 (0, 465)
	Winner	+	+	+	=	+	+	+	+	+	+	+	+
F_4 (T+, T-)	p-value (0, 465)	1.73E-06 (0, 465)	1.73E-06 (0, 465)	1.73E-06 (0, 465)	1.73E-06 (0, 465)	1.73E-06 (0, 465)	1.73E-06 (0, 465)	1.73E-06 (0, 465)	1.73E-06 (0, 465)	1.73E-06 (0, 465)	1.73E-06 (0, 465)	1.73E-06 (0, 465)	1.73E-06 (0, 465)
	Winner	+	+	+	=	+	+	+	+	+	+	+	+
F_5 (T+, T-)	p-value (7, 458)	3.52E-06 (410, 55)	2.61E-04 (410, 55)	1.73E-06 (0, 465)	1.73E-06 (0, 465)	1.73E-06 (0, 465)	1.02E-05 (18, 447)	1.73E-06 (0, 465)	2.61E-04 (410, 55)	1.73E-06 (0, 465)	1.73E-06 (0, 465)	1.73E-06 (0, 465)	1.73E-06 (0, 465)
	Winner	-	+	+	=	+	+	+	-	+	+	+	+
F_6 (T+, T-)	p-value (0, 435)	2.45E-06 (0, 465)	1.73E-06 (0, 465)	1.73E-06 (0, 465)	1.73E-06 (0, 465)	1.73E-06 (0, 465)	1.73E-06 (0, 465)	1.73E-06 (0, 465)	1.73E-06 (0, 465)	1.73E-06 (0, 465)	0.5 (0, 3)	1 (0, 0)	1.73E-06 (0, 465)
	Winner	+	+	+	=	+	+	+	+	+	=	=	+
F_7 (T+, T-)	p-value (0, 465)	1.73E-06 (0, 465)	1.73E-06 (0, 465)	1.73E-06 (0, 465)	0.46528 (197, 268)	1.73E-06 (0, 465)	1.73E-06 (0, 465)	1.73E-06 (0, 465)	1.73E-06 (0, 465)	1.73E-06 (0, 465)	1.73E-06 (0, 465)	1.73E-06 (0, 465)	1.73E-06 (0, 465)
	Winner	+	+	+	=	+	+	+	+	+	+	+	+
Total (+/-/-)	7/0/0	6/0/1	7/0/0	7/0/0	4/3/0	7/0/0	7/0/0	6/0/1	7/0/0	7/0/0	6/1/0	6/1/0	7/0/0

LSE. Nevertheless, it can be clearly stated that AISA has a satisfactory performance when all experimental analysis is considered.

5. Experiments on engineering problems

Up to this point, the performance of AISA algorithm was investigated on standard test problems with respect to different performance measures. However, in order to test performance of the proposed approach for real-time applications, it is applied to solve IIR filter-based system identification problem and the inverse kinematics problem of a seven degrees of freedom (7-DOF) serial robot manipulator.

5.1. Adaptive IIR system identification

Infinite impulse response (IIR) filter is a type of digital filter and has been used for engineering applications in signal processing, control, communication and many more. As the IIR filter

has a recursive structure, the current output depends upon not only on present input but also the previous inputs and outputs. The main task of the system identification is to determine the parameters of the adaptive IIR filter iteratively using an optimization algorithm until the output of filter is matched to the output of unknown system when the same input is applied synchronically to both the adaptive filter and unknown system. In general, the error surface of identification system can be nonlinear, non-differentiable and multimodal [82]. To overcome these difficulties, many metaheuristic algorithms have been in demand for IIR system identification and filter design [83]. A system identification configuration using an adaptive IIR filter is shown in Fig. 13.

The input-output relationship of an adaptive IIR filter is governed by the following difference equation:

$$y(n) + \sum_{i=1}^M a_i y(n-i) = \sum_{j=0}^N b_j x(m-j) \quad (29)$$

Table 18

The results of two-sided Wilcoxon signed-rank test with $\alpha = 0.05$ for $F_1 - F_7$ with 50 dimensions.

<i>F</i>	PSO	ABC	GSA	BA	GWO	MFO	VS	JA	SCA	SSA	TSA	DE	ES
F_1 (T+, T-) Winner	1.73E-06 (0, 465)	1.73E-06 (0, 465)	1.73E-06 (0, 465)	1.73E-06 (0, 465)	1 (0, 0)	1.36E-06 (0, 465)	1.73E-06 (0, 465)	1.73E-06 (0, 465)	1.73E-06 (0, 465)	1.73E-06 (0, 465)	1.73E-06 (0, 465)	1.73E-06 (0, 465)	1.73E-06 (0, 465)
	+ +	+ +	+ +	+ +	= =	+ +	+ +	+ +	+ +	+ +	+ +	+ +	+ +
F_2 (T+, T-) Winner	1.73E-06 (0, 465)	1.73E-06 (0, 465)	1.73E-06 (0, 465)	1.73E-06 (0, 465)	1 (0, 0)	1.68E-06 (0, 465)	1.73E-06 (0, 465)	1.73E-06 (0, 465)	1.73E-06 (0, 465)	1.73E-06 (0, 465)	1.73E-06 (0, 465)	1.73E-06 (0, 465)	1.73E-06 (0, 465)
	+ +	+ +	+ +	+ +	= =	+ +	+ +	+ +	+ +	+ +	+ +	+ +	+ +
F_3 (T+, T-) Winner	1.73E-06 (0, 465)	1.73E-06 (0, 465)	1.73E-06 (0, 465)	1.73E-06 (0, 465)	1.73E-06 (0, 465)	1.73E-06 (0, 465)	1.73E-06 (0, 465)	1.73E-06 (0, 465)	1.73E-06 (0, 465)	1.73E-06 (0, 465)	1.73E-06 (0, 465)	1.73E-06 (0, 465)	1.73E-06 (0, 465)
	+ +	+ +	+ +	+ +	= =	+ +	+ +	+ +	+ +	+ +	+ +	+ +	+ +
F_4 (T+, T-) Winner	1.73E-06 (0, 465)	1.73E-06 (0, 465)	1.73E-06 (0, 465)	1.73E-06 (0, 465)	1.73E-06 (0, 465)	1.73E-06 (0, 465)	1.73E-06 (0, 465)	1.73E-06 (0, 465)	1.73E-06 (0, 465)	1.73E-06 (0, 465)	1.73E-06 (0, 465)	1.73E-06 (0, 465)	1.73E-06 (0, 465)
	+ +	+ +	+ +	+ +	= =	+ +	+ +	+ +	+ +	+ +	+ +	+ +	+ +
F_5 (T+, T-) Winner	3.38E-03 (90, 375)	3.18E-06 (459, 6)	2.77E-03 (378, 87)	0.42843 (271, 194)	1.73E-06 (0, 465)	2.05E-04 (52, 413)	1.73E-06 (0, 465)	3.18E-06 (459, 6)	1.73E-06 (0, 465)	1.15E-04 (45, 420)	3.16E-03 (89, 376)	0.01480 (351, 114)	1.73E-06 (0, 465)
	+ -	- -	- -	= =	+ +	+ +	+ +	- +	+ +	+ +	+ +	- -	+ +
F_6 (T+, T-) Winner	1.73E-06 (0, 465)	1.73E-06 (0, 465)	1.73E-06 (0, 465)	1.73E-06 (0, 465)	1.73E-06 (0, 465)	1.66E-06 (0, 465)	1.73E-06 (0, 465)	1.73E-06 (0, 465)	1.73E-06 (0, 465)	1.73E-06 (0, 465)	1.73E-06 (0, 465)	1.73E-06 (0, 465)	1.73E-06 (0, 465)
	+ +	+ +	+ +	+ +	= =	+ +	+ +	+ +	+ +	+ +	+ +	= =	+ +
F_7 (T+, T-) Winner	1.73E-06 (0, 465)	1.73E-06 (0, 465)	1.73E-06 (0, 465)	1.73E-06 (0, 465)	1.64E-05 (23, 442)	1.73E-06 (0, 465)	1.73E-06 (0, 465)	1.73E-06 (0, 465)	1.73E-06 (0, 465)	1.73E-06 (0, 465)	1.73E-06 (0, 465)	1.73E-06 (0, 465)	1.73E-06 (0, 465)
	+ +	+ +	+ +	+ +	= =	+ +	+ +	+ +	+ +	+ +	+ +	+ +	+ +
Total (+/-/-)	7/0/0	6/0/1	6/0/1	6/1/0	5/2/0	7/0/0	7/0/0	6/0/1	7/0/0	7/0/0	7/0/0	5/1/1	7/0/0

Table 19

The results of two-sided Wilcoxon signed-rank test with $\alpha = 0.05$ for $F_8 - F_{13}$ with 10 dimensions.

<i>F</i>	PSO	ABC	GSA	BA	GWO	MFO	VS	JA	SCA	SSA	TSA	DE	ES
F_8 (T+, T-) Winner	1.73E-06 (0, 465)	1 (0, 0)	1.73E-06 (0, 465)	1.73E-06 (0, 465)	1.73E-06 (0, 465)	1.72E-06 (0, 276)	2.65E-05 (0, 153)	2.93E-04 (0, 465)	1.73E-06 (0, 465)	1.73E-06 (0, 465)	1.46E-04 (0, 171)	0.25 (0, 6)	1.73E-06 (0, 465)
	+ =	+ +	+ +	+ +	= =	+ +	+ +	+ +	+ +	+ +	+ +	= =	+ +
F_9 (T+, T-) Winner	1.11E-05 (0, 325)	1 (0, 0)	1.56E-06 (0, 465)	1.73E-06 (0, 465)	1 (0, 0)	1.73E-06 (0, 465)	1.73E-06 (0, 465)	1.73E-06 (0, 465)	1 (0, 0)	1.73E-06 (0, 465)	1.19E-05 (0, 325)	1 (0, 0)	1.73E-06 (0, 465)
	+ =	+ =	+ +	+ +	= =	+ +	+ +	+ +	+ +	+ +	+ +	= =	+ +
F_{10} (T+, T-) Winner	6.80E-08 (0, 465)	1.01E-07 (0, 465)	1.73E-06 (0, 465)	1.73E-06 (0, 465)	4.32E-08 (0, 435)	2.40E-07 (0, 465)	1.24E-06 (0, 231)	4.32E-08 (0, 465)	4.59E-06 (0, 465)	1.73E-06 (0, 465)	4.32E-08 (0, 465)	2.03E-07 (0, 378)	1.73E-06 (0, 465)
	+ +	+ +	+ +	+ +	= =	+ +	+ +	+ +	+ +	+ +	+ +	= =	+ +
F_{11} (T+, T-) Winner	1.73E-06 (0, 465)	5.60E-06 (0, 378)	4.88E-04 (0, 78)	1.73E-06 (0, 465)	0.01563 (0, 28)	1.73E-06 (0, 465)	1.73E-06 (0, 465)	1.73E-06 (0, 465)	0.5 (0, 3)	1.73E-06 (0, 465)	2.56E-06 (0, 435)	1 (0, 0)	1.73E-06 (0, 465)
	+ +	+ +	+ +	+ +	= =	+ +	+ +	+ +	= =	+ +	+ +	= =	+ +
F_{12} (T+, T-) Winner	0.125 (0, 10)	1.73E-06 (0, 465)	1.73E-06 (0, 465)	1.73E-06 (0, 465)	1.73E-06 (0, 465)	1.78E-05 (0, 300)	1.73E-06 (0, 465)	1.73E-06 (0, 465)	1.73E-06 (0, 465)	1.73E-06 (0, 465)	1 (0, 0)	1 (0, 0)	1.73E-06 (0, 465)
	= +	+ +	+ +	+ +	= =	+ +	+ +	+ +	+ +	+ +	= =	= =	+ +
F_{13} (T+, T-) Winner	1 (0, 0)	1.73E-06 (0, 465)	1.73E-06 (0, 465)	1.73E-06 (0, 465)	1.73E-06 (0, 465)	6.81E-06 (0, 351)	1.73E-06 (0, 465)	1.73E-06 (0, 465)	1 (0, 1)	1.73E-06 (0, 465)	1 (0, 465)	1 (0, 0)	1.73E-06 (0, 465)
	= +	+ +	+ +	+ +	= =	+ +	+ +	+ +	+ +	+ +	= =	= =	+ +
Total (+/-/-)	4/2/0	4/2/0	6/0/0	6/0/0	5/1/0	6/0/0	6/0/0	6/0/0	4/2/0	6/0/0	4/2/0	1/5/0	6/0/0

Table 20

The results of two-sided Wilcoxon signed-rank test with $\alpha = 0.05$ for $F_8 - F_{13}$ with 30 dimensions.

<i>F</i>	PSO	ABC	GSA	BA	GWO	MFO	VS	JA	SCA	SSA	TSA	DE	ES	
F_8 (T+, T-) Winner	1.73E-06 (0, 465)	1.54E-05 (0, 300)	1.73E-06 (0, 465)	6.10E-05 (0, 120)	1.73E-06 (0, 465)	1.73E-06 (0, 465)	1.73E-06 (0, 465)	1.61E-05 (0, 300)	1.73E-06 (0, 465)					
	+ +	+ +	+ +	+ +	= =	+ +	+ +	+ +	+ +	+ +	+ +	= =	+ +	
F_9 (T+, T-) Winner	1.72E-06 (0, 465)	2.58E-06 (0, 406)	1.68E-06 (0, 465)	1.73E-06 (0, 465)	1 (0, 0)	1.73E-06 (0, 465)	1.73E-06 (0, 465)	0.25 (0, 6)	1.73E-06 (0, 465)					
	+ +	+ +	+ +	+ +	= =	+ +	+ +	+ +	+ +	+ +	+ +	= =	+ +	
F_{10} (T+, T-) Winner	6.47E-07 (0, 465)	1.36E-06 (0, 465)	1.73E-06 (0, 465)	1.73E-06 (0, 465)	1.96E-07 (0, 465)	1.73E-06 (0, 465)	1.51E-06 (0, 465)	1.70E-06 (0, 465)	1.71E-06 (0, 465)	1.73E-06 (0, 465)	2.57E-07 (0, 465)	1.24E-06 (0, 435)	1.73E-06 (0, 465)	
	+ +	+ +	+ +	+ +	= =	+ +	+ +	+ +	+ +	+ +	+ +	= =	+ +	
F_{11} (T+, T-) Winner	1.18E-05 (0, 325)	2.52E-06 (0, 435)	1 (0, 0)	1.73E-06 (0, 465)	1 (0, 0)	3.99E-05 (0, 253)	1.73E-06 (0, 465)	1.31E-04 (0, 190)	1 (0, 0)	1.73E-06 (0, 465)	0.5 (0, 3)	1 (0, 0)	1.73E-06 (0, 465)	
	+ +	+ +	= =	+ +	= =	+ +	+ +	+ +	= =	+ +	= =	= =	+ +	
F_{12} (T+, T-) Winner	3.65E-06 (0, 406)	1.73E-06 (0, 465)	1 (0, 1)	1 (0, 0)	1.73E-06 (0, 465)									
	+ +	+ +	+ +	+ +	= =	+ +	+ +	+ +	+ +	+ +	= =	= =	+ +	
F_{13} (T+, T-) Winner	1.16E-05 (0, 325)	1.73E-06 (0, 465)	1.73E-06 (0, 465)	1.73E-06 (0, 465)	1.73E-06 (0, 465)	1.37E-06 (0, 465)	1.73E-06 (0, 465)	1.73E-06 (0, 465)	7.61E-05 (0, 210)	1.73E-06 (0, 465)	1.73E-06 (0, 465)	0.5 (0, 3)	1 (0, 0)	1.73E-06 (0, 465)
	+ +	+ +	+ +	+ +	= =	+ +	+ +	+ +	+ +	+ +	= =			

Table 21

The results of two-sided Wilcoxon signed-rank test with $\alpha = 0.05$ for $F_8 - F_{13}$ with 50 dimensions.

<i>F</i>	PSO	ABC	GSA	BA	GWO	MFO	VS	JA	SCA	SSA	TSA	DE	ES
F_8 (T+, T-) Winner	1.73E-06 (0, 465)	3.11E-05 (30, 435)	1.73E-06 (0, 465)	1.73E-06 (0, 465)	1.73E-06 (0, 465)	1.73E-06 (0, 465)	1.92E-06 (1, 464)	4.90E-05 (25, 381)	1.73E-06 (0, 465)	1.73E-06 (0, 465)	3.18E-06 (6, 459)	1.73E-06 (0, 465)	3.11E-05 (30, 435)
	p-value + +												
F_9 (T+, T-) Winner	1.73E-06 (0, 465)	1.73E-06 (0, 465)	1.71E-06 (0, 465)	1.73E-06 (0, 465)	1 (0, 0)	1.73E-06 (0, 465)	1.73E-06 (0, 465)	0.01563 (0, 28)	1.73E-06 (0, 465)				
	p-value + +												
F_{10} (T+, T-) Winner	1.53E-06 (0, 465)	1.68E-06 (0, 465)	1.73E-06 (0, 465)	1.73E-06 (0, 465)	4.11E-07 (0, 465)	1.73E-06 (0, 465)	1.69E-06 (0, 465)	1.73E-06 (0, 465)	1.71E-06 (0, 465)	1.73E-06 (0, 465)	3.26E-07 (0, 465)	1.73E-06 (0, 465)	
	p-value + +												
F_{11} (T+, T-) Winner	6.10E-05 (0, 120)	1.72E-06 (0, 465)	0.25 (0, 6)	1.73E-06 (0, 465)	1 (0, 0)	8.30E-06 (0, 351)	1.72E-06 (0, 465)	5.54E-06 (0, 378)	0.5 (0, 3)	1.73E-06 (0, 465)	1 (0, 0)	1 (0, 0)	1.73E-06 (0, 465)
	p-value + +												
F_{12} (T+, T-) Winner	1.73E-06 (0, 465)	1.73E-06 (0, 465)	1.73E-06 (0, 465)	1.73E-06 (0, 465)	1.73E-06 (0, 465)	1.71E-06 (0, 465)	1.73E-06 (0, 465)	1.73E-06 (0, 465)	1.73E-06 (0, 465)	1.73E-06 (0, 465)	1 (0, 0)	1 (0, 0)	1.73E-06 (0, 465)
	p-value + +												
F_{13} (T+, T-) Winner	1.67E-06 (0, 465)	1.73E-06 (0, 465)	1.73E-06 (0, 465)	1.73E-06 (0, 465)	1.73E-06 (0, 465)	1.61E-06 (0, 465)	1.72E-06 (0, 465)	2.36E-06 (0, 435)	1.73E-06 (0, 465)	1.73E-06 (0, 465)	1 (0, 0)	1 (0, 0)	1.73E-06 (0, 465)
	p-value + +												
Total (+/-/-)	6/0/0	6/0/0	5/1/0	6/0/0	4/2/0	6/0/0	6/0/0	6/0/0	5/1/0	6/0/0	5/1/0	3/3/0	6/0/0

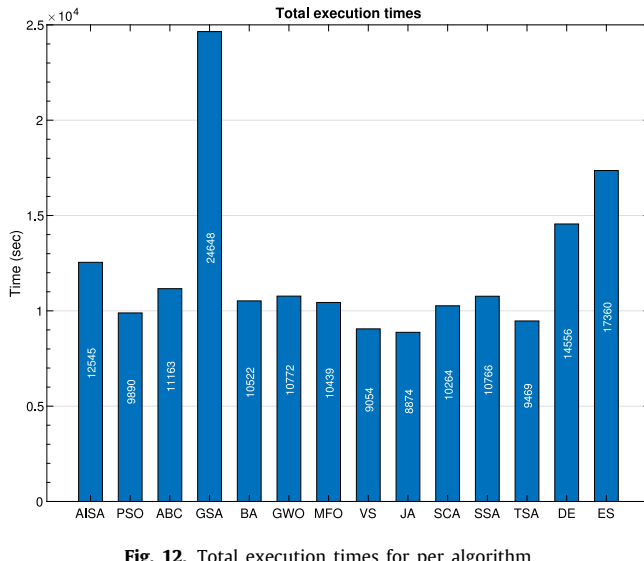


Fig. 12. Total execution times for per algorithm.

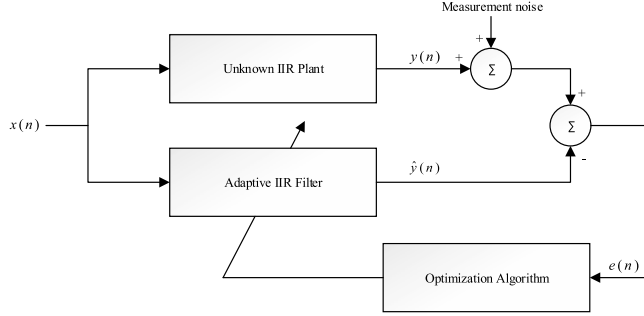


Fig. 13. System identification configuration using an adaptive IIR filter.

where a_i ($i = 1, 2, \dots, M$) and b_j ($j = 0, 1, 2, \dots, N$) are the filter coefficients, $x(n)$ and $y(n)$ are the input and output of the plant at a time instant n , and $M(\geq N)$ is the order of filter, respectively. The transfer function of the adaptive IIR filter is expressed as follows.

$$H(z) = \frac{b_0 + b_1 z^{-1} + \dots + b_N z^{-N}}{1 + a_1 z^{-1} + \dots + a_M z^{-M}} \quad (30)$$

The adaptive IIR system identification has been used to estimate an equivalent model that mimics unknown system behavior. In the its design process, the input samples are first generated to be used on both systems, and then they are applied synchronically to both the adaptive filter and unknown system. Finally, the coefficients of the adaptive IIR filter are estimated by an optimizer in a way to closely match the outputs from both systems. In other words, an objective function between the desired and estimated outputs is minimized. In this work, mean square error (MSE) is considered as the objective function,

$$MSE = \frac{1}{N_s} \sum_{n=1}^{N_s} e(n)^2 \quad (31)$$

where N_s is the number of input-output pairs, $e(n) = y(n) - \hat{y}(n)$ is the identification error signal; $\hat{y}(n)$ is the response of adaptive IIR filter, respectively. Furthermore, MSE can be expressed based on decibel (dB) for practical applications as follows.

$$MSE (\text{dB}) = 10 \log\left(\frac{1}{N_s} \sum_{n=1}^{N_s} e(n)^2\right) \quad (32)$$

In the application part of the identification, two benchmark plants (Ex. 1–2) are used to demonstrate the capability of the proposed ASIA algorithm. The input/test signal is a white noise with zero mean, unit variance, uniform distribution with 256 samples ($N_s = 256$). For the fair comparison of the competitor algorithms, the maximum number of function evaluations is set as used in Section 4.3 and the control parameters of algorithms are used in the same manner which are already given in Table 6.

5.1.1. Example I

In this example, a fourth-order plant is considered as an unknown plant [84] where its transfer function is given as

$$H_s(z) = \frac{1 - 0.9z^{-1} + 0.81z^{-2} - 0.729z^{-3}}{1 + 0.04z^{-1} + 0.2775z^{-2} - 0.2101z^{-3} + 0.14z^{-4}} \quad (33)$$

Case 1: In this case, the unknown fourth-order plant (33) is modeled using a fourth-order IIR filter $H_{af}(z)$. Hence, the transfer function of the adaptive IIR filter model is assumed as

$$H_{af}(z) = \frac{b_0 + b_1 z^{-1} + b_2 z^{-2} + b_3 z^{-3}}{1 - a_1 z^{-1} - a_2 z^{-2} - a_3 z^{-3} - a_4 z^{-4}} \quad (34)$$

Table 22The results of two-sided Wilcoxon signed-rank test with $\alpha = 0.05$ for $F_{14} - F_{23}$.

<i>F</i>	PSO	ABC	GSA	BA	GWO	MFO	VS	JA	SCA	SSA	TSA	DE	ES	
F_{14} (T+, T-) Winner	<i>p</i> -value (0, 253)	1.38E-05 (0, 0)	1 (0, 0)	1.73E-06 (0, 465)	1.73E-06 (0, 465)	1.73E-06 (0, 465)	6.10E-05 (0, 120)	0.01563 (0, 28)	1.73E-06 (0, 465)	1.73E-06 (0, 465)	2.19E-06 (0, 300)	1 (0, 0)	1 (0, 465)	
	+ =	= +	= +	= +	= +	= +	= +	= +	= +	= +	= +	= =	= +	
F_{15} (T+, T-) Winner	<i>p</i> -value (0, 465)	1.73E-06 (0, 465)	1.73E-06 (0, 465)	1.73E-06 (0, 465)	1.73E-06 (0, 465)	1.72E-06 (0, 465)	1.73E-06 (0, 465)	8.11E-06 (3.5, 374.5)	1.73E-06 (0, 465)	1.73E-06 (0, 465)	1.73E-06 (0, 465)	8.00E-04 (16.5, 193.5)	1.73E-06 (0, 465)	
	+ =	= +	= +	= +	= +	= +	= +	= +	= +	= +	= +	= +	= +	
F_{16} (T+, T-) Winner	<i>p</i> -value (36, 0)	7.81E-03 (21, 0)	0.03125 (28, 0)	0.01563 (28, 0)	1.73E-06 (0, 465)	1.73E-06 (0, 465)	3.91E-03 (45, 0)	0.03125 (21, 0)	1.73E-06 (0, 465)	1.73E-06 (0, 465)	5.90E-06 (15, 450)	3.91E-03 (45, 0)	3.91E-03 (45, 0)	1.73E-06 (0, 465)
	- =	- =	- =	- +	- +	- -	- -	- +	- +	- +	- -	- =	- +	
F_{17} (T+, T-) Winner	<i>p</i> -value (0, 0)	1 (0, 0)	1 (0, 0)	1 (0, 0)	1.73E-06 (0, 465)	1.73E-06 (0, 465)	1 (0, 0)	1 (0, 0)	1.73E-06 (0, 465)	1.15E-05 (0, 325)	1 (0, 0)	1 (0, 0)	1.73E-06 (0, 465)	
	= =	= =	= =	= +	= +	= =	= =	= =	= +	= +	= =	= =	= +	
F_{18} (T+, T-) Winner	<i>p</i> -value (115.5, 94.5)	0.65472 (36, 315)	2.47E-04 (12.5, 393.5)	2.55E-06 (0, 465)	1.73E-06 (0, 465)	1.73E-06 (105, 105)	1 (37.5, 287.5)	1.57E-04 (0, 465)	1.73E-06 (0, 465)	1.73E-06 (0, 465)	1.73E-06 (0, 465)	3.47E-04 (189, 21)	4.22E-06 (312, 13)	1.73E-06 (0, 465)
	= =	= +	= +	= +	= +	= =	= +	= +	= +	= +	= -	= -	= +	
F_{19} (T+, T-) Winner	<i>p</i> -value (0, 0)	1 (0, 0)	1 (0, 0)	1 (0, 0)	1.73E-06 (0, 465)	1.73E-06 (0, 465)	1 (0, 0)	0.06250 (0, 15)	1 (0, 0)	1.73E-06 (0, 465)	1.42E-06 (0, 465)	1 (0, 0)	1 (0, 0)	1.73E-06 (0, 465)
	= =	= =	= =	= +	= +	= =	= =	= =	= +	= +	= =	= =	= +	
F_{20} (T+, T-) Winner	<i>p</i> -value (32, 88)	0.11847 (10, 0)	0.125 (10, 0)	0.125 (10, 0)	4.86E-05 (35, 430)	4.53E-04 (62, 403)	0.01071 (27, 126)	1.39E-03 (9, 144)	4.65E-04 (8.5, 127.5)	1.73E-06 (0, 465)	3.52E-06 (7, 458)	0.125 (10, 0)	0.22656 (18, 48)	5.75E-06 (12, 453)
	= =	= =	= =	= +	= +	= +	= +	= +	= +	= +	= =	= =	= +	
F_{21} (T+, T-) Winner	<i>p</i> -value (0, 45)	3.91E-03 (0, 10)	0.125 (0, 78)	4.88E-04 (0, 465)	1.73E-06 (0, 465)	1.73E-06 (0, 136)	1 (0, 0)	8.67E-05 (0, 210)	1.73E-06 (0, 465)	1.73E-06 (0, 465)	0.03125 (0, 21)	1 (0, 0)	1.73E-06 (0, 465)	
	+ =	= =	= +	= +	= +	= +	= =	= +	= +	= +	= +	= =	= +	
F_{22} (T+, T-) Winner	<i>p</i> -value (0, 3)	0.5 (0, 6)	0.25 (0, 0)	1 (0, 0)	1.73E-06 (0, 465)	1.73E-06 (0, 465)	9.77E-04 (0, 66)	1 (0, 0)	2.44E-04 (0, 91)	1.73E-06 (0, 465)	1.73E-06 (0, 465)	0.03125 (0, 21)	1 (0, 0)	1.73E-06 (0, 465)
	= =	= =	= =	= +	= +	= +	= =	= +	= +	= +	= +	= =	= +	
F_{23} (T+, T-) Winner	<i>p</i> -value (0, 6)	0.25 (0, 66)	9.77E-04 (0, 0)	1 (0, 0)	1.73E-06 (0, 465)	1.73E-06 (0, 465)	1.22E-04 (0, 105)	1 (0, 0)	2.44E-04 (0, 91)	1.73E-06 (0, 465)	1.73E-06 (0, 465)	0.125 (0, 10)	1 (0, 0)	1.73E-06 (0, 465)
	= =	= +	= =	= +	= +	= +	= =	= +	= +	= +	= +	= =	= +	
Total (+/-/-)	3/6/1	3/6/1	4/5/1	10/0/0	10/0/0	6/3/1	4/5/1	8/2/0	10/0/0	10/0/0	3/5/2	1/7/2	10/0/0	

Table 23The results of two-sided Wilcoxon signed-rank test with $\alpha = 0.05$ for $F_{24} - F_{29}$.

<i>F</i>	PSO	ABC	GSA	BA	GWO	MFO	VS	JA	SCA	SSA	TSA	DE	ES	
F_{24}	<i>p</i> -value (T+, T-) Winner	2.38E-04 (15, 238) +	1.73E-06 (0, 465) +	1.73E-06 (0, 465) +	1.73E-06 (0, 465) +	7.63E-06 (0, 351) +	0.01449 (104.5, 330.5) +	1.73E-06 (0, 465) +	1.73E-06 (0, 465) +	1.73E-06 (0, 465) +	4.67E-03 (45, 231) +	0.01178 (49, 204) +	1.73E-06 (0, 465) +	
F_{25}	<i>p</i> -value (T+, T-) Winner	1.80E-05 (24, 441) +	0.02849 (126, 339) +	1.73E-06 (0, 465) +	1.73E-06 (0, 465) +	1.02E-05 (18, 447) +	1.48E-03 (78, 387) +	2.77E-03 (87, 378) +	6.98E-06 (14, 451) +	2.88E-06 (5, 460) +	9.27E-03 (106, 359) +	0.07190 (145, 320) =	0.36953 (176, 259) =	3.06E-04 (57, 408) +
F_{26}	<i>p</i> -value (T+, T-) Winner	0.53044 (202, 263) =	8.19E-05 (424, 41) -	1.36E-05 (444, 21) -	1.73E-06 (0, 465) +	4.68E-03 (95, 370) -	1.36E-05 (21, 444) +	0.01044 (108, 357) +	1.73E-06 (0, 465) +	1.73E-06 (0, 465) +	3.85E-03 (92, 373) +	0.12544 (307, 158) =	8.94E-04 (394, 71) -	0.17791 (167, 298) =
F_{27}	<i>p</i> -value (T+, T-) Winner	5.29E-04 (64, 401) +	2.35E-06 (3, 462) +	1.36E-05 (21, 444) +	1.73E-06 (0, 465) +	1.04E-03 (73, 392) +	1.73E-06 (0, 465) +	6.84E-03 (101, 364) +	1.73E-06 (0, 465) +	1.73E-06 (0, 465) +	3.72E-05 (32, 433) +	2.41E-04 (54, 411) +	0.17138 (166, 299) =	1.92E-06 (1, 464) +
F_{28}	<i>p</i> -value (T+, T-) Winner	8.47E-06 (16, 449) +	1.73E-06 (0, 465) +	1.92E-06 (1, 464) +	1.73E-06 (0, 465) +	4.29E-06 (9, 456) +	1.73E-06 (0, 465) +	0.03501 (120, 315) +	1.73E-06 (0, 465) +	1.73E-06 (0, 465) +	2.84E-05 (29, 436) +	2.05E-04 (52, 413) +	7.73E-04 (62, 373) +	1.73E-06 (0, 465) +
F_{29}	<i>p</i> -value (T+, T-) Winner	2.60E-05 (28, 437) +	2.58E-03 (86, 379) +	3.41E-05 (31, 434) +	2.35E-06 (3, 462) +	2.13E-06 (2, 463) +	4.45E-05 (34, 431) +	0.01790 (108, 327) +	6.339E-06 (13, 452) +	0.079710 (220, 245) =	0.12044 (157, 308) =	0.06511 (122, 284) =	4.27E-03 (50, 250) +	1.92E-06 (1, 464) =
Total (+/-/-)		5/1/0	5/0/1	5/0/1	6/0/0	5/0/1	6/0/0	6/0/0	6/0/0	5/1/0	5/1/0	3/3/0	3/2/1	4/2/0

Table 24

The results of two-sided Wilcoxon signed-rank test with $\alpha = 0.05$ for $F_{30} - F_{39}$.

<i>F</i>	PSO	ABC	GSA	BA	GWO	MFO	VS	JA	SCA	SSA	TSA	DE	ES	
F_{30}	<i>p</i> -value (T+, T-) Winner	1.73E-06 (0, 465)	1.73E-06 (0, 465)	1.73E-06 (0, 465)	1.73E-06 (0, 465)	1.73E-06 (0, 465)	1.73E-06 (0, 465)	1.73E-06 (0, 465)	1.73E-06 (0, 465)	1.73E-06 (0, 465)	1.73E-06 (0, 465)	1.73E-06 (0, 465)	1.73E-06 (0, 465)	
		+	+	+	+	+	+	+	+	+	+	+	+	
F_{31}	<i>p</i> -value (T+, T-) Winner	1.73E-06 (0, 465)	1.73E-06 (0, 465)	1.73E-06 (0, 465)	1.73E-06 (0, 465)	1.73E-06 (0, 465)	1.73E-06 (0, 465)	1.73E-06 (0, 465)	1.73E-06 (0, 465)	1.73E-06 (0, 465)	1.73E-06 (0, 465)	1.73E-06 (0, 465)	1.73E-06 (0, 465)	
		+	+	+	+	+	+	+	+	+	+	+	+	
F_{32}	<i>p</i> -value (T+, T-) Winner	0.53648 (128.5, 171.5)	6.64E-04 (67, 398)	0.02840 (66, 210)	1.73E-06 (0, 465)	2.77E-03 (87, 378)	2.35E-06 (3, 462)	9.09E-04 (45, 306)	1.73E-06 (0, 465)	1.73E-06 (0, 465)	7.69E-06 (15, 450)	1.73E-06 (0, 465)	1.73E-06 (0, 465)	
		=	+	+	+	+	+	+	+	+	+	+	+	
F_{33}	<i>p</i> -value (T+, T-) Winner	1.73E-06 (0, 465)	4.68E-03 (370, 95)	1.73E-06 (0, 465)	1.73E-06 (0, 465)	0.05193 (138, 327)	1.92E-06 (1, 464)	0.03160 (128, 337)	1.92E-06 (1, 464)	1.73E-06 (0, 465)	1.60E-04 (49, 416)	3.61E-03 (91, 374)	7.27E-03 (363, 102)	6.04E-03 (99, 366)
		+	-	+	+	=	+	+	+	+	+	+	-	
													+	
F_{34}	<i>p</i> -value (T+, T-) Winner	1.48E-04 (48, 417)	2.35E-06 (462, 3)	1.73E-06 (465, 0)	1.73E-06 (0, 465)	1.73E-06 (0, 465)	2.37E-05 (27, 438)	3.88E-06 (8, 457)	1.73E-06 (0, 465)	1.73E-06 (0, 465)	3.18E-06 (6, 459)	4.53E-04 (62, 403)	0.06564 (322, 143)	1.73E-06 (0, 465)
		+	-	-	+	+	+	+	+	+	+	+	=	
													+	
F_{35}	<i>p</i> -value (T+, T-) Winner	8.47E-06 (16, 449)	7.51E-05 (40, 425)	3.32E-04 (58, 407)	1.73E-06 (0, 465)	0.01852 (118, 347)	1.73E-06 (0, 465)	4.11E-03 (372, 93)	1.73E-06 (0, 465)	1.73E-06 (0, 465)	7.51E-05 (40, 425)	9.71E-05 (422, 43)	0.65833 (211, 254)	9.32E-06 (17, 448)
		+	+	+	+	+	+	-	+	+	+	-	=	
													+	
F_{36}	<i>p</i> -value (T+, T-) Winner	8.47E-06 (16, 449)	1.73E-06 (465, 0)	1.73E-06 (0, 465)	1.73E-06 (0, 465)	1.38E-03 (77, 388)	1.73E-06 (0, 465)	0.01319 (112, 353)	1.73E-06 (0, 465)	1.73E-06 (0, 465)	6.89E-05 (39, 426)	2.60E-06 (4, 461)	0.03501 (335, 130)	0.07865 (318, 147)
		+	-	+	+	+	+	+	+	+	+	-	=	
													=	
F_{37}	<i>p</i> -value (T+, T-) Winner	4.73E-06 (10, 455)	0.03160 (128, 337)	1.73E-06 (0, 465)	1.73E-06 (0, 465)	1.06E-04 (44, 421)	1.73E-06 (0, 465)	7.27E-03 (102, 363)	1.73E-06 (0, 465)	1.92E-06 (1, 464)	1.49E-05 (22, 443)	1.73E-06 (0, 465)	0.16503 (165, 300)	6.89E-05 (39, 426)
		+	+	+	+	+	+	+	+	+	+	+	=	
													+	
F_{38}	<i>p</i> -value (T+, T-) Winner	2.13E-06 (2, 463)	2.88E-06 (5, 460)	2.13E-06 (463, 2)	1.73E-06 (0, 465)	2.88E-06 (5, 460)	1.73E-06 (0, 465)	3.59E-04 (59, 406)	1.73E-06 (0, 465)	1.73E-06 (0, 465)	2.35E-06 (3, 462)	1.73E-06 (0, 465)	7.69E-06 (15, 450)	1.73E-06 (0, 465)
		+	+	-	+	+	+	+	+	+	+	+	+	
													+	
F_{39}	<i>p</i> -value (T+, T-) Winner	3.61E-03 (91, 374)	0.03327 (129, 336)	0.24519 (176, 289)	0.01566 (115, 350)	7.69E-06 (15, 450)	4.20E-04 (61, 404)	0.14139 (161, 304)	1.73E-06 (0, 465)	1.92E-06 (1, 464)	0.03001 (127, 338)	1.73E-06 (0, 465)	1.83E-03 (81, 384)	0.01108 (109, 356)
		+	+	=	+	+	+	=	+	+	+	+	+	
													+	
Total (+/-=)	9/1/0	7/0/3	7/1/2	10/0/0	9/1/0	10/0/0	8/1/1	10/0/0	10/0/0	10/0/0	9/0/1	5/3/2	9/1/0	

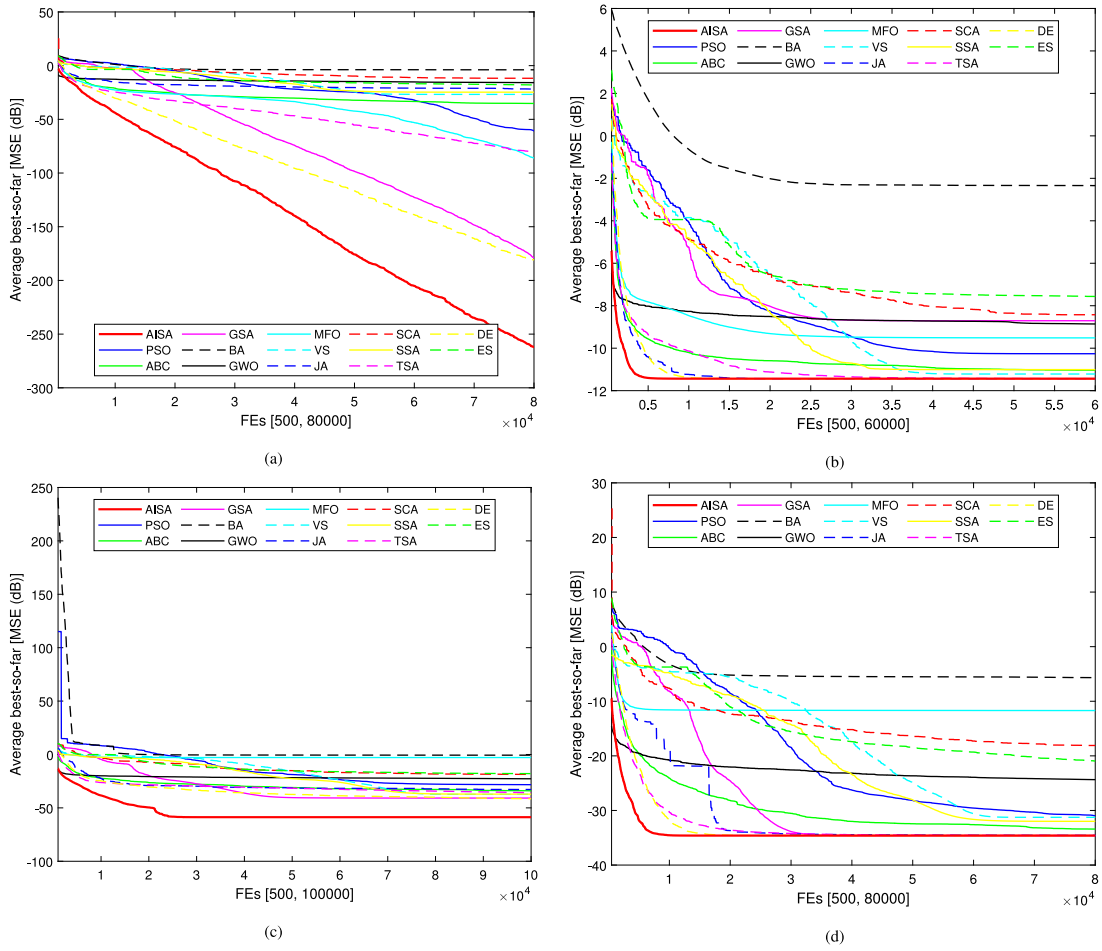


Fig. 14. Convergence characteristics of the algorithms for examples and their cases (a) Example 1 – Case 1; (b) Example 1 – Case 2; (c) Example 2 – Case 1; (d) Example 2 – Case 2.

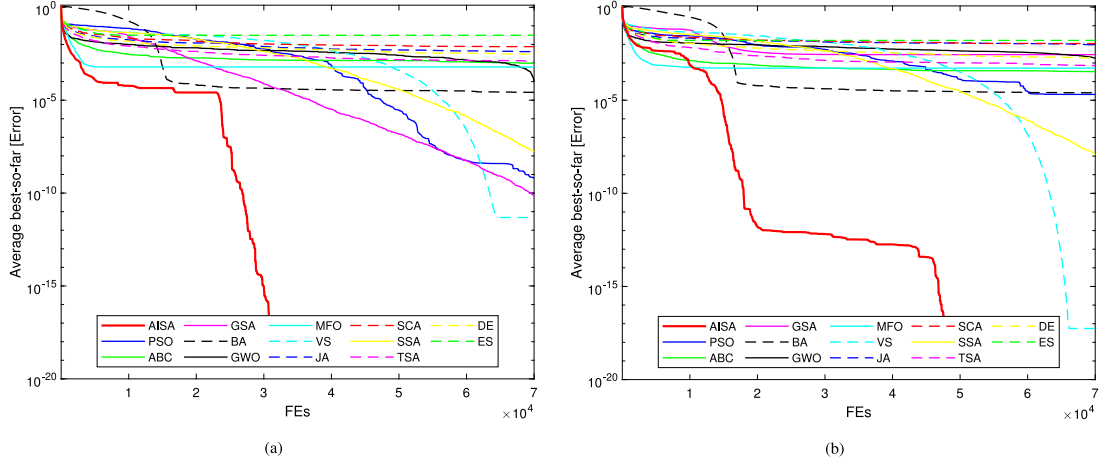


Fig. 15. Convergence curves of the algorithms for inverse kinematics problems (a) $P_{desired1}$; (b) $P_{desired2}$.

Case 2: In this case, it is considered that the fourth-order plant (33) is modeled by a third-order IIR filter presented as

$$H_{af}(z) = \frac{b_0 + b_1 z^{-1} + b_2 z^{-2}}{1 - a_1 z^{-1} - a_2 z^{-2} - a_3 z^{-3}} \quad (35)$$

5.1.2. Example II

In this example, a fifth-order IIR plant is considered as an unknown plant [84] and its transfer function is given as follows.

$$H_s(z) = \frac{0.1084 + 0.5419z^{-1} + 1.0837z^{-2} + 1.0837z^{-3} + 0.5419z^{-4} + 0.1084z^{-5}}{1 + 0.04z^{-1} + 0.2775z^{-2} - 0.2101z^{-3} + 0.14z^{-4}} \quad (36)$$

Case 1: In this case the fifth-order plant $H_s(z)$ is modeled using fifth-order IIR filter $H_{af}(z)$. Thereby, the transfer function of the adaptive IIR filter model is assumed as

$$H_{af}(z) = \frac{b_0 + b_1 z^{-1} + b_2 z^{-2} + b_3 z^{-3} + b_4 z^{-4} + b_5 z^{-5}}{1 - a_1 z^{-1} - a_2 z^{-2} - a_3 z^{-3} - a_4 z^{-4} - a_5 z^{-5}} \quad (37)$$

Table 25Results based on test category of two-sided Wilcoxon signed-rank test ($\alpha = 0.05$).

Test category	PSO	ABC	GSA	BA	GWO	MFO	VS	JA	SCA	SSA	TSA	DE	ES
Unimodal ($n = 10$)	6/1/0	7/0/0	7/0/0	7/0/0	5/2/0	7/0/0	7/0/0	7/0/0	7/0/0	7/0/0	6/1/0	6/1/0	7/0/0
Unimodal ($n = 30$)	7/0/0	6/0/1	7/0/0	7/0/0	4/3/0	7/0/0	7/0/0	6/0/1	7/0/0	7/0/0	6/1/0	6/1/0	7/0/0
Unimodal ($n = 50$)	7/0/0	6/0/1	6/0/1	6/1/0	5/2/0	7/0/0	7/0/0	6/0/1	7/0/0	7/0/0	7/0/0	5/1/1	7/0/0
Multimodal ($n = 10$)	4/2/0	4/2/0	6/0/0	6/0/0	5/1/0	6/0/0	6/0/0	4/2/0	6/0/0	4/2/0	4/2/0	1/5/0	6/0/0
Multimodal ($n = 30$)	6/0/0	6/0/0	5/1/0	5/1/0	6/0/0	4/2/0	6/0/0	6/0/0	4/2/0	6/0/0	3/3/0	3/3/0	6/0/0
Multimodal ($n = 50$)	6/0/0	6/0/0	5/1/0	6/0/0	4/2/0	6/0/0	6/0/0	5/1/0	6/0/0	5/1/0	3/3/0	3/3/0	6/0/0
Fixed-dimension multimodal	3/6/1	3/6/1	4/5/1	10/0/0	10/0/0	6/3/1	4/5/1	8/2/0	10/0/0	10/0/0	3/5/2	1/7/2	10/0/0
Composite	5/1/0	5/0/1	5/0/1	6/0/0	5/0/1	6/0/0	6/0/0	5/1/0	5/1/0	5/1/0	3/3/0	3/2/1	4/2/0
CEC 2019	9/1/0	7/0/3	7/1/2	10/0/0	9/1/0	10/0/0	8/1/1	10/0/0	10/0/0	10/0/0	9/0/1	5/3/2	9/1/0
Total (+/-/-)	53/11/1	50/8/7	52/8/5	64/1/0	61/13/1	61/3/1	57/6/2	61/2/2	59/6/0	64/1/0	46/16/3	33/26/6	62/3/0

Case 2: In this case, it is considered that the fifth-order plant as in (36) is modeled by a fourth-order IIR filter presented as

$$H_{af}(z) = \frac{b_0 + b_1 z^{-1} + b_2 z^{-2} + b_3 z^{-3}}{1 - a_1 z^{-1} - a_2 z^{-2} - a_3 z^{-3} - a_4 z^{-4}} \quad (38)$$

MSE and MSE (dB) values are reported in Tables 26–29 sequentially for all different consecutive examples and their cases. From the tables, it is clearly observed that AISA and JA obtain the best results in the Case 2 of Example 1, while AISA outperforms other competitor algorithms in terms of average results in other cases.

The non-parametric Wilcoxon Signed-Rank Test is performed as another comparison criterion based on the results obtained from 30 independent trials. The results of the AISA versus other algorithms based on the Wilcoxon Signed-Rank Test are tabulated in Table 30. In the Case 2 of Example 1, p -value corresponding to JA algorithm is greater than 0.05 (5% significance level). This means that there is no strict difference between AISA and JA. However, in other cases, p -values are less than 0.05. This is a strong evidence against the null hypothesis, establishing significant superiority of the proposed approach.

The convergence curves of the algorithms on IIR filter-based system identification problems are shown in Fig. 14. It should be noted that preliminary results of up to 500 evaluations are not illustrated to prevent scaling issues. As may be seen in Fig. 14, AISA convergence much faster than other competitor algorithms. Overall, it can be concluded that the proposed algorithm has a remarkable success rate in IIR system identification problems.

5.2. Inverse kinematics solution of 7-DOF serial robot manipulator

The robot manipulators with seven degrees of freedom (7-DOF) are widely used in the industry since they can easily escape from the obstacle, move flexibly and work in a larger space. Inverse kinematics is basically defined as finding the joint parameters/angles by using kinematics equations for a desired end-effector position. Inverse kinematics problems can be considered as challenging optimization problems due to their complex nonlinear structure [85].

In order to obtain kinematic equations of a serial industrial robot, Denavit–Hartenberg (DH) parameters are widely used and listed in Table 31 where a_i , α_i , d_i and θ_i denote link length, link twist, link offset and joint angle, respectively. It is also worth noting that interested reader can see it in [86] for more detailed information on the configuration of the robot manipulator.

The general homogeneous transformation matrix can be expressed by

$${}_{i-1}^i T = \begin{bmatrix} c\theta_i & -c\alpha_i s\theta_i & s\alpha_i s\theta_i & a_i c\theta_i \\ s\theta_i & c\alpha_i c\theta_i & -c\theta_i s\alpha_i & a_i s\theta_i \\ 0 & s\alpha_i & c\alpha_i & d_i \\ 0 & 0 & 0 & 1 \end{bmatrix} \quad (39)$$

where ${}_{i-1}^i T$ is the transformation matrix relating joint $(i-1)$ to joint i , s and c denote sine and cosine functions, respectively. Individual transformation matrices for robot manipulator are explicitly obtained by substituting DH parameters in Table 31, in Eq. (40) as follows.

$$\begin{aligned} {}_0^1 T &= \begin{bmatrix} c\theta_1 & 0 & -s\theta_1 & 0 \\ s\theta_1 & 0 & c\theta_1 & 0 \\ 0 & -1 & 0 & l_1 \\ 0 & 0 & 0 & 1 \end{bmatrix}, & {}_1^2 T &= \begin{bmatrix} c\theta_2 & 0 & s\theta_2 & l_2 c\theta_2 \\ s\theta_2 & 0 & -c\theta_2 & l_2 s\theta_2 \\ 0 & 1 & 0 & 0 \\ 0 & 0 & 0 & 1 \end{bmatrix}, \\ {}_2^3 T &= \begin{bmatrix} c\theta_3 & 0 & -s\theta_3 & l_3 c\theta_3 \\ s\theta_3 & 0 & c\theta_3 & l_3 s\theta_3 \\ 0 & -1 & 0 & 0 \\ 0 & 0 & 0 & 1 \end{bmatrix}, & {}_3^4 T &= \begin{bmatrix} c\theta_4 & 0 & s\theta_4 & l_4 c\theta_4 \\ s\theta_4 & 0 & -c\theta_4 & l_4 s\theta_4 \\ 0 & 1 & 0 & 0 \\ 0 & 0 & 0 & 1 \end{bmatrix}, & {}_4^5 T &= \begin{bmatrix} c\theta_5 & 0 & -s\theta_5 & l_5 c\theta_5 \\ s\theta_5 & 0 & c\theta_5 & l_5 s\theta_5 \\ 0 & -1 & 0 & 0 \\ 0 & 0 & 0 & 1 \end{bmatrix}, \\ {}_5^6 T &= \begin{bmatrix} c\theta_6 & -s\theta_6 & 0 & l_6 c\theta_6 \\ s\theta_6 & c\theta_6 & 0 & l_6 s\theta_6 \\ 0 & 0 & 1 & 0 \\ 0 & 0 & 0 & 1 \end{bmatrix}, & {}_6^7 T &= \begin{bmatrix} c\theta_7 & -s\theta_7 & 0 & l_7 c\theta_7 \\ s\theta_7 & c\theta_7 & 0 & l_7 s\theta_7 \\ 0 & 0 & 1 & d_7 \\ 0 & 0 & 0 & 1 \end{bmatrix}. \end{aligned} \quad (40)$$

Then, the forward kinematics of the manipulator can be obtained by multiplying the individual transformation matrices as

$$T_{\text{End-Effector}} = {}_0^7 T = {}_0^1 T \cdot {}_1^2 T \cdot {}_2^3 T \cdot {}_3^4 T \cdot {}_4^5 T \cdot {}_5^6 T \cdot {}_6^7 T = \begin{bmatrix} R_{3 \times 3} & P_x \\ 0 & 0 & 0 & 1 \end{bmatrix} \quad (41)$$

where $T_{\text{End-Effector}}$ is the homogeneous transformation matrix of the end-effector with respect to the base frame, $R_{3 \times 3}$ indicates the orientation matrix and $[P_x \ P_y \ P_z]^T$ is the position vector of end-effector.

The main task of the inverse kinematics problem of 7-DOF serial robot manipulator is to determine joint angles $(\theta_1, \theta_2, \dots, \theta_7)$ according to the desired positions of end-effector in the Cartesian coordinate system. The position error, which is calculated based on the Euclidean distance between the desired and predicted position vectors, is considered as the objective function to be minimized as

$$\text{fitness} = \|P_{\text{desired}} - P_{\text{predicted}}\| \quad (42)$$

Table 26

Results of MSE and MSE (dB) metrics for Example 1 (Case 1) modeled using a fourth order IIR filter over 30 runs.

MSE	AISA	PSO	ABC	GSA	BA	GWO	MFO	VS	JA	SCA	SSA	TSA	DE	ES
Best	3.58E-30	1.39E-18	1.60E-05	4.18E-19	2.32E-07	8.60E-07	2.39E-19	1.66E-18	2.10E-03	1.90E-02	3.78E-14	9.05E-15	7.93E-21	1.93E-03
Best (dB)	-294.4604	-178.5740	-47.9577	-183.7881	-66.3454	-60.6553	-186.2170	-177.7988	-26.7786	-17.2119	-134.2239	-140.4340	-201.0078	-27.1339
Mean	6.14E-27	8.36E-07	3.01E-04	1.24E-18	4.10E-01	2.63E-02	2.52E-09	2.10E-03	6.64E-03	6.67E-02	3.39E-03	8.16E-09	8.36E-19	1.59E-02
Mean (dB)	-262.1154	-60.7771	-35.2213	-179.0833	-3.8713	-15.8069	-85.9780	-26.7690	-21.7760	-11.7557	-24.7029	-80.8846	-180.7754	-17.9776
Std	1.49E-26	3.29E-06	3.14E-04	6.07E-19	1.35E+00	5.12E-02	1.08E-08	1.15E-02	5.08E-03	3.94E-02	1.31E-02	3.40E-08	2.74E-18	1.39E-02
Std (dB)	-258.2687	-54.8233	-35.0346	-182.1663	1.3157	-12.9069	-79.6833	-19.3834	-22.9413	-14.0486	-18.8233	-74.6853	-175.6244	-18.5708

The bold values indicate the best solutions found by the algorithms.

Table 2

Results of MSE and MSE (dB) metrics for Example 1 (Case 2) modeled using a third order IIR filter over 30 runs.

MSE	AISA	PSO	ABC	GSA	BA	GWO	MFO	VS	JA	SCA	SSA	TSA	DE	ES
Best	0.07186	0.07186	0.07224	0.07186	0.07186	0.07500	0.07186	0.07186	0.07186	0.08347	0.07186	0.07186	0.07186	0.07613
Best (dB)	-11.4353	-11.4353	-11.4120	-11.4353	-11.4353	-11.2493	-11.4353	-11.4353	-11.4353	-10.7849	-11.4353	-11.4353	-11.4353	-11.1844
Mean	0.07186	0.09419	0.07875	0.13471	0.58313	0.13005	0.11183	0.07558	0.07186	0.14374	0.07930	0.07189	0.07186	0.17529
Mean (dB)	-11.4353	-10.2602	-11.0374	-8.7059	-2.3423	-8.8590	-9.5145	-11.2161	-11.4353	-8.4242	-11.0073	-11.4331	-11.4353	-7.5625
Std	3.47E-17	4.54E-02	5.00E-03	5.30E-02	1.19E+00	4.79E-02	1.79E-01	2.04E-02	3.98E-17	4.64E-02	2.83E-02	7.60E-05	4.09E-16	7.43E-02
Std (dB)	-164.6004	-13.4279	-23.0087	-12.7601	0.7470	-13.1962	-7.4737	-16.9077	-163.9968	-13.3383	-15.4787	-41.1898	-153.8830	-11.2886

The bold values indicate the best solutions found by the algorithms.

Table 28

Results of MSE and MSE (dB) metrics for Example 2 (Case 1) modeled using a fifth order IIR filter over 30 runs.

MSE	AISA	PSO	ABC	GSA	BA	GWO	MFO	VS	JA	SCA	SSA	TSA	DE	ES
Best	1.34E–06	1.99E–06	8.54E–05	1.87E–05	2.32E–06	9.71E–05	7.70E–06	1.39E–06	2.02E–06	4.70E–03	1.71E–06	5.01E–05	3.63E–06	2.02E–04
Best (dB)	–58.7154	–57.0168	–40.6843	–47.2913	–56.3362	–40.1260	–51.1338	–58.5660	–56.9497	–23.2754	–57.6609	–42.9980	–54.4048	–36.9459
Mean	1.34E–06	1.49E–03	3.98E–04	8.28E–05	8.59E–01	5.31E–03	5.16E–01	1.85E–04	5.27E–04	1.37E–02	1.93E–04	2.67E–04	7.16E–05	1.62E–02
Mean (dB)	–58.7154	–28.2778	–34.0056	–40.8183	–0.6605	–22.7476	–2.8765	–37.3266	–32.7852	–18.6172	–37.1471	–35.7430	–41.4507	–17.9131
Std	1.36E–20	5.26E–03	2.21E–04	3.16E–05	1.68E+00	4.65E–03	1.20E+00	8.70E–05	8.56E–04	5.26E–03	1.34E–04	1.35E–04	4.08E–05	3.29E–02
Std (dB)	–198.6741	–22.7901	–36.5503	–44.9966	2.2489	–23.3273	0.8044	–40.6040	–30.6752	–22.7914	–38.7222	–38.7010	–43.8889	–14.8291

The bold values indicate the best solutions found by the algorithms.

Table 29

Results of MSE and MSE (dB) metrics for Example 2 (Case 2) modeled using a fourth order IIR filter over 30 runs.

MSE	AISA	PSO	ABC	GSA	BA	GWO	MFO	VS	JA	SCA	SSA	TSA	DE	ES
Best	3.47E-04	3.47E-04	3.55E-04	3.47E-04	3.47E-04	3.55E-04	3.47E-04	3.47E-04	3.47E-04	5.78E-03	3.47E-04	3.47E-04	3.47E-04	8.58E-04
Best (dB)	-34.6023	-34.6023	-34.5020	-34.6023	-34.5996	-34.5008	-34.6023	-34.6022	-34.5939	-22.3826	-34.6023	-34.6023	-34.6023	-30.6641
Mean	3.47E-04	8.00E-04	4.56E-04	3.47E-04	2.71E-01	3.67E-03	6.76E-02	7.49E-04	3.50E-04	1.55E-02	6.32E-04	3.48E-04	3.47E-04	8.03E-03
Mean (dB)	-34.6023	-30.9703	-33.4089	-34.6023	-5.6706	-24.3541	-11.7009	-31.2563	-34.5607	-18.0975	-31.9913	-34.5886	-34.6023	-20.9525
Std	1.65E-19	1.98E-03	1.24E-04	4.92E-19	6.16E-01	4.48E-03	3.68E-01	1.40E-03	1.68E-06	9.09E-03	9.60E-04	2.48E-06	2.28E-15	7.27E-03
Std (dB)	-187.8305	-27.0252	-39.0501	-183.0801	-2.1030	-23.4854	-4.3376	-28.5332	-57.7371	-20.4153	-30.1779	-56.0515	-146.4270	-21.3818

The bold values indicate the best solutions found by the algorithms.

Table 30

The results of Wilcoxon signed-rank test for IIR filters.

		PSO	ABC	GSA	BA	GWO	MFO	VS	JA	SCA	SSA	TSA	DE	ES
Example 1	Case 1	p-value (T+, T-)	1.73E-06 (0, 465)											
	Winner	+	+	+	+	+	+	+	+	+	+	+	+	+
Example 2	Case 1	p-value (T+, T-)	1.73E-06 (0, 465)	1.73E-06 (0, 465)	1.37E-06 (0, 465)	1.73E-06 (0, 465)	1.73E-06 (0, 465)	1.73E-06 (0, 465)	1.73E-06 (9, 6)	1.73E-06 (0, 465)	1.73E-06 (0, 465)	1.73E-06 (0, 465)	4.18E-07 (0, 465)	1.73E-06 (0, 465)
	Winner	+	+	+	+	+	+	=	+	+	+	+	+	+
Example 2	Case 2	p-value (T+, T-)	1.73E-06 (0, 465)	1.73E-06 (0, 465)	1.01E-07 (0, 465)	1.73E-06 (0, 465)								
	Winner	+	+	+	+	+	+	+	+	+	+	+	+	+
Total (+/-=)		4/0/0	4/0/0	4/0/0	4/0/0	4/0/0	4/0/0	4/0/0	3/1/0	4/0/0	4/0/0	4/0/0	4/0/0	4/0/0

Table 31

The DH parameters of the 7-DOF robot manipulator.

i	a_i (m)	α_i ($^{\circ}$)	d_i (m)	θ_i ($^{\circ}$) Range
1	0	-90	$l_1 = 0.5$	$-180 < \theta_1 < 180$
2	$l_2 = 0.2$	90	0	$-90 < \theta_2 < 30$
3	$l_3 = 0.25$	-90	0	$-90 < \theta_3 < 120$
4	$l_4 = 0.3$	90	0	$-90 < \theta_4 < 90$
5	$l_5 = 0.2$	-90	0	$-90 < \theta_5 < 90$
6	$l_6 = 0.2$	0	0	$-90 < \theta_6 < 90$
7	$l_7 = 0.1$	0	$d_7 = 0.05$	$-30 < \theta_7 < 90$

where $\|\cdot\|$ denotes the Euclidean distance, $P_{desired}$ represents desired position vector of robot manipulator, $P_{predicted}$ represents predicted position vector that found by substituting a candidate solution of optimizers in the forward kinematics equations.

In the simulation part, in order to verify performance of AISA, two different desired position vectors are selected as $P_{desired1} = [-25 \ 100 \ 50]^T$ and $P_{desired2} = [50 \ -25 \ 75]^T$ in centimeter. For a fair comparison of the competitor algorithms, the maximum number of function evaluations is set as used in Section 4.3 and the control parameters of algorithms are used in the same manner which are already given in Table 6.

Tables 32 and 33 illustrate the numerical optimization results of AISA with 13 other comparators on the inverse kinematics problems for two different desired position coordinates of end-effector. From the optimization results in these tables, it is seen that proposed AISA outperforms other algorithms in inverse kinematics problems in terms of mean performance results. The results obtained from 30 runs of the AISA versus other algorithms based on the Wilcoxon Signed-Rank Test are tabulated in Tables 34 and 35. As seen from these tables, the proposed AISA exhibits better performance against other algorithms except MFO in the first scenario and VS in the second one. The convergence histories of the algorithms on inverse kinematics problems are shown in Fig. 15 where AISA converges much faster than other competitor algorithms. The overall optimization results on inverse kinematics problems reveal that AISA provides optimal values in this engineering problem that reflecting the applicability of AISA to real engineering problem.

6. Results and discussion

In the present study, the proposed AISA algorithm is compared with PSO, ABC, GSA, BA, GWO, MFO, VS, JA, SCA, SSA, TSA, DE and ES. The results and comparisons in previous sections are summarized below.

Tables 7–9 depict the obtained results for AISA versus other optimizers in dealing with scalable unimodal functions. AISA attains the best results for 100%, 85.7% and 85.7% of 10-, 30- and 50-dimensional unimodal functions, respectively. With regard

to Wilcoxon Signed-Rank Test in Tables 16–18, it is detected that AISA achieves the best values in almost all cases, with the exception of function F_5 .

Tables 10–12 show the quantitative results by all optimizers in dealing with scalable multimodal functions. AISA attains the best results for 100%, 100% and 83.3% of 10-, 30- and 50-dimensional multimodal functions, respectively. According to the non-parametric statistical results given in Tables 19–21, AISA has higher performance than others in almost all cases.

The convergence graphs of AISA and other optimizers are given in Figs. 7–9 on unimodal and multimodal functions with different dimensions. As seen from these figures, AISA achieves consistent convergence success on both unimodal and multimodal functions with different dimensions.

When the results for scalable benchmark functions are discussed, the performance of AISA seems to be reducing; however, the optimal results obtained in F_2 , F_3 , F_4 , F_7 and F_{12} functions, as opposed to F_5 , F_8 , and F_{10} functions, get better as the problem size increases.

The results in Table 13 present the obtained results for AISA versus other optimizers on fixed-dimension multimodal functions. While the success rate of AISA is 70% in dealing with these functions, that of DE is 80%. Based on Wilcoxon Signed-Rank Test in Table 22, AISA is in competition with PSO, ABC, TSA and DE algorithms and the numerical results provided for these algorithms is not sufficient to make a statistically convincing inference.

Table 14 depicts numerical results of all algorithms on complex composite test functions. AISA attains the best results for 66.7% of these functions. In addition, with regard to Wilcoxon Signed-Rank Test in Table 23, AISA achieves the best values in almost all cases, with the exception of function F_{26} .

Table 15 shows the statistical results of the algorithms on modern CEC 2019 test functions. It is observed that AISA is successful in results 50% of the problems. With regard to Wilcoxon Signed-Rank Test in Table 24, AISA exhibits similarly competitive performance. It is also emphasized here that the performance success of AISA in these functions is relatively low compared to others. This fits in with “No-Free-Lunch” (NFL) theorem.

Figs. 10 and 11 shows the convergence graphs of all algorithms on fixed-dimension multimodal, composite and CEC 2019 benchmarks. It is observed that AISA exhibits a remarkable convergence rate on more than half functions.

Fig. 12 visually compares the total running time for each algorithm. As seen from this figure, it performs faster than well-established optimizers such as GSA, DE and ES although the proposed algorithm uses a modeling approach optimized by LSE.

The results in Tables 26–29 present the obtained results for the optimizers on real-life adaptive IIR system identification problems. AISA attains the best results for 100% of these problems. In

Table 32

Comparative results of all optimizers for $P_{desired1} = [-25 \quad 100 \quad 50]^T$ (cm) over 30 runs.

	AISA	PSO	ABC	GSA	BA	GWO	MFO	VS	JA	SCA	SSA	TSA	DE	ES
Best	0.00E+00	0.00E+00	1.45E-04	1.69E-11	1.11E-05	9.03E-06	0.00E+00	0.00E+00	5.37E-04	1.69E-03	1.58E-09	8.32E-07	3.26E-04	2.27E-03
Mean	0.00E+00	6.40E-10	9.78E-04	7.33E-11	2.66E-05	9.75E-05	6.07E-04	4.84E-12	4.12E-03	7.62E-03	1.67E-08	1.20E-03	3.00E-03	3.10E-02
Std	0.00E+00	3.27E-09	7.06E-04	3.38E-11	1.05E-05	8.50E-05	3.33E-03	1.94E-11	2.09E-03	3.93E-03	1.04E-08	1.78E-03	1.81E-03	1.93E-02

The bold values indicate the best solutions found by the algorithms.

Table 33

Comparative results of all optimizers for $P_{desired2} = [50 \quad -25 \quad 75]^T$ (cm) over 30 runs.

	AISA	PSO	ABC	GSA	BA	GWO	MFO	VS	JA	SCA	SSA	TSA	DE	ES
Best	0.00E+00	0.00E+00	8.70E-05	7.30E-12	9.53E-06	1.46E-05	0.00E+00	0.00E+00	4.40E-03	2.42E-03	2.41E-09	8.99E-07	4.20E-05	1.41E-03
Mean	0.00E+00	2.05E-05	3.46E-04	2.81E-03	2.53E-05	1.78E-03	5.27E-04	5.55E-18	9.51E-03	1.11E-02	1.20E-08	7.24E-04	1.85E-03	1.63E-02
Std	0.00E+00	1.12E-04	1.94E-04	1.54E-02	9.80E-06	9.22E-03	2.89E-03	2.11E-17	5.94E-03	4.60E-03	6.04E-09	7.18E-04	2.31E-03	1.00E-02

The bold values indicate the best solutions found by the algorithms.

Table 34

The results of Wilcoxon signed-rank test for $P_{desired1} = [-25 \quad 100 \quad 50]^T$ (cm).

	PSO	ABC	GSA	BA	GWO	MFO	VS	JA	SCA	SSA	TSA	DE	ES
p-value	4.88E-04	1.73E-06	1.73E-06	1.73E-06	1.73E-06	0.0625	1.93E-04	1.73E-06	1.73E-06	1.73E-06	1.73E-06	1.73E-06	1.73E-06
(T+, T-)	(0, 78)	(0, 465)	(0, 465)	(0, 465)	(0, 465)	(0, 15)	(0, 171)	(0, 465)	(0, 465)	(0, 465)	(0, 465)	(0, 465)	(0, 465)
Winner	+	+	+	+	+	=	+	+	+	+	+	+	+

Table 35

The results of Wilcoxon signed-rank test for $P_{desired2} = [50 \quad -25 \quad 75]^T$ (cm).

	PSO	ABC	GSA	BA	GWO	MFO	VS	JA	SCA	SSA	TSA	DE	ES
p-value	8.81E-05	1.73E-06	1.73E-06	1.73E-06	1.73E-06	7.81E-03	0.25	1.73E-06	1.73E-06	1.73E-06	1.73E-06	1.73E-06	1.73E-06
(T+, T-)	(0, 210)	(0, 465)	(0, 465)	(0, 465)	(0, 465)	(0, 36)	(0, 6)	(0, 465)	(0, 465)	(0, 465)	(0, 465)	(0, 465)	(0, 465)
Winner	+	+	+	+	+	+	=	+	+	+	+	+	+

addition, with regard to Wilcoxon Signed-Rank Test in [Table 23](#) and convergence analysis given in [Fig. 14](#), AISA produces better results than others. The results reveal that AISA provides superior performance compared to other algorithms when solving IIR system identification problems.

[Tables 32](#) and [33](#) show the statistical results of all optimizers on the inverse kinematics problems. The results reveal that AISA is capable of achieving to high-quality solutions and outperforming other competitors. Inspecting the Wilcoxon Signed-Rank Test results in [Tables 34](#) and [35](#) and convergence graphs in [Fig. 15](#), it is detected that AISA is the best optimizer in dealing with inverse kinematics problems and can attain superior results compared to other algorithms.

When the overall optimization results are discussed, it should be mentioned that better or competitive results are obtained by the proposed AISA. The reason behind it is that the proposed algorithm has been conscientiously designed to possess different search capabilities. AISA has three mechanisms (phases) manipulated by the parameter r_4 . The first mechanism is designed to focus the algorithm on exploitation. In this mechanism, the best feature vector (\mathbf{x}^*) is found using a CFLN optimized by LSE at the start of each iteration, and the individual is directed towards this vector by using step size r_1 . The second mechanism is designed to ensure that the algorithm has a more balanced exploitation, which means that the algorithm has a tendency towards the best solution/role model (\mathbf{x}^{rm}), but struggles to avoid immature convergence by using another individual \mathbf{x}^p . The third mechanism is designed to focus the algorithm on exploration. In this mechanism, the algorithm has a tendency towards negative identity vector \mathbf{x}^q by using random vector \mathbf{r}_3 , which assists to span unexplored regions. These features can theoretically assist us to understand search behavior of AISA. While AISA possesses a strong and robust capability to produce superior optimization performance over other competitor metaheuristic algorithms in solving both standard benchmark functions and real-life engineering problems, it has a computational load for

feature extraction layer via LSE when large parameter space exists. In addition, a problem may arise from the inversion of ill-conditioned matrix in LSE. Therefore, pseudoinverse may be used, or recursive type improvements are planned to improve.

7. Conclusion and future directions

A novel metaheuristic algorithm called Adolescent Identity Search Algorithm (AISA) is proposed for solving unconstrained optimization problems. The proposed AISA can be included in both population-based and human-based classes. The AISA mimics the adolescent identity formation within a peer group. Identity behaviors of adolescents were mathematically modeled on the basis of observing and reasoning the features of individuals in the group, imitating a role model and adopting an undesirable feature. In addition, the most important characteristic that distinguishes the proposed optimizer from other metaheuristics is that it attempts to find partial fitness values using a CFLN optimized by LSE. Firstly, thirty-nine test functions consisting of five different types including unimodal, multimodal, fixed-dimensional multimodal, composite and CEC 2019 were employed in order to test the performance of proposed optimizer in respect to exploration, exploitation, local optima avoidance, and convergence. The results reveal that AISA was capable of finding excellent solutions compared to thirteen well-regarded state-of-the-art metaheuristic algorithms (PSO, ABC, GSA, BA, GWO, MFO, VS, JA, SCA, SSA, TSA, DE and ES) in terms of standard statistical analysis, scalability analysis, Wilcoxon signed-rank test, converge analysis and computational time analysis. Then, the performance of proposed optimizer was investigated on IIR system identification and inverse kinematics problem of a 7-DOF robot manipulator found in engineering. The overall results reveal that AISA exhibits a superior and very competitive performance.

Moreover, this work is open to new ideas for future studies. First of all, new perspectives can be injected into the algorithm since adolescent identity development is a complex concept in the psychosocial framework. Secondly, different network

structure may be integrated instead of the proposed orthogonal Chebyshev network. Thirdly, different versions such as the binary and multi-objective of the AISA algorithm may be advanced. In addition, the proposed algorithm can be implemented to solve other optimization problems situated in real world.

CRediT authorship contribution statement

Esref Bogar: Conceptualization, Investigation, Methodology, Software, Validation, Writing - original draft. **Selami Beyhan:** Conceptualization, Software, Writing - original draft, Writing - review & editing.

Declaration of competing interest

The authors declare that they have no known competing financial interests or personal relationships that could have appeared to influence the work reported in this paper.

Acknowledgment

Author E.B. offers his profound thanks to the Scientific and Technological Research Council of Turkey (TUBITAK Programme, 2211-A) for their bursary support.

Appendix

MATLAB codes of all competitive algorithms used in this work can be obtained from the following links:

- AISA: <http://www.pau.edu.tr/ebogar/tr/aisa>
- PSO: <http://www.alimirjalili.com/GWO.html>
- ABC: <https://abc.erciyes.edu.tr/>
- GSA: <https://www.mathworks.com/matlabcentral/fileexchange/27756-gravitational-search-algorithm-gsa>
- BA: <https://www.mathworks.com/matlabcentral/fileexchange/37582-bat-algorithm-demo>
- GWO: <http://www.alimirjalili.com/GWO.html>
- MFO: <http://www.alimirjalili.com/MFO.html>
- VS: <https://web.itu.edu.tr/bdogan/VortexSearch/VS.htm>
- JA: <https://sites.google.com/site/jayaalgorithm/>
- SCA: <http://www.alimirjalili.com/SCA.html>
- SSA: <http://www.alimirjalili.com/SSA.html>
- TSA: <http://mskiran.kisisel.selcuk.edu.tr/tsa/>
- DE: <https://academic.csuohio.edu/simond/bbo/>
- ES: <https://academic.csuohio.edu/simond/bbo/>

References

- [1] G. Dhiman, V. Kumar, Emperor penguin optimizer: A bio-inspired algorithm for engineering problems, *Knowl.-Based Syst.* 159 (2018) 20–50.
- [2] A. Gogna, A. Tayal, Metaheuristics: review and application, *J. Exp. Theor. Artif. Intell.* 25 (4) (2013) 503–526.
- [3] A.A. Heidari, S. Mirjalili, H. Faris, I. Aljarah, M. Mafarja, H. Chen, Harris hawks optimization: Algorithm and applications, *Future Gener. Comput. Syst.* 97 (2019) 849–872.
- [4] S. Mirjalili, S.M. Mirjalili, A. Lewis, Grey wolf optimizer, *Adv. Eng. Softw.* 69 (2014) 46–61.
- [5] E. Alba, B. Dorronsoro, The exploration/exploitation tradeoff in dynamic cellular genetic algorithms, *IEEE Trans. Evol. Comput.* 9 (2) (2005) 126–142.
- [6] S. Mirjalili, S.M. Mirjalili, A. Hatamlou, Multi-verse optimizer: a nature-inspired algorithm for global optimization, *Neural Comput. Appl.* 27 (2) (2016) 495–513.
- [7] J.H. Holland, *Adaptation in Natural and Artificial Systems*, second ed., University of Michigan Press, Ann Arbor, MI, 1975, 1992.
- [8] R. Storn, K. Price, Differential evolution – a simple and efficient heuristic for global optimization over continuous spaces, *J. Global Optim.* 11 (4) (1997) 341–359.
- [9] I. Rechenberg, *Evolutionsstrategie : OPTimierung Technischer Systeme Nach Prinzipien Der Biologischen Evolution*, Frommann-Holzboog, 1973.
- [10] L.J. A., L. Pedro, *Estimation of Distribution Algorithms: a New Tool for Evolutionary Computation*, Kluwer Academic, 2002.
- [11] D. Simon, Biogeography-based optimization, *IEEE Trans. Evol. Comput.* 12 (6) (2008) 702–713.
- [12] J. Kennedy, R. Eberhart, Particle swarm optimization, in: *Proceedings of the IEEE International Conference on Neural Networks*, 1995, pp. 1942–1948.
- [13] M. Dorigo, V. Maniezzo, A. Colorni, Ant system: optimization by a colony of cooperating agents, *IEEE Trans. Syst. Man Cybern. B* 26 (1) (1996) 29–41.
- [14] D. Karaboga, B. Basturk, A powerful and efficient algorithm for numerical function optimization: artificial bee colony (abc) algorithm, *J. Global Optim.* 39 (3) (2007) 459–471.
- [15] S.-C. Chu, P.-w. Tsai, J.-S. Pan, Cat swarm optimization, in: Q. Yang, G. Webb (Eds.), *PRICAI 2006: Trends in Artificial Intelligence*, Springer Berlin Heidelberg, Berlin, Heidelberg, 2006, pp. 854–858.
- [16] X.Y. and, Cuckoo search via levy flights, in: *2009 World Congress on Nature Biologically Inspired Computing (NaBIC)*, 2009, pp. 210–214.
- [17] X.-S. Yang, Firefly algorithms for multimodal optimization, in: O. Watanabe, T. Zeugmann (Eds.), *Stochastic Algorithms: Foundations and Applications*, Springer Berlin Heidelberg, Berlin, Heidelberg, 2009, pp. 169–178.
- [18] X.-S. Yang, *A New Metaheuristic Bat-Inspired Algorithm*, Springer Berlin Heidelberg, Berlin, Heidelberg, 2010, pp. 65–74.
- [19] A.H. Gandomi, A.H. Alavi, Krill herd: A new bio-inspired optimization algorithm, *Commun. Nonlinear Sci. Numer. Simul.* 17 (12) (2012) 4831–4845.
- [20] W.-T. Pan, A new fruit fly optimization algorithm: Taking the financial distress model as an example, *Knowl.-Based Syst.* 26 (2012) 69–74.
- [21] A. Baykasoglu, S. Akpinar, Weighted superposition attraction (wsa): A swarm intelligence algorithm for optimization problems – part 2: Constrained optimization, *Appl. Soft Comput.* 37 (2015) 396–415.
- [22] S.A. Uymaz, G. Tezel, E. Yel, Artificial algae algorithm (aaa) for nonlinear global optimization, *Appl. Soft Comput.* 31 (2015) 153–171.
- [23] A. Askarzadeh, A novel metaheuristic method for solving constrained engineering optimization problems: Crow search algorithm, *Comput. Struct.* 169 (2016) 1–12.
- [24] S. Mirjalili, A. Lewis, The whale optimization algorithm, *Adv. Eng. Softw.* 95 (2016) 51–67.
- [25] S. Saremi, S. Mirjalili, A. Lewis, Grasshopper optimisation algorithm: Theory and application, *Adv. Eng. Softw.* 105 (2017) 30–47.
- [26] S. Mirjalili, A.H. Gandomi, S.Z. Mirjalili, S. Saremi, H. Faris, S.M. Mirjalili, Salp swarm algorithm: A bio-inspired optimizer for engineering design problems, *Adv. Eng. Softw.* 114 (2017) 163–191.
- [27] E. Jahani, M. Chizari, Tackling global optimization problems with a novel algorithm – mouth brooding fish algorithm, *Appl. Soft Comput.* 62 (2018) 987–1002.
- [28] M. Jain, V. Singh, A. Rani, A novel nature-inspired algorithm for optimization: Squirrel search algorithm, *Swarm Evol. Comput.* 44 (2019) 148–175.
- [29] H. Yapici, N. Cetinkaya, A new meta-heuristic optimizer: Pathfinder algorithm, *Appl. Soft Comput.* 78 (2019) 545–568.
- [30] I.F. Jr., X. Yang, I. Fister, J. Brest, D. Fister, A brief review of nature-inspired algorithms for optimization, 2013, arXiv preprint. [arXiv:1307.4186](https://arxiv.org/abs/1307.4186).
- [31] S. Kirkpatrick, C.D. Gelatt, M.P. Vecchi, Optimization by simulated annealing, *Science* 220 (1983) 671–680.
- [32] O.K. Erol, I. Eksin, A new optimization method: Big bang–big crunch, *Adv. Eng. Softw.* 37 (2) (2006) 106–111.
- [33] E. Rashedi, H. Nezamabadi-pour, S. Saryazdi, Gsa: A gravitational search algorithm, *Inform. Sci.* 179 (13) (2009) 2232–2248.
- [34] A.Y.S. Lam, V.O.K. Li, Chemical-reaction-inspired metaheuristic for optimization, *IEEE Trans. Evol. Comput.* 14 (3) (2010) 381–399.
- [35] A. Kaveh, S. Talatahari, A novel heuristic optimization method: charged system search, *Acta Mech.* 213 (3) (2010) 267–289.
- [36] A. Kaveh, M. Khayatazarad, A new meta-heuristic method: Ray optimization, *Comput. Struct.* 112–113 (2012) 283–294.
- [37] A. Hatamlou, Black hole: A new heuristic optimization approach for data clustering, *Inform. Sci.* 222 (2013) 175–184.
- [38] M. Abdechiri, M.R. Meybodi, H. Bahrami, Gases brownian motion optimization: an algorithm for optimization (gbmo), *Appl. Soft Comput.* 13 (5) (2013) 2932–2946.
- [39] B. Javidy, A. Hatamlou, S. Mirjalili, Ions motion algorithm for solving optimization problems, *Appl. Soft Comput.* 32 (2015) 72–79.
- [40] B. Doğan, T. Ölmez, A new metaheuristic for numerical function optimization: Vortex search algorithm, *Inform. Sci.* 293 (2015) 125–145.
- [41] S. Salcedo-Sanz, Modern meta-heuristics based on nonlinear physics processes: A review of models and design procedures, *Phys. Rep.* 655 (2016) 1–70.

- [42] F. Glover, Future paths for integer programming and links to artificial intelligence, *Comput. Oper. Res.* 13 (5) (1986) 533–549.
- [43] R. Rao, V. Savsani, D. Vakharia, Teaching-learning-based optimization: A novel method for constrained mechanical design optimization problems, *Comput. Aided Des.* 43 (3) (2011) 303–315.
- [44] A. Sadollah, A. Bahreininejad, H. Eskandar, M. Hamdi, Mine blast algorithm: A new population based algorithm for solving constrained engineering optimization problems, *Appl. Soft Comput.* 13 (5) (2013) 2592–2612.
- [45] A.H. Gandomi, Interior search algorithm (isa): A novel approach for global optimization, *ISA Trans.* 53 (4) (2014) 1168–1183.
- [46] N. Ghorbani, E. Babaei, Exchange market algorithm, *Appl. Soft Comput.* 19 (2014) 177–187.
- [47] S.-A. Ahmadi, Human behavior-based optimization: a novel metaheuristic approach to solve complex optimization problems, *Neural Comput. Appl.* 28 (1) (2017) 233–244.
- [48] R. Moghdani, K. Salimifard, Volleyball premier league algorithm, *Appl. Soft Comput.* 64 (2018) 161–185.
- [49] A.M. Fathollahi-Fard, M. Hajighaei-Keshteli, R. Tavakkoli-Moghaddam, The social engineering optimizer (seo), *Eng. Appl. Artif. Intell.* 72 (2018) 267–293.
- [50] D.H. Wolpert, W.G. Macready, No free lunch theorems for optimization, *IEEE Trans. Evol. Comput.* 1 (1) (1997) 67–82.
- [51] S. Mirjalili, Moth-flame optimization algorithm: A novel nature-inspired heuristic paradigm, *Knowl.-Based Syst.* 89 (2015) 228–249.
- [52] W. Al-Ani, M. Kadhum, The study of unhealthy eating habits among secondary schools students in babel governorate, *Mustansiriya Med. J.* 12 (1) (2018).
- [53] H.D. Grotewalt, Coming to terms with adoption, *Adopt. Quart.* 1 (1) (1997) 3–27.
- [54] S. Tsang, E. Hui, B. Law, Positive identity as a positive youth development construct: A conceptual review, *Sci. World J.* 2012 (2012) 1–7.
- [55] E.H. Erikson, *Childhood and Society*, second ed., Norton, New York, NY, 1963.
- [56] J.E. Marcia, Development and validation of ego-identity status, *J. Personal. Soc. Psychol.* 3 (5) (1966) 551–558.
- [57] S.B. Campbell, *Behavior Problems in Preschool Children: Clinical and Developmental Issues*, The Guilford Press, 2006.
- [58] A. Bandura, *Social Foundations of Thought and Action : A Social Cognitive Theory*, Prentice Hall, Englewood Cliffs, NJ, 1986.
- [59] A. Bandura, *Social Learning Theory*, General Learning Press, 1971.
- [60] N.M. Hurd, M.A. Zimmerman, Role models, in: *Encyclopedia of Adolescence*, Springer New York, 2011, pp. 2399–2404.
- [61] T. Rageliene, Links of adolescents identity development and relationship with peers: a systematic literature review, *J. Can. Acad. Child. Adolesc. Psychiatry* 25 (2) (2016) 97–105.
- [62] M. Çetin, B. Bahtiyar, S. Beyhan, Adaptive uncertainty compensation-based nonlinear model predictive control with real-time applications, *Neural Comput. Appl.* 31 (2) (2019) 1029–1043.
- [63] J.C. Patra, A.C. Kot, Nonlinear dynamic system identification using cheby-shev functional link artificial neural networks, *IEEE Trans. Syst. Man Cybern. B* 32 (4) (2002) 505–511.
- [64] M.-Y. Cheng, D. Prayogo, Symbiotic organisms search: A new metaheuristic optimization algorithm, *Comput. Struct.* 139 (2014) 98–112.
- [65] P. Civicioglu, Backtracking search optimization algorithm for numerical optimization problems, *Appl. Math. Comput.* 219 (15) (2013) 8121–8144.
- [66] E. Crocetti, Identity formation in adolescence: The dynamic of forming and consolidating identity commitments, *Child. Dev. Perspect.* 11 (2) (2017) 145–150.
- [67] K. Sørensen, Metaheuristics—the metaphor exposed, *Int. Trans. Oper. Res.* 22 (1) (2015) 3–18.
- [68] D. Weyland, A rigorous analysis of the harmony search algorithm, *Int. J. Appl. Metaheuristics Comput.* 1 (2) (2010) 50–60.
- [69] D. Molina, J. Poyatos, J.D. Ser, S. Garcia, A. Hussain, F. Herrera, Comprehensive taxonomies of nature- and bio-inspired optimization: inspiration versus algorithmic behavior, critical analysis and recommendations, 2020, arXiv:2002.08136.
- [70] J.D. Ser, E. Osaba, D. Molina, X.-S. Yang, S. Salcedo-Sanz, D. Camacho, S. Das, P.N. Suganthan, C.A.C. Coello, F. Herrera, Bio-inspired computation: Where we stand and what's next, *Swarm Evol. Comput.* 48 (2019) 220–250.
- [71] X.-S. Yang, Nature-inspired optimization algorithms: Challenges and open problems, *J. Comput. Sci.* (2020) 101–104.
- [72] J.J. Liang, P.N. Suganthan, K. Deb, Novel composition test functions for numerical global optimization, in: *Proceedings 2005 IEEE Swarm Intelligence Symposium*, 2005. SIS 2005., 2005, pp. 68–75.
- [73] R. Salomon, Re-evaluating genetic algorithm performance under coordinate rotation of benchmark functions. a survey of some theoretical and practical aspects of genetic algorithms, *Biosystems* 39 (3) (1996) 263–278.
- [74] K. Price, N. Awad, M. Ali, P. Suganthan, Problem definitions and evaluation criteria for the 100-digit challenge special session and competition on single objective numerical optimization, in: *Technical Report*, Nanyang Technological University, 2018.
- [75] R.V. Rao, Jaya: A simple and new optimization algorithm for solving constrained and unconstrained optimization problems, *Int. J. Ind. Eng. Comput.* 7 (1) (2016) 19–34.
- [76] S. Mirjalili, Sca: A sine cosine algorithm for solving optimization problems, *Knowl.-Based Syst.* 96 (2016) 120–133.
- [77] M.S. Kiran, Tsa: Tree-seed algorithm for continuous optimization, *Expert Syst. Appl.* 42 (19) (2015) 6686–6698.
- [78] S. Das, S.S. Mukherjee, P. Suganthan, Recent advances in differential evolution – an updated survey, *Swarm Evol. Comput.* 27 (2016) 1–30.
- [79] H.-P.P. Schwefel, *Evolution and Optimum Seeking: The Sixth Generation*, John Wiley & Sons, Inc., 1993.
- [80] X. Hu, Particle swarm optimization tutorial, 2006, <https://titan.csit.rmit.edu.au/~e46507/publications/psotutorial-seal06.pdf>.
- [81] J. Derrac, S. García, D. Molina, F. Herrera, A practical tutorial on the use of nonparametric statistical tests as a methodology for comparing evolutionary and swarm intelligence algorithms, *Swarm Evol. Comput.* 1 (1) (2011) 3–18.
- [82] P. Lagos-Eulogio, J.C. Seck-Tuoh-Mora, N. Hernandez-Romero, J. Medina-Marin, A new design method for adaptive iir system identification using hybrid cso and de, *Nonlinear Dynam.* 88 (4) (2017) 2371–2389.
- [83] A. Gotmare, S.S. Bhattacharjee, R. Patidar, N.V. George, Swarm and evolutionary computing algorithms for system identification and filter design: A comprehensive review, *Swarm Evol. Comput.* 32 (2017) 68–84.
- [84] G. Panda, P.M. Pradhan, B. Majhi, Iir system identification using cat swarm optimization, *Expert Syst. Appl.* 38 (10) (2011) 12671–12683.
- [85] M. Toz, Chaos-based vortex search algorithm for solving inverse kinematics problem of serial robot manipulators with offset wrist, *Appl. Soft Comput.* 89 (2020) 106074.
- [86] S. Dereli, R. Köker, A meta-heuristic proposal for inverse kinematics solution of 7-dof serial robotic manipulator: quantum behaved particle swarm algorithm, *Artif. Intell. Rev.* 53 (2) (2019) 949–964.